

Cycle to Cycle Feedback Control of Manufacturing Processes

by

Tsz-Sin Siu

B.A.Sc., Engineering Science
University of Toronto, 1999

Submitted to the Department of Mechanical Engineering
in Partial Fulfillment of the Requirements for the Degree of
Master of Science in Mechanical Engineering

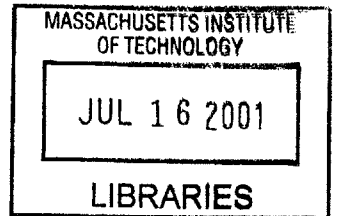
at the

Massachusetts Institute of Technology

February 2001

©2001 Massachusetts Institute of Technology
All rights reserved

BARKER



Signature of Author

.....
Department of Mechanical Engineering
January 29, 2001

Certified by

.....
David E. Hardt
Professor of Mechanical Engineering
Thesis Supervisor

Accepted by

.....
Ain A. Sonin
Chairman, Department Committee on Graduate Students

Cycle to Cycle Feedback Control of Manufacturing Processes

by

Tsz-Sin Siu

Submitted to the Department of Mechanical Engineering on
January 29, 2001 in Partial Fulfillment of the Requirements for the
Degree of Master of Science in Mechanical Engineering

Abstract

A new concept of process control in manufacturing called Cycle-to-Cycle (CTC) feedback control is introduced in this research. It is done by applying feedback from the final output of a manufacturing process, using the information from the current cycle to improve quality for the following cycles. Run-by-Run (RbR) control in semiconductor industry is found to use a similar idea of discrete feedback control. CTC control will be a complement to existing RbR technologies by presenting a stronger emphasis on control theory and expanding the application to other manufacturing processes.

Models for different process components are presented for CTC systems. Theories of discrete control system are used for analysis. Proportional and integral controls for CTC systems are analyzed using a linear process gain model with additive disturbance.

Two manufacturing processes - metal bending and injection molding - are carried out to demonstrate the advantages of CTC control and also to verify the accuracy of the models. As predicted, we found that CTC control can increase variation on uncorrelated process such as metal bending and reduce variation on correlated processes such as injection molding. Even for uncorrelated processes, however, CTC control can be used to reject common disturbances and bring the process closer to the desired target. As a result, CTC control is able to improve overall process capability by either reducing the variance or by removing the mean shift from the target.

It is shown experimentally that the linear additive models of the process and the disturbance are accurate. Analytical and graphical tools are very useful in predicting behavior of actual systems. It is also shown in the experiments that an optimization technique, which is based on the minimization of mean squared error, is effective in designing an optimal controller for the metal bending process.

Thesis Supervisor: David E. Hardt
Title: Professor of Mechanical Engineering

Acknowledgements

Achieving success in life is about achieving equilibrium. During my stay here at MIT, I learned to reach the state of equilibrium that had transformed me into a different person. I achieved that balance with the guidance of people around me (or engineers would call it “feedback”). I met more people from different background than ever before. I learned to share and give.

I would like to sincerely thank my research advisor, Professor David Hardt, for his ample and enthusiastic support for this research, and particularly his timely motivations that constantly re-energized my interest during the course of the project. Although my stay here at MIT has been quite short, your influence on me would certainly last for the rest of my life. Thanks also to SMA (Singapore-MIT Alliance) for generously providing the funding for this project. Thank you Gerry, Dave, Bob and Mark in the machine shop for helping me on the experiments during this project.

Everyone in the research group help made this thesis possible. Lisa helped with all the administrative stuff. Walt helped share my worries about job search. John showed me how to learn and think scientifically and rationally. Benny kept me up to date with new discovery on literatures.

To my father Bun-Wing, my mother Ching and my brother Peter for their support. I certainly miss the times I stayed at home but my encounter at MIT helped develop myself to be a complete person.

My roommate Kai is always pessimistic about life. I know you had a roller coaster experience here, but at least you made it and got a decent job earlier than any one of us. I hope you will learn to be optimistic and enjoy your work in California. Josh provides the daily dose of lunchtime relief and thanks for sharing a lot of interesting stories. Chee Wei is a lucky man, I wish Maggie and you the best. Keng Hui is a smart and witty guy, and I hope your generosity will lead you far and high in your career. Allen is full of surprises, and Saturday Haymarket trips are definitely the most memorable experience. Winston is most organized person that I have ever met, and by chance he is also a Canadian. Thank you for teaching me how to stay on my goals. Thank you Ceani for helping me to find the job at graduate admissions so I could get through my studies smoothly. Rhonda helped me solve a lot of problems while I was finishing this research. Well Ada, I don't know where to mention you, but thank you for being a close friend for more than 8 years.

I want to say thanks to Simon, Federico, Rogelio, Andrew, Shivanshu, Sascha, Yogesh, Carlos, and Cesar for sharing memorable moments with me. Thank you for teaching me things in life. Thanks to all my friends in Mechanical Engineering, especially those in the LMP, for their everyday support that allows me to overcome all the hurdles.

Before I started my studies here at MIT, Professor Ely Sachs told me that I would work harder than I have ever worked before. It certainly lived up to his comment. Thank you for helping me reach my potential. I also learned to enjoy life, as we all only live once and work is only part of life. Keeping a balance life not only enhances my efficiency at work, it also may research work more enjoyable and meaningful. Thank you Professor Sanjay Sarma for providing the comic relief during the stressful days as a teaching assistant; and you still owe me a coffee. And to all the students in the class, good luck in your future endeavor.

Quite unexpected for my stay here at MIT, I met a lot of people outside the academic circle. For my job as a database consultant, I got to meet a lot of people that assist the administration of the institution. I certainly learned a lot through the experience. It expanded my views and understanding of the cultures, history, religion and politics by interacting with different people all around the campus. Marina, Bette, Elizabeth, Linda, Monica and Tammy at the graduate admissions office especially gave me the care and guided me through my toughest times. They deserve my deepest gratitude as a pupil and friend.

MIT is a place that affects people. Through its rich culture of academics and research, it attracts the brightest and the most passionate scholars from around the world. President Vest calls MIT a learning institute. Whether it is an undergraduate student taking an introductory course to fulfill a degree requirement or a post-doctoral associate conducting cutting edge research trying to push the envelope of existing knowledge, we all have a common goal. The goal is to investigate and learn the truth about the natural and the artificial in a rational and scientific manner. What distinguishes MIT from other schools is not the course material being taught in classes, but rather the deep heritage that it embodies. At MIT, people work diligently to be the leaders of tomorrow; people work hard to achieve what they want; and people work endlessly to change the world. I am lucky to try to be one of them. So last but certainly not least, I must thank MIT for giving me the opportunity to learn with you, and to achieve some of the goals that I would never have achieved elsewhere.

Table of Contents

Abstract	3
Acknowledgements	5
Table of Contents	7
List of Figures	11
List of Tables.....	13
Glossary.....	15
Chapter 1: Introduction	17
1.1. Definition of Quality	17
1.2. Conventional Methods of Quality Control.....	18
1.2.1. Acceptance Sampling.....	18
1.2.2. Statistical Process Control and its notion of feedback	19
1.3. Automatic Feedback Control	20
1.3.1. Cycle-to-cycle feedback control.....	20
1.3.2. Difference between CTC control and machine control	21
1.4. Research Goals.....	23
1.4.1. Discrete control tools for CTC control.....	24
1.4.2. Experiments of CTC control on new processes	24
1.5. Expected Reader Background and Thesis Outline.....	24
Chapter 2: Literature Review	27
2.1. The Pioneers.....	27
2.1.1. Box and Kramer	27
2.1.2. Sachs, Hu and Ingolfsson	29
2.1.3. Vander Wiel and Tucker	31
2.2. More Recent Developments.....	32
2.2.1. T. Smith and D. Boning.....	32
2.2.2. Del Castillo and Hurwitz.....	32
2.2.3. Del Castillo.....	33
2.2.4. Valjavec and Hardt.....	33
2.3. The Future	34
2.3.1. The Next-Generation Manufacturing Project.....	34
2.4. Motivation for Cycle-to-Cycle feedback control	35
Chapter 3: Theoretical Background.....	37
3.1. Cycle-to-Cycle System Models.....	37
3.1.1. Process and Disturbance models	37
3.1.2. Delay models.....	39
3.2. Discrete Control System Analysis	40
3.2.1. Z-transform and analysis.....	40
3.2.2. Adding Randomness to the system.....	42
3.3. Characterizing Cycle-to-Cycle Control Systems	42

3.3.1. Root locus diagram in Z-plane.....	42
3.3.2. Steady-state error analysis	43
3.3.3. Settling time analysis	45
3.4. Analysis of Cycle-to-Cycle Control Systems	45
3.4.1. Proportional control with direct feedback.....	45
3.4.2. Integral control with direct feedback	50
3.5. Analysis Summary	55

Chapter 4: Design of Minimum Quality Loss Controller.....57

4.1. Introduction to Controller Design.....	57
4.2. Performance Measuring Techniques	58
4.2.1. Performance metrics used in Manufacturing Quality Control	58
4.3. Cycle-to-Cycle feedback control scheme and its design criteria.....	59
4.3.1. Performance Metric of Cycle-to-Cycle feedback controller.....	60
4.4. Optimal Controller Design for Cycle-to-Cycle Systems	62
4.5. Step disturbance example	63

Chapter 5: Application to Sheet Metal Bending Process..... 69

5.1. Introduction.....	69
5.1.1. Manufacturing Process Taxonomy	69
5.1.2. Selection of appropriate processes for experimentation	70
5.1.3. Description of Air Bending process.....	71
5.1.4. Process Model and Assumptions	72
5.2. Experimental Setup.....	73
5.2.1. Expected Results.....	75
5.3. Experimental Procedure and Observations.....	76
5.4. Results and Analysis.....	78
5.4.1. Characterization of Process Gains	78
5.4.2. Open-loop Run.....	80
5.4.3. Closed-loop with no deterministic disturbance.....	81
5.4.4. Closed-loop with step disturbance (sudden shift of material properties).....	84
5.4.5. Closed-loop with ramp disturbance (gradual change of tailstock position).....	86
5.4.6. Optimally designed gain with material shift.....	88
5.5. Conclusions.....	91

Chapter 6: Application to Injection Molding Processes 93

6.1. Introduction.....	93
6.1.1. Description of Injection Molding Process	93
6.1.2. Process Model and Assumptions	95
6.2. Experimental Setup.....	96
6.3. Experimental Procedure and Observations.....	99
6.3.1. Procedures.....	99
6.3.2. Observations	100
6.4. Data analysis	101
6.4.1. Design of experiment to characterize process gain.....	101
6.4.2. Closed-loop control of the process with P-controller	104

6.4.3. Closed-loop control of the process with I-controller..... 109
6.5. Conclusions..... 111

Chapter 7: Conclusions and Recommendations..... 113

7.1. Summary of results 113
 7.1.1. Experimental results 113
 7.1.2. Additional insights 114
7.2. Recommended future work 115
 7.2.1. Short-term research goals 115
 7.2.2. Long-term research goals 115
7.3. Final words..... 116

Appendix A..... 117

Appendix B..... 127

References 133
Bibliographical Note 136

List of Figures

Figure 1.1: Acceptance sampling implementation.....	18
Figure 1.2: Classical Control System View of SPC implementation.....	19
Figure 1.3: Cycle-to-cycle discrete-time control implementation	21
Figure 1.4: Material variations are outside the loop of machine state control	22
Figure 1.5: Process control that includes material control.....	22
Figure 1.6: Process control by feeding back critical output parameters	23
Figure 3.1: Control system blocks	37
Figure 3.2: An appropriate process model	38
Figure 3.3: A simple additive disturbance model	38
Figure 3.4: Pure process delay model	39
Figure 3.5: Control Block Diagram for proportional controller.....	41
Figure 3.6: A first order correlated disturbance	42
Figure 3.7: Comparison of root locus plot in s-plane (left) and z-plane (right).....	43
Figure 3.8: Matlab verification of the analytical result for a P-controller with NIDI disturbance... 48	48
Figure 3.9: Time dependence of variance amplification for P-controller	49
Figure 3.10: Matlab simulation result showing variance reduction for a P-controller.....	50
Figure 3.11: Control Block Diagram for Integral Controller	50
Figure 3.12: Root locus plot for a closed-loop integral control system	51
Figure 3.13: Matlab verification of the analytical result for I- controller with NIDI disturbance ... 53	53
Figure 3.14: Time dependence of variance amplification for I-controller	54
Figure 3.15: Matlab and frequency analysis results showing variance reduction for I-controller... 55	55
Figure 4.1: Discrete-time feedback implementation of a P-controller with random disturbance 60	60
Figure 4.2: Variation of performance parameters for a P-controller with random disturbance	61
Figure 4.3: The two types of disturbances:	63
Figure 4.4: Block diagram of a feedback control system with an I-controller on a shifted process 64	64
Figure 4.5: Control block diagram for a PI-controller	66
Figure 4.6: Root locus diagram for a PI-controller (with $K=1$, so the open-loop zero is at 0.5) 67	67
Figure 5.1: Manufacturing Process Taxonomy	69
Figure 5.2: Illustration of Air Bending Process	71
Figure 5.3: Model Schematics for Air Bending Process.....	72
Figure 5.4: Setup for the metal air bending experiment on a lathe	73
Figure 5.5: Punch depth control using the precision dial on a lathe	74

Figure 5.6: A Vernier Protractor measuring part angle	75
Figure 5.7: Steps showing different bend angles at different punch depths	76
Figure 5.8: Feedback Control schematics for air bending process	77
Figure 5.9: Simulated deterministic output using optimal feedback gain	88
Figure 5.10: Performance Index minimization by K_c	89
Figure 6.1: Illustration of Injection Molding Process	94
Figure 6.2: Model Schematics for Injection Molding Process	95
Figure 6.3: Injection Molding Machine used for experiment	96
Figure 6.4: Injection Molding Machine controller panel	97
Figure 6.5: Injection Molding Die Close-up with Part	97
Figure 6.6: Dial Caliper measuring an injection molded part	98
Figure 6.7: Output Part Dimension	98
Figure 6.8: Feedback Control schematics for Injection Molding process	100
Figure 6.9: Comparison of a good and bad part	101
Figure 6.10: Correlation plot between hot and cold measurement	104
Figure 6.11: P-controller closed-loop run	105
Figure 6.12: Autocorrelation comparison between open-loop process	106
Figure 6.13: P-controller closed-loop run with gain change	107
Figure 6.14: Root locus diagram for P-controller	108
Figure 6.15: Closed-loop P-controller target shifted	109
Figure 6.16: I-controller closed-loop run	110
Figure 6.17: Root locus diagram for I-controller	111
Figure 6.18: Illustration of a thermoformed part	112
Figure 6.19: The side of a thermoformed part is tapered at the bottom	112

List of Tables

Table 5.1: Results of Process Gain Characterization experiments.....	79
Table 5.2: Results of open-loop run experiments	80
Table 5.3: Results from undisturbed closed-loop experiment with P-controller	82
Table 5.4: Results from undisturbed closed-loop experiment with I-controller	83
Table 5.5: Results from shifted closed-loop experiment	85
Table 5.6: Results from closed-loop experiment with ramp disturbance.....	87
Table 5.7: Experimental result for Minimum Quality Loss I-controller design	90
Table 6.1: Input parameters and the range of operations	101
Table 6.2: Design of experiment input levels used	102
Table 6.3: First round ANOVA table.....	102
Table 6.4: Second round design of experiment result.....	103
Table 6.5: Run statistics for P-controller run	105
Table 6.6: Run statistics for disturbed P-controller run	107
Table 6.7: Run statistics for P-controller with varying target.....	109
Table 6.8: Run statistics for I-controller	110

Glossary

SPC – Statistical Process Control

CTC control – Cycle-to-Cycle control

RbR control – Run-by-Run control

NGM – Next-Generation Manufacturing

P-controller – Proportional controller

PI-controller – Proportional Integral controller

I-controller – Integral controller

MSE – Minimum squared error

ST controller – Self-tuning controller

MISO – Multiple-Input Single-Output

DOE – Design of Experiment

ANOVA – Analysis of Variance

Chapter 1: Introduction

This thesis is about expanding the traditional concept of quality control in manufacturing: using feedback from the output of a manufacturing process, measured after each process cycle, as a means of systematic quality improvement. We call this Cycle-to-Cycle (CTC) feedback control. In this chapter, we will summarize some of the quality control techniques that are commonly used in industry today. We will show that in some of the traditional techniques, the notion of feedback control has long existed. The problem, however, lies on the fact that most of the control schemes are based on subjective operator judgments. We will also present the traditional use of in-process control in machine design to improve the process and how CTC feedback control can be implemented to further improve the quality of the process.

1.1. Definition of Quality

In manufacturing processes, quality is how well the process output conforms to the design specifications. Output refers to the critical dimension or critical property of the output. In machining, for example, the output is the critical dimension of the machined part and the accuracy of the machined part determines the quality of the output. In annealing process, the output is the average hardness of the annealed part and the quality is the uniformity of the hardness on the output part.

Quality is also defined as inversely proportional to variability [1]. Since variability can be described only in statistical terms, statistical measures such as process capability¹ and quality loss² are commonly used for quality improvement.

1.2. Conventional Methods of Quality Control

1.2.1. Acceptance Sampling

Acceptance sampling, also known as 100 percent inspection, is an end-of-pipeline solution to quality control. One can imagine this as a “quality filter” at the output of the process that only allows the acceptable parts to pass through. By inspecting every single output of the process, the quality of the products is guaranteed. Figure 1.1 shows how acceptance sampling is conducted.

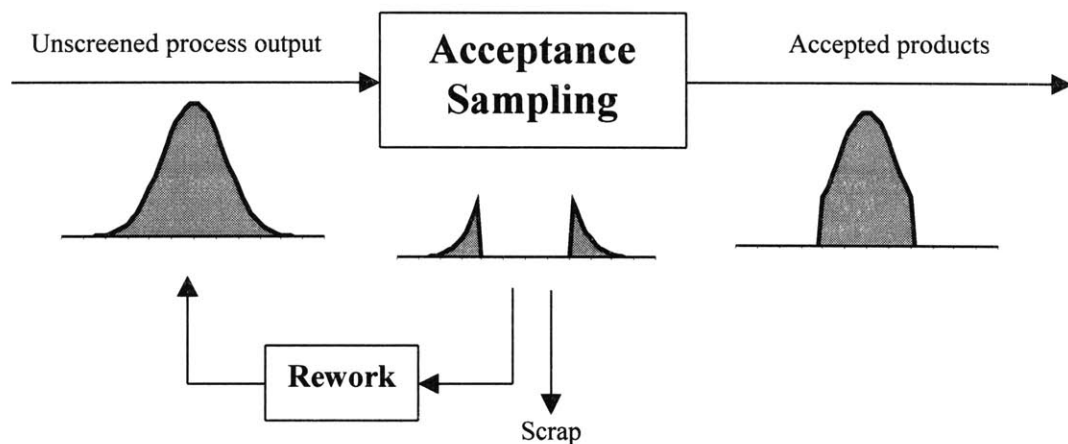


Figure 1.1: Acceptance sampling implementation

Source: DeVor [2], p. 28

¹ Process capability, C_{pk} , is a statistical parameter commonly used to measure quality. It is defined as

$$C_{pk} = \min\left(\frac{USL - \mu}{3\sigma}, \frac{\mu - LSL}{3\sigma}\right),$$

where μ and σ are the mean and standard deviation of the process, and

USL and LSL are the specification limits. A process with higher C_{pk} has better quality.

² Quality loss, L , is usually a quadratic function describing the cost of being off target and is defined as $L = (x - T)^2$, where x is the actual output and T is the desired output. We want to minimize the value L .

The advantage of acceptance sampling, obviously, is its 100% quality assurance. For mission critical parts that need to meet stringent quality requirements, acceptance sampling is the only way to guarantee complete compliance to specification. The disadvantages, on the other hand, are large quantities of wasted parts, lower production rate and high cost of inspection and rework.

Although acceptance sampling guarantees the quality of the output, it does not improve the process itself. The variability of the process output is still high, and this limits the process capability of the process.

1.2.2. Statistical Process Control and its notion of feedback

Statistical Process Control (SPC) is probably one of the most widely used techniques in quality control today. Samples of the process output are obtained and the collected data are usually averaged (like a low pass filter) and plotted on a graph called a run chart. If a sample point is found to lie outside the process limits (usually $\pm 3\sigma$ from the true mean of the process, where σ is the standard deviation of the process), an alarm is signaled. The operator would then check for anomalies in the machine, the material or the process itself and see if adjustments are needed. SPC allows the detection of assignable or special causes such as tool wear, material changes or human errors. Figure 1.2 below shows the feedback loop of SPC methodology.

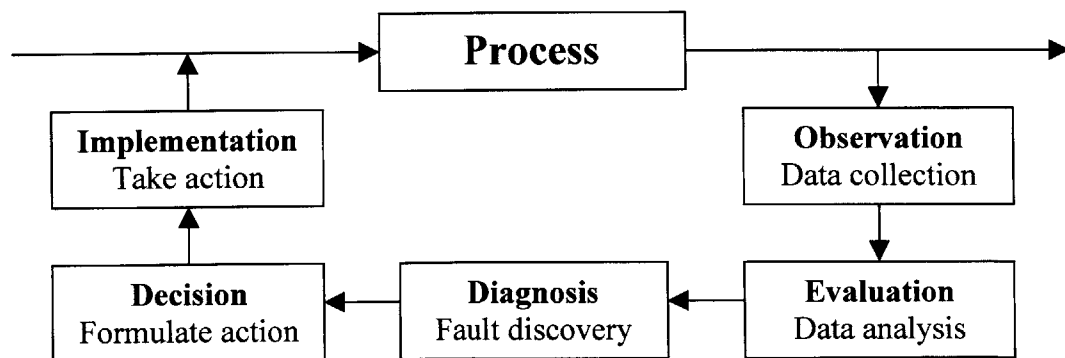


Figure 1.2: Classical Control System View of SPC implementation

Source: DeVor [2], p. 134

Advantages of SPC include lower cost on inspection and rework, higher quality than without inspection, and lower waste than acceptance sampling. Its ability to signal critical problems in machine, material and operating procedure is also an important advantage. Compared to acceptance sampling, however, SPC does not have 100% quality assurance. Slow response to disturbances in input parameters due to the averaging effect is also a disadvantage.

In SPC, the goal is to maintain the output within the 3σ limits. Quality control is a task performed by human decision. The control action can be inconsistent and arbitrary, so the variability is still high and the process capability limited.

1.3. Automatic Feedback Control

As seen in Figure 1.2, SPC uses the notion of feedback in quality control. The feedback signal, however, is only being used as a monitoring tool as opposed to a decision tool. In other words, SPC does not provide the user with a specific direction to improve the process. The ability to improve the performance of a process relies completely on the operator or production engineer's knowledge and experience. It is desirable, therefore, to devise an autonomous feedback control scheme that would automatically and intelligently fine tune the manufacturing process to achieve optimal performance.

For continuous processes, feedback control theory in the continuous domain can be applied to achieve desired dynamic behavior. For discrete part manufacturing, similar continuous feedback control can be used for the time period within each process cycle (herein referred to as "in-process" control). The final output, however, cannot be obtained until the discrete process cycle is complete. Our interest is in investigating the use of discrete control theory on data obtained after each process cycle, hereafter referred to as CTC feedback control.

1.3.1. Cycle-to-cycle feedback control

Cycle-to-cycle feedback control is the focus of this research. It can be thought of as a combination of acceptance sampling and automatic feedback control. In acceptance sampling, all output parts are sampled for quality assurance. By contrast, CTC control feeds back the information acquired from the sampling in an analytical manner to adjust and improve the process.

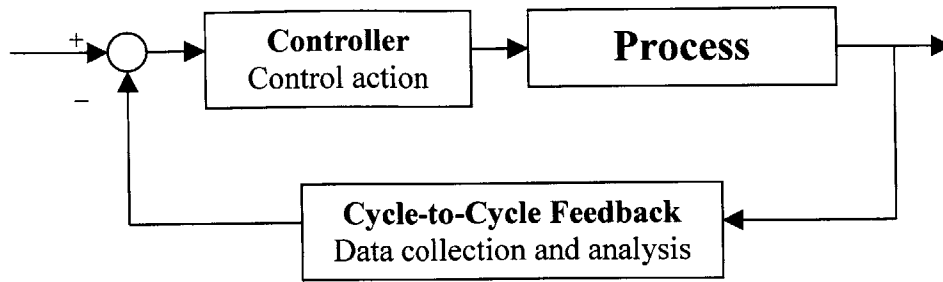


Figure 1.3: Cycle-to-cycle discrete-time control implementation

The obvious advantages of CTC control include a systematic control strategy that does not require subjective human decision-making and predictable performance based on theory. The disadvantages of CTC control are the cost of measurement and the inability to diagnose assignable causes in the process. In order to popularize the use of CTC control, some of these disadvantages need to be overcome.

1.3.2. Difference between CTC control and machine control

Another way to look at CTC control is from a machine control point of view. One might ask what is the difference between traditional machine control and the proposed CTC control. Most high volume machines have sophisticated controllers to maintain machine parameters such as position, flow rate, pressure and temperature. But these controllers only control the machine states. The most important attribute of a process is its output, which can only be indirectly controlled by these machine state controllers. In addition, imperfection in the modeling of the relationship between machine parameters and the output can lead to output errors.

Variation in material properties is also a major cause of error on the output; and machine state control cannot possibly adjust for the variation in the material because material is out of the loop of machine state control (Figure 1.4 shows why machine state control cannot control material variation). We can see that both the machine and material have variations in their property (stiffness, yield stress, melting point) and state (temperature, internal stress, shape). Machine state

control only compensates for the machine part of the process and thus leaves the variation of the output dependent on material variation.

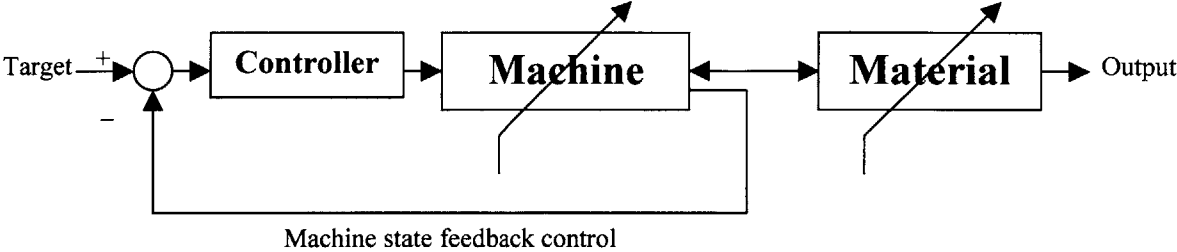


Figure 1.4: Material variations are outside the loop of machine state control
Source: Hardt [3]

A natural step to tackle this problem is to impose control on the material. Figure 1.5 below shows the control model that includes material control as well. It can be observed that this type of control still does not control the output directly. Because the interactions between the machine and the material can be unpredictable, the output variation is still high.

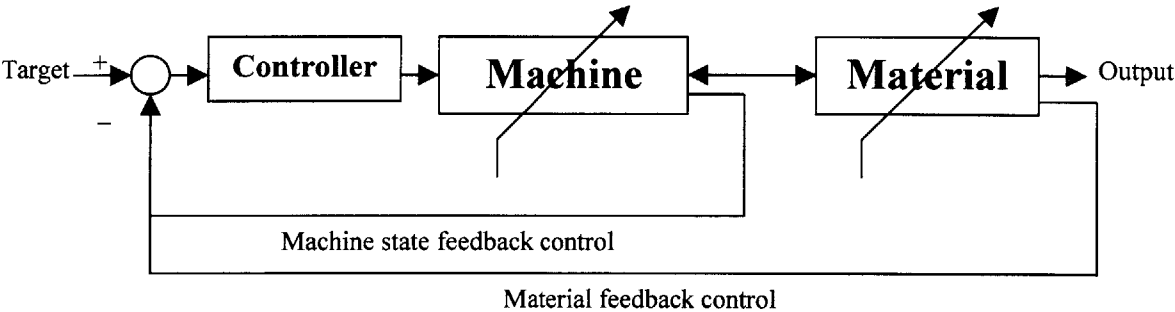


Figure 1.5: Process control that includes material control
Source: Hardt [3]

To achieve direct control on the output, measurements of critical output parameters have to be obtained and fed back for adjustment. As shown in Figure 1.6, output feedback considers variations imposed by both the machine and the materials. We could, of course, implement machine state control and material control in conjunction with critical output control to reduce the amplitude of adjustment in the outer loop.

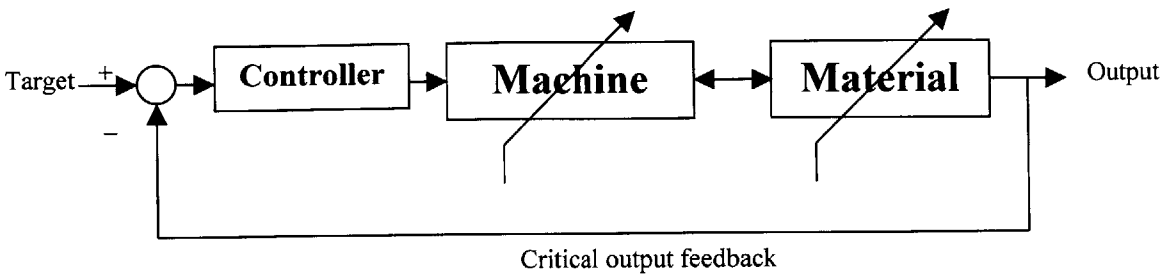


Figure 1.6: Process control by feeding back critical output parameters

Source: Hardt [3]

In certain manufacturing processes such as chemical mixing, direct output feedback control can be achieved within the manufacturing cycle so the output can be controlled precisely for each individual cycle. In most other cases, however, the critical output parameter (typically a dimension) will not be accessible until the manufacturing cycle is finished; by which time the current output, even if out of specification, cannot be changed anymore. Cycle-to-cycle control is the use of this final output to adjust the proper input parameter for the following cycle. Cycle-to-cycle control is, therefore, discrete in nature and it can be applied to batch continuous processes and discrete parts manufacturing.

1.4. Research Goals

We started this research believing that CTC control would be a breakthrough in quality control. It was a subtle but important improvement towards conventional SPC scheme. As will be shown in chapter 2, it is found that substantial research had been done in the development of similar quality control scheme for semiconductor manufacturing. In reading through this literature, it was found that most of the theoretical development had been conducted from a statistical point of view. Some of the analyses were long and tedious; and more importantly, most of the theories lacked simple graphical design tools that are familiar to control engineers. The complexity of the statistics can be a hindrance in the widespread used of CTC control.

1.4.1. Discrete control tools for CTC control

The theories of discrete control have been in existent for a long time. In areas such as discrete signal processing, digital communications and digital control system, applications of the theories are diverse and comprehensive. Tools such as z-transformation and root locus plot on a unit circle can greatly ease the analysis and design process. We will bring some of these tools to CTC control and show examples of effective application.

1.4.2. Experiments of CTC control on new processes

Two applications of CTC control are carried out to verify analytical results and to demonstrate the use of design tools to predict system behavior. The three-point bending or air bending process represents a family of processes that has uncorrelated disturbances. It also has regular shifts or ramps that are somewhat predictable. In short run manufacturing situations, we could effectively use CTC control tools to optimally improve the process capability.

The injection molding process, on the other hand, has highly correlated disturbances. It represents a family of thermal processes that can take benefit of the variance reduction capability of CTC control.

1.5. Expected Reader Background and Thesis Outline

In order to take full advantage of the discussions in this thesis, it is expected that the reader be familiar with classical feedback control theory, elementary statistics, manufacturing processes and some knowledge on difference equations and matrix operations.

This thesis highlights the two main focuses of the research of CTC feedback control: theoretical development and application by experimentation. One who is familiar with run-by-run control can skim through chapter 2 and focus more on the discrete control theories presented in chapters 3 and 4. Those who are familiar with discrete stochastic control theory may elect to skip chapter 3.

In this chapter, the advantages of CTC feedback control compared to traditional quality control methodologies were presented. The theoretical work revolves around the development of discrete

stochastic control theory, with short run manufacturing and correlated disturbances some of the important themes. Chapter 2 presents a thorough review of the history of CTC feedback control and summarizes the current state-of-the-art of the field. It also seeks to define a vision on which CTC feedback control can be integrated into manufacturing equipment design in the future. The essential theoretical background of the CTC feedback control, which is extracted from discrete feedback control, is presented in chapter 3. Several graphical and analytical tools for discrete feedback control are also presented.

Chapter 4 contains an analytical framework for designing minimum quality loss controller and the method is later used in the air bending process to illustrate the concepts.

Applying the theory to existing manufacturing processes is a non-trivial task and the advantage of CTC may not be immediately appealing to engineers or managers. Chapter 5 deals with the appropriate application of CTC feedback control to manufacturing processes. Common manufacturing processes are categorized. Chapters 5 and 6 also contain experimental results that verify and illustrate some of the issues presented in the theoretical development. The sheet metal air bending process represents an uncorrelated process and is summarized in chapter 5. Injection molding is a correlated process and the results are included in chapter 6.

Not only are the equipment nowadays not designed with CTC feedback control in mind, the manufacturing systems cannot be integrated to take advantage of the technology. The conclusion of the thesis is not about a particular application, rather it tries to envision the power of CTC feedback control in a more general framework of manufacturing system. It suggests exploration into related fields and search for new ideas and theories.

Chapter 2: Literature Review

While searching through the literature that made up the so-called Run-by-Run (RbR) control in the semiconductor industry, it was found that the idea of discrete feedback control in manufacturing processes surfaced at the end of the 1980's. The concept was quickly adopted to be used in semiconductor manufacturing. Until recently, most work has been related to RbR control. This chapter is organized to first present the early literature in this field; giving an idea of how it started. It is followed by the more recent developments in the field, again mostly in semiconductor manufacturing. It concludes with motivation for new analytical tools that are easier to use and for expanding the field.

2.1. The Pioneers

To precisely identify how and when the notion of discrete feedback process control initiated is subjective and inaccurate. This is an attempt to distinguish several important works that furthered the area by either developing new theories or applying the theory to real processes.

2.1.1. Box and Kramer

Statistical Process Control and Automatic Process Control, 1990

This is one of the earliest attempts to provide a formal introduction to discrete feedback control in manufacturing. It argues that statistical process control and automatic process control are similar in nature but originate from different industries. SPC is developed for the “parts” industry while APC is designed for the “process” industry. The major differences in the two industries are as follows:

1. The two industries have different goals. The parts industry wants to achieve the smallest possible variation while the process industry wants the highest yield.
2. Different disturbances are associated with the two industries. The parts industry has small variations in material properties while the process industry has higher sensitivity to external disturbances such as temperature and pressure.
3. Cost of adjustment is high for the parts industry relative to the process industry.

The authors then point out that the dividing line between the two industries is fading. The primary reason is the need for higher quality using control. The emergence of hybrid manufacturing processes such as semiconductor manufacturing and the coexistence of both processes in a single company urge the combined usage of both methodologies.

The authors then propose a quality control perspective from a feedback control point of view. A generalized disturbance model (Z_t) combining a white noise disturbance and an integrated moving average model is presented:

$$Z_t = \hat{Z}_t + a_t \quad (2.1)$$

where $\hat{Z}_t = \lambda \cdot (Z_{t-1} + \theta \cdot Z_{t-2} + \theta^2 \cdot Z_{t-3} + \dots)$, λ and θ are the weighing factors for the moving average and a_t is a white noise sequence.

They also propose a simple first order dynamic model describing the process with a generalized inertia:

$$Y_t = \delta \cdot Y_{t-1} + g \cdot (1 - \delta) \cdot X_{t-1} + c \quad (2.2)$$

where g is the systems gain, δ is the first order dynamic parameter and c is a constant.

Given the models in equations (2.1) and (2.2), the minimum mean square error (MMSE) PI-controller for the process is found to have the following values:

$$k_p = \frac{\lambda \delta}{g \cdot (1 - \delta)} \text{ and } k_i = \frac{\lambda}{g} \quad (2.3)$$

Using the optimal controller parameters, the authors show variance reduction on the output. In addition to the MMSE optimization scheme, the authors also present an optimal control methodology that takes into account the cost of adjusting input parameters and the cost of measuring output variables.

2.1.2. Sachs, Hu and Ingolfsson

Run-by-Run Process Control: Combining SPC and Feedback Control, 1995

Stability and Sensitivity of an EWMA Controller, 1993

Based on some of the arguments and theories developed by Box and Kramer, this research represents one of the first applications of discrete feedback control to manufacturing process. This paper contains results in the 1991 MS thesis by Ingolfsson at MIT.

The authors believe that SPC is a “binary view of the condition of a process; i.e. either it is running satisfactorily or not”. And that SPC does not or cannot prescribe correction action. They also note that the SPC paradigm believes as long as the process behaves in a random and stable manner, applying feedback control will only increase the variability of the process. There are, however, some commonly encountered situations where the SPC paradigm may not be satisfied, and therefore doing feedback control would help eliminate assignable causes.

A real-time run-by-run controller is implemented for a silicon epitaxy process to reduce variability. Three modes of operations are used to accommodate the common types of disturbances:

1. Optimization mode using sequential design of experiments to locally optimize the process
2. Rapid mode to quickly adjust the input to correct for large step disturbances ($>2\sigma$)
3. Gradual mode to slowly adjust for slow drift disturbances ($1\sigma/100$ runs)

An EWMA filter is used to estimate the intercept of the linear model of the process ($Y_i = a_i + b \cdot X_i$, where Y_i and X_i are the output and input of the process, a_i and b are the y-intercept and the slope of linear model respectively) and it is shown that it works just like an integral controller with the following equation:

$$X_i = -\frac{w}{b} \cdot \sum_{i=1}^{i-1} (Y_i - T) + X_1 \quad (2.4)$$

where w is the weight on the EWMA filter and T is the desired output.

Experiments are performed on an Epitaxy Reactor and they show a 2.7 times improvement in the process capability, C_{pks} , in the gradual mode. The results also show the ability to reject step disturbances quickly in the rapid mode.

In the second paper based on the 1991 MS thesis by Ingolfsson, some of the stability issues associated with increasing the gain of an EWMA run-by-run controller are illustrated.

Convergence analysis is performed on two process models: a deterministic first order process and a deterministic second order process. The first order process is specified as follows:

$$Y_t = \alpha + \beta \cdot x_t \quad (2.5)$$

where Y_t and X_t are the output and input of the process, α and β are actual parameters of the physical plant and are not exactly known.

The authors also discuss the stability of the system. Using the feedback system with control law stated in equation (2.4), it is found that the system would be stable if:

$$0 < \frac{w \cdot \beta}{b} < 2 \quad (2.6)$$

where $0 < w < 1$ is the weight on the EWMA filter and b is the estimated value of the actual slope β .

For a deterministic second order process with quadratic behavior:

$$Y_t = \alpha + \beta \cdot x_t + \delta \cdot x_t^2 \quad (2.7)$$

Using the same updating equation of the form of an EWMA filter, it is shown that the system is stable if:

$$\left| \frac{w \cdot \mu}{b} \right| < 2 \quad (2.8)$$

where $\mu = \left. \frac{dY_t}{dx_t} \right|_{Y_t=T}$ is the local process gain.

The authors also discuss the effect on the output if a more realistic probabilistic model is used:

$$Y_t = \alpha + \beta \cdot x_t + \kappa \cdot \sigma \cdot t + e_t \quad (2.9)$$

where $\kappa \cdot \sigma \cdot t$ represents a drift (ramp) disturbance, κ determines the slope of the ramp disturbance and e_t is a white noise sequence with mean of zero and standard deviation of σ . The result of statistical analysis shows that the asymptotic mean squared deviation (MSD), which is the

expected value of the squared of the difference between Y_∞ and the target T , has the following expression:

$$\frac{MSD}{\sigma^2} = \frac{2b/\beta}{2b/\beta - w} + \left(\frac{\kappa b/\beta}{w} \right)^2 \quad (2.10)$$

The ratio is always greater than zero, which indicates that the MSD is greater than σ . One limiting case of the equation is when $\kappa=0$ and $b=\beta$. Equation (2.10) becomes $\frac{2}{2-w}$, which is minimized at $w=0$. As a result, if the process has no ramp disturbance component, it is best to simply leave the process alone in open loop (with system gain, $\frac{w}{b}$, equal to zero).

A similar result on a wandering (random walk) noise model is given and experimental results based on controlling an epitaxial growth process are also presented.

2.1.3. Vander Wiel and Tucker

Algorithmic Statistical Process Control: Concepts and an Application, 1992

This is another paper that tries to apply the concept of CTC feedback control to a manufacturing process. It is based on experiments of controlling intrinsic viscosity from a particular General Electric polymerization process. It reiterates many of the equations and concepts proposed by Box and Kramer in [4]. The main contribution of this paper to the field is the four-step application guideline that the authors proposed:

1. Develop a time series transfer-function model of the process including process dynamics caused by measurement delays.
2. Design a suitable controller based on the model of the process.
3. Put in SPC charts to monitor the closed-loop process to detect any unexpected events happening.
4. If an SPC alarm signals, search for assignable causes and remove it if possible.

2.2. More Recent Developments

Since the formal introduction of discrete process control by Box and Kramer, most theoretical developments and practical work have been in the semiconductor industry, which has led to the development of run-by-run control. Actively pursued topics include self-tuning controllers and multivariate control theory for run-by-run control³. Research on discrete process control for the sheet metal forming industry is also included below where reconfigurable dies are used.

2.2.1. T. Smith and D. Boning

A Self-Tuning EWMA Controller Utilizing Artificial Neural Network Function Approximation Techniques, 1996

This paper presents an extension to the Exponentially Weighted Moving Average (EWMA) controller to dynamically update the EWMA weights via an Artificial Neural Network to provide better control. The effects of EWMA weights on the responses of systems with different disturbances are discussed, and the determination of optimal EWMA weights using disturbance state mapping is also presented.

The authors believe that the performance of a regular EWMA controller is highly dependent on the choice of the EWMA weights, and the ability to dynamically update the EWMA weight value is important for systems in which the process model does not accurately represent the true process dynamics. Simulation results show an improvement ranging from 9% in small drift and high noise processes to 38.7% in high drift and low noise processes.

2.2.2. Del Castillo and Hurwitz

Run-to-Run Process Control: Literature Review and Extensions, 1997

This paper discusses the concepts behind RbR control with particular emphasis on EWMA based controllers. The authors point out that this type of controller is well suited for processes where the cost of an output being off-target is high and where the cost of control action is relative

³ A more comprehensive literature listing on RbR control can be found on the MIT Microsystems Technology Laboratories Website - <http://www-mtl.mit.edu/rbrBench/RbRLit.html>

inexpensive. They also believe that the run-by-run control techniques are well suited for short-run discrete part manufacturing processes.

Limitations of these controllers include lagged response and the sluggish performance. A self-tuning (ST) controller is presented to rectify some of these problems by separating the estimation problem from the control problem. The type of controller discussed is called “indirect ST” controller where the control equation is derived and then parameter estimates are substituted for the true values. Simulation results are presented and it shows that the ST controller could provide more robust control against a wider variety of distributions and system configurations than could certain EWMA controllers found in the literature.

The authors also perform analysis on a ST with an SPC deadband. This means that the controller would not be activated unless the feedback data moved outside a SPC deadband. It is demonstrated by Box, Jenkins and Reinsel in [5] that this would reduce the frequency of control action changes that might be costly for some processes. Simulation shows that a deadband to give approximately the same output standard deviation with a reduction in the number of control action changes by about 33%.

2.2.3. Del Castillo

A multivariate self-tuning controller for run-to-run process control under shift and trend disturbances, 1996

The author presents a self-tuning multiple-input multiple-output controller for run-by-run control. A sensitivity analysis is presented to show the performance of the controller under various simulated system noise combinations.

2.2.4. Valjavec and Hardt

A closed-loop shape control methodology for flexible stretch forming over a reconfigurable tool, 1999

This is one of few research works related to CTC feedback control that are not in the process industry. It provides validation that CTC feedback control can be applied effectively to discrete parts manufacturing processes.

The author develops a self-tuning feedback shape control algorithm for stretch forming on a reconfigurable forming tool. Based on empirical estimation results of process parameters from calibration trials, a system identification strategy called the deformation transfer function is used to recursively estimate the tool shape required to achieve desired part shape. Stability is achieved for the control strategy on laboratory and full-scale experiments.

In addition, the same control methodology is used to compensate for the combined shape distortions in a series of manufacturing operations (stretch forming, chemical milling and trimming).

2.3. The Future

Although most current applications are in the area of semiconductor manufacturing, the potential of discrete feedback control is far beyond that. In most manufacturing processes, from discrete parts manufacturing to batch continuous processes, discrete feedback control can provide the next level of automation and quality control that complements the control of machine states alone. The following publication provides a vision for the future of manufacturing that allows manufacturing companies to succeed in the future marketplace of immense industry competition and globalization.

2.3.1. The Next-Generation Manufacturing Project

Next-Generation Manufacturing – A framework for Action, 1997

The Next-Generation Manufacturing (NGM) Project is a collaboration between industry, government and academia that seeks to provide a framework for developing answers to the challenges for change.

The NGM framework uses a hierarchical cause and effect structure that tries to identify the Global Drivers of new marketplace. From this set of Global Drivers one could determine the necessary “attributes” and “dilemmas” that companies should possess and overcome. Finally, based on the “NGM imperatives” one could provide specific “action recommendations” that would allow manufacturing companies to succeed in the future.

One aspect of the NGM paradigm that is particularly relevant to the topic of CTC feedback control is the Next-Generation Manufacturing Processes and Equipment. The NGM paradigm calls for faster responsiveness to customer requirements. And doing so would require reconfigurable, scalable, cost-effective physical plants and equipment. Instead of relying on experience-based knowledge for process improvement, science-based knowledge would be utilized in the future. Rather than using hard tooling, soft tooling and tool-less processes would be preferred. Automatic equipment would be replaced by autonomous equipment where high quality can be achieved without supervision. It requires the development of new intelligent processes and equipment hardware to achieve optimized process configurations using modular machine tools and modern computer control equipment.

2.4. Motivation for Cycle-to-Cycle feedback control

As evidenced by the amount of literature related to CTC feedback control, it is an important tool to improving the quality of manufacturing processes in a scientific and systematic manner. In addition, the NGM project envisions the future of manufacturing embodying more scientific content and pushing beyond the current envelope of automatic equipment. Productivity and quality are two of the most important features of successful modern manufacturing enterprise. The two attributes are closely tied together. Better quality means less waste or rework, and the overall productivity increases. The CTC feedback control framework enables Next-Generation Manufacturing Equipment to achieve this goal by controlling the output of the process rather than the states of the machine. Since humans perform poorly in supervisory positions such as SPC monitoring [6], why not let machines carry out the task. In addition, information collected from the output measurement can be used by subsequent processes to collaboratively improve the quality of the system [7].

A variant of CTC feedback control has been used extensively in the semiconductor industry for close to a decade now. Significant research work has been done on the development of theory and some issues of implementation. CTC control would further the field by introducing some elegant tools that are simpler to use; and also by proposing a more powerful application framework that would promote the broader use of CTC control. We seek to contribute to field in the follow ways:

1. Provide a more general theoretical framework to the problem; namely discrete feedback control theory, with analytical and graphical tools for design.
2. Investigate applying the theory to other manufacturing processes, and provide guidelines for the implementation of the control strategy.

In the next chapter, we will introduce some of the theories about stochastic discrete control that are the building blocks of CTC control. We also show some analysis of simple CTC systems.

Chapter 3: Theoretical Background

3.1. Cycle-to-Cycle System Models

Cycle-to-cycle control requires the modeling of discrete manufacturing processes as a discrete-time dynamic systems. As shown in Figure 3.1, all control systems have a model for the plant (the process), the feedback loop (the delay) and the disturbance. In this section, we will present the models and assumptions that we use for the cycle-to-cycle control.

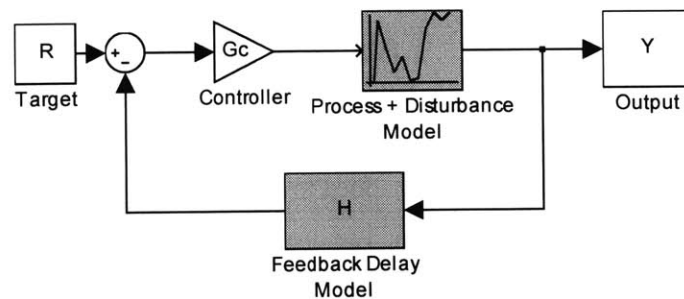


Figure 3.1: Control system blocks

3.1.1. Process and Disturbance models

All processes have variations and disturbances. For some manufacturing processes, especially for processes that involve thermal processing, there are low frequency dynamics in the process output. From a process point of view, separating the process model from the disturbance model can be difficult. Take metal forming for example. The output is the shape of the formed part. The major

source of uncertainty is a result of springback in metals and this is caused by the variation in material property. We cannot simply separate the process model from the disturbance model because the process gain is a function of the material property and yet the variation is mainly on the material property. An accurate model for the example would be as shown in Figure 3.2, where the disturbance model is embedded into the process model. We call this the “varying gain” process model.

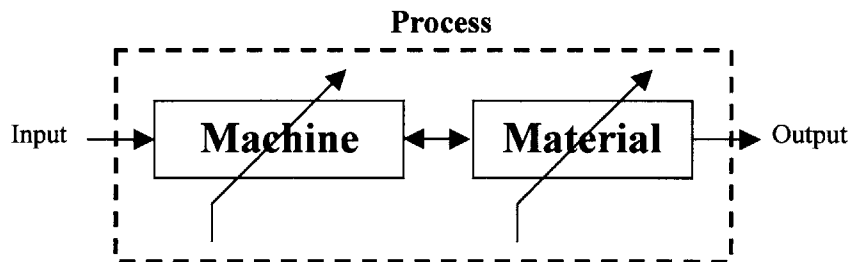


Figure 3.2: An appropriate process model

In mathematical terms, however, this model is difficult to analyze because it is not a linear stochastic system. So in CTC control, we will separate the disturbance model from the process. Our assumption is that all “in-process” transients are fully settled before the end of the cycle, meaning that the process dynamics does not exist in the process model. Dynamics are represented in a separate disturbance block. This disturbance is added to the output of a deterministic process model and can be as simple as a constant process gain. The disturbance model can be a random white-noise process or a combination of random and deterministic (step and ramp disturbances) components. This model is represented in Figure 3.3.

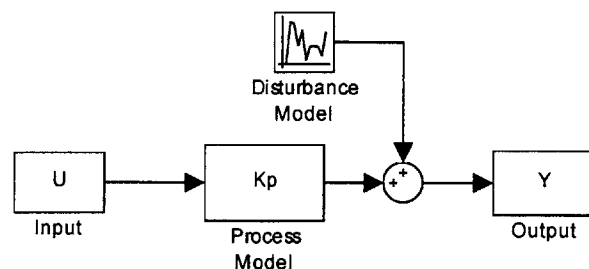


Figure 3.3: A simple additive disturbance model

One can see that the only stochastic input to the system is from the disturbance. The advantage of such a model is the ability to carry out conventional control system analysis separately from the stochastic analysis. This allows the use of discrete control tools in predicting disturbance rejection capability and steady state property of a system. Since most processes have a linear process gain, the additive disturbance model would produce an output similar to the varying gain process model.

The difference between the two models is evident when we close the feedback loop (the closed-loop analysis will be presented in the next section). With the varying gain process model, the varying process gain (K_p) makes the loop gain ($K_c \cdot K_p$) fluctuate. The closed-loop system behavior such as response time becomes difficult to predict. The additive model is physically reasonable for processes with small process gain variations.

3.1.2. Delay models

In CTC systems, there is an inherent delay of one cycle in the process model. As mentioned before, one can only use the output of the current cycle as the feedback for the next cycle. Nothing can be done to the current output after it is taken out of the machine. So the current output is a result of the input entered one cycle ago. A diagram of the process delay is shown in Figure 3.4 below.

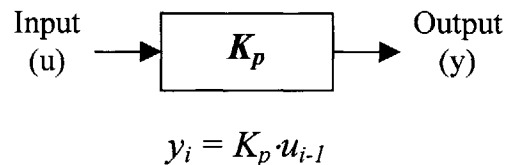


Figure 3.4: Pure process delay model

Source: Hardt [16]

In addition to process delays, there are also measurement delays. Measurements may not be quickly obtained so more delays can occur in the feedback loop. In SPC, for example, measurements are usually not used until after N cycles and only the average is used for feedback purposes. The average of the SPC measurement given in equation (3.1) shows an N -cycle delay:

$$(Average)_i = \frac{1}{N} \cdot \sum_{k=N \cdot (i-1)}^{N \cdot i} y_k \quad (3.1)$$

Other feedback filters include running average and exponentially weighted moving average.

3.2. Discrete Control System Analysis

3.2.1. Z-transform and analysis

As seen in the previous section, CTC control contains discrete time delay operators and they can be mathematically represented by difference equations. The pure process delay ($y_i = K_p \cdot u_{i-1}$), for example, is a first order ordinary difference equation. Detailed definitions and examples of difference equation can be referred to Mickens [17].

The z-transform is a mathematical operation that transforms discrete variables into functions of a continuous variable z. It facilitates greatly the analysis of difference equations. It does so by applying the following operation to a discrete sequence $\{x_n\}$:

$$X_n(z) = \sum_{k=0}^{\infty} X_k(z) \cdot z^{-k} \quad (3.2)$$

The sequence $\{x_n\}$ can be the output sequence of a discrete manufacturing process. The simplicity comes when we compare values in a sequence that are separated by n cycles, their relationship in z-domain is $U_{i-n}(Z) = U_i(z) \cdot z^{-n}$. For the pure process delay of one cycle shown in Figure 3.4 ($y_i = K_p \cdot u_{i-1}$), the z-transform becomes $Y(z) = K_p \cdot U(z) \cdot z^{-1}$.

For an EWMA measurement filter, the difference equation is $y_{i+1} = p \cdot y_i + p \cdot u_i$ (y_i and u_i are the output and input of the process and p is the weight for the EWMA function). The corresponding equation in z-domain is $z \cdot Y(z) = p \cdot Y(z) + p \cdot U(z)$. We can also obtain the transfer function

$$G(z) = \frac{Y(z)}{U(z)} = \frac{p}{z - p} \text{ for the EWMA filter.}$$

For an integral controller, we sum all the errors (e_i) from previous cycles. The difference equation becomes $y_{i+1} = y_i + e_{i+1}$ and the transfer function for the integral controller is

$$G(z) = \frac{Y(z)}{E(z)} = \frac{z}{z-1}.$$

Figure 3.5 shows a simple proportional control system with a one-cycle process delay. By tracing through all the components in the loop, we can obtain the following relationship between the disturbance and the output:

$$z \cdot Y(z) = z \cdot D(z) - K_c \cdot K_p \cdot Y(z) \quad (3.3)$$

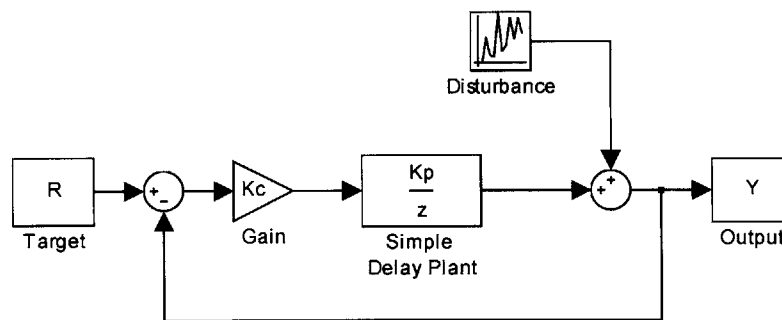


Figure 3.5: Control Block Diagram for proportional controller

From equation (3.3), we can arrange the $Y(z)$ together and divide by $D(z)$. We will get the disturbance transfer function of the closed-loop system:

$$G(z) = \frac{Y(z)}{D(z)} = \frac{z}{z - K_c \cdot K_p} \quad (3.4)$$

This transfer function is useful in analyzing a closed-loop system because it allows the prediction of important properties such as steady-state error and settling time that is presented in the next section. The term, $K_c \cdot K_p$, is the loop gain ⁴.

⁴ The loop gain is a product of the controller gain (K_c) and the process gain (K_p) and is used to interpret root locus diagrams. For the rest of the thesis, we will assume that K_p is unity because K_c is the only parameter that can be varied in designing a controller. The only gain that is mentioned in our root locus interpretation is K_c . It should be noted that in real processes, K_p is never one (for the experiments presented in chapters 5 and 6, K_p 's are manually adjusted to be one).

3.2.2. Adding Randomness to the system

Randomness can be added to the system through the disturbance model. One commonly used random variable is the Normal Identically Distributed and Independent (NIDI) distribution. This type of distribution has no correlation and is normally distributed.

Correlation can be added to the process by passing the NIDI distribution through a correlation filter. Figure 3.6 below shows a first order correlated disturbance. The correlation filter in this case is the same as an EWMA filter.

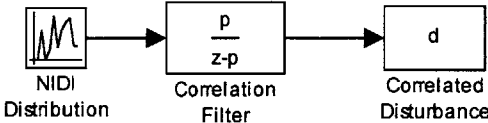


Figure 3.6: A first order correlated disturbance

3.3. Characterizing Cycle-to-Cycle Control Systems

Modeling CTC control systems as discrete control systems allows the use of conventional control tools that help study the behavior of the system. We present here some analytical tools from discrete control systems.

3.3.1. Root locus diagram in Z-plane

The root locus diagram displays the loci of the closed-loop system poles as the closed-loop gain increases. Plotting root locus diagram in the z-plane for discrete system is the same as plotting root locus diagram on a s-plane for continuous system. The only difference is in the interpretation of the plot. To show the difference, consider a closed-loop proportional control system with a process delay of unity. For a discrete system (see Figure 3.5 for schematics, K_p is assumed to be 1), the unit delay plant has a transfer function of $\frac{1}{z}$ and the open-loop transfer function is $\frac{K_c}{z}$. We have the

open-loop pole at the origin and the root locus goes to negative infinity along the real axis. For a

continuous system, the delay plant with a time constant of one has a transfer function of $\frac{1}{s+1}$ and the open-loop transfer function is $\frac{K_c}{s+1}$. We have the open-loop pole at -1 and the root locus goes to negative infinity along the real axis. Figure 3.7 below shows the root locus plots for both the continuous system and the discrete system. As controller gain increases, the closed-loop pole moves towards the left to negative infinity. The solid dot on the plots shows the closed-loop pole when K_c equals 0.5. The region of stability is indicated as the part of the plot that contains grid lines. On the s-plane for continuous systems, the stability region is to the left of the imaginary axis and the response is non-oscillatory if closed-loop poles are on the real axis. The continuous system is stable for all $K_c > 0$. For the z-plane, it is stable when the closed-loop pole is within the unit circle; closed-loop poles on the positive real axis are non-oscillatory. The discrete proportional control system is stable for $0 < K_c < 1$. (Refer to Van De Vegte [18] for complete instructions on plotting root locus diagrams for both discrete and continuous control systems.)

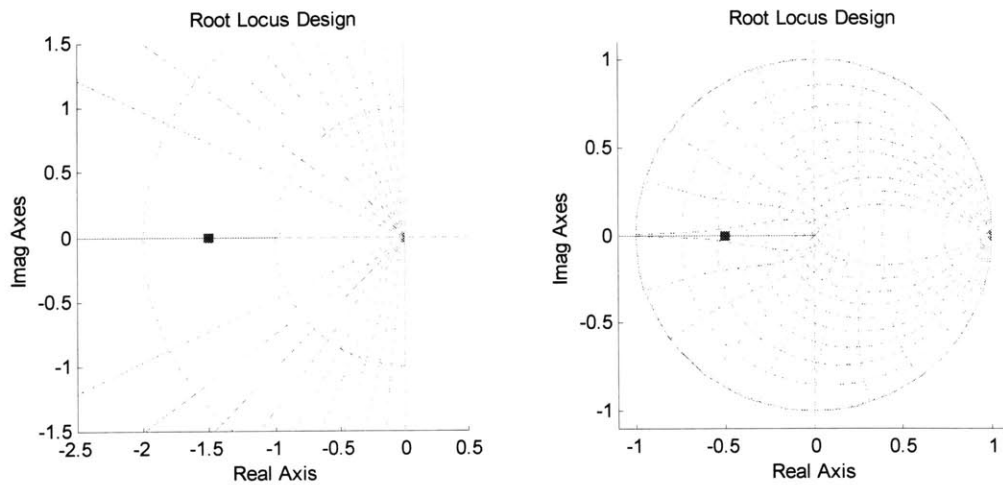


Figure 3.7: Comparison of root locus plot in s-plane (left) and z-plane (right)

3.3.2. Steady-state error analysis

Steady-state error can be caused by step or ramp disturbances. It represents the inability of the control system to adjust input fast enough to meet the target. Steady-state error can be obtained using the final value theorem:

$$e_{ss} = \lim_{z \rightarrow 1} (z-1) \cdot E(z) \quad (3.5)$$

For a proportional control system in Figure 3.5, the output equation is (assume $K_p = 1$):

$$Y(z) = \left(\frac{z}{z + K_c} \right) \cdot D(z) \quad (3.6)$$

The error is the difference between target and output:

$$E(z) = - \left(\frac{z}{z + K_c} \right) \cdot D(z) \quad (3.7)$$

For a step disturbance that has a step size of C , the transfer function is $C \cdot \frac{z}{z-1}$, the steady-state error is:

$$e_{ss} = \lim_{z \rightarrow 1} \left\{ -C \cdot (z-1) \cdot \frac{z}{z + K_c} \cdot \frac{z}{z-1} \right\} = -\frac{C}{1 + K_c} \quad (3.8)$$

From equation (3.8), we can see that there is always a steady-state error for step disturbance in a proportional control system. This has the same result as the continuous time analysis in s-domain.

If we use an integral control system, we will have an extra $\frac{z}{z-1}$ term in the formulation and the steady-state error for a step disturbance is completely removed.

For a ramp disturbance that has a slope of m , its transfer function is $m \cdot \left(\frac{z}{z-1} \right)^2$. The steady-state error becomes:

$$e_{ss} = \lim_{z \rightarrow 1} \left\{ -m \cdot (z-1) \cdot \frac{z}{z + K_c} \cdot \left(\frac{z}{z-1} \right)^2 \right\} = \infty \quad (3.9)$$

This result is same as in continuous time case, and the P-controller is not able to keep up with a ramp disturbance. The steady-state error will become finite if an integral controller is used:

$$e_{ss} = \lim_{z \rightarrow 1} \left\{ -m \cdot (z-1) \cdot \frac{z-1}{z-1 + K_c} \cdot \left(\frac{z}{z-1} \right)^2 \right\} = -\frac{m}{K_c} \quad (3.10)$$

3.3.3. Settling time analysis

The root locus diagram can also tell the speed of response of a system. On the z-plane, the closer the closed-loop poles are to the origin, the faster the speed of response. From the root locus diagram on a z-plane, the 5% settling time can be calculated using the distance from the closed-loop pole to the origin, r , according to the following equation:

$$t_s|_{5\%} = \frac{3}{|\ln(r)|} \quad (3.11)$$

Simple limiting cases can verify the equation. When $r = 0$, the closed-loop pole is at the origin. The system is infinitely fast and so the settling time is zero. When $r = 1$, the closed-loop pole is on the unit circle. The system is marginally stable and thus never settles.

3.4. Analysis of Cycle-to-Cycle Control Systems

Using the mathematical tools presented above, we can analyze CTC systems with relative ease. The following are two examples of CTC control system analysis that include stochastic analysis. One is a proportional control system and the other an integral control system. The analytical results are also compared to Matlab simulation results for verification. The goal of the following analyses is to demonstrate variance propagation in the closed-loop system.

3.4.1. Proportional control with direct feedback

The first system to be considered is the closed-loop proportional control system given in Figure 3.5. This is the simplest CTC system and we expect that the output variance (σ_y^2) to be greater than the variance of the injected disturbance (σ^2) when the sequence of disturbances, d_i 's, are independent and uncorrelated. Intuitively, if there is no correlation between subsequent outputs, there is no useful information in the feedback link that will help improve the process. As mentioned before, we will assume that the process gain (K_p) is one to simplify the analysis. By tracing the closed-loop system in z-domain, we can obtain the following equation:

$$z \cdot Y(z) = z \cdot D(z) - K_c \cdot Y(z) \quad (3.12)$$

The root locus plot of the system is shown in Figure 3.7 (the plot on the right) and the stability region is $K_c < 1$. Taking the inverse z-transform of equation (3.12), we can obtain a first order difference equation of the system:

$$y_{n+1} = d_{n+1} - K_c \cdot y_n \quad (3.13)$$

We can solve this recursive difference equation by substituting $y_n = d_n - K_c \cdot y_{n-1}$ and $y_{n-1} = d_{n-1} - K_c \cdot y_{n-2}$ etc into the equation, and we will get the following series ⁵:

$$y_{n+1} = \sum_{i=0}^n [(-K_c)^i \cdot d_{n-i+1}] + (-K_c)^{n+1} \cdot y_0 \quad (3.14)$$

From equation (3.14), we can assume that y_0 is deterministic and does not contribute to the variance analysis. So given a normally distributed disturbance sequence with the mean of zero and variance σ^2 , $d_i \sim (0, \sigma^2)$, we can estimate the variance of the next output (y_{n+1}) using the linear variance

analysis formula given by Rice [20]. It states that, $Var\left(\sum_{i=1}^n b_i \cdot X_i\right) = \sum_{i=0}^n \sum_{j=0}^n [b_i \cdot b_j \cdot Cov(X_i, X_j)]$.

We can obtain the variance for y_{n+1} as:

$$\sigma_{y_{n+1}}^2 = \sum_{i=0}^n \sum_{j=0}^n [(-K_c)^i \cdot (-K_c)^j \cdot Cov(d_i, d_j)] \quad (3.15)$$

Equation (3.14) can be expressed as compact matrix products:

$$y_{n+1} = K^T \cdot D + (-K_c)^{n+1} \cdot y_0 \quad (3.16)$$

where, $K = \begin{bmatrix} 1 \\ -K_c \\ \vdots \\ (-K_c)^n \end{bmatrix}$ is a column matrix that contains the coefficients of summation and

$D = \begin{bmatrix} d_n \\ d_{n-1} \\ \vdots \\ d_0 \end{bmatrix}$ is the sequence of discrete random numbers, also expressed as a column matrix.

⁵ A similar result for a first order difference equation is also given in Boyce and DiPrima [19].

So using equation (3.16), we can express the variance of the output also in matrix form as follows:

$$\begin{aligned} \sigma_{y_{n+1}}^2 & \quad (3.17) \\ &= K^T \cdot \sum_{y_{n+1}} \cdot K \\ &= \begin{bmatrix} 1 & -K_c & \cdots & (-K_c)^n \end{bmatrix} \cdot \begin{bmatrix} \text{Cov}(d_1, d_1) & \text{Cov}(d_1, d_2) & \cdots & \text{Cov}(d_1, d_n) \\ \text{Cov}(d_2, d_1) & \text{Cov}(d_2, d_2) & \ddots & \vdots \\ \vdots & \ddots & \ddots & \vdots \\ \text{Cov}(d_n, d_1) & \cdots & \cdots & \text{Cov}(d_n, d_n) \end{bmatrix} \cdot \begin{bmatrix} 1 \\ -K_c \\ \vdots \\ (-K_c)^n \end{bmatrix} \end{aligned}$$

where $\sum_{y_{n+1}}$ is the auto-covariance matrix of the discrete disturbance signal matrix D .

$\sigma_{y_{n+1}}^2$ is positive by definition, which means that the matrix $\sum_{y_{n+1}}$ must be positive definite⁶.

When d_i 's are NIDI

If $d_i \sim (0, \sigma^2)$ is a Normal Identically Distributed Independent (NIDI) process, then

$$\text{Cov}(d_i, d_j) = \begin{cases} \sigma^2 & ; \text{if } i = j \\ 0 & ; \text{if } i \neq j \end{cases}$$

This means that the value of the numbers in the sequence is independent of any other numbers in the sequence. Equation (3.15) can then be reduced to:

$$\sigma_{y_{n+1}}^2 = \sum_{i=0}^n [(-K_c)^{2i} \cdot \sigma^2] = \sigma^2 \cdot \sum_{i=0}^n (K_c^2)^i \quad (3.18)$$

The stability region of the system is $K_c < 1$. So equation (3.18) can be simplified as a finite sum geometric series with parameter $K_c^2 < 1$. The simplified expression is as follows:

$$\sigma_{y_n}^2 = \sigma^2 \cdot \left[\frac{1 - K_c^{2n}}{1 - K_c^2} \right] \quad (3.19)$$

⁶ An analogy can be made with its scalar counterpart: if $Y = a \cdot X$ where $X \sim (0, \sigma_x^2)$, then $\sigma_y^2 = a^2 \cdot \sigma_x^2 = a \cdot \sigma_x^2 \cdot a$. A definition of positive definiteness is given in Rice [20].

Several observations can be made from equation (3.19):

1. As K_c increases, $\sigma_{y_{n+1}}^2$ also increases. Intuitively, a larger K_c feeds back more useless information (because d_i 's are independent) for control that would increase the dispersion of the output.
2. The value of $\sigma_{y_{n+1}}^2$ is always above one, which indicates that the feedback loop always increases the variance of the output, regardless of the control gain.
3. The value of $\sigma_{y_{n+1}}^2$ depends on the time step, n , as well. This means there is a transient behavior before a steady state $\sigma_{y_{n+1}}^2$ is obtained.
4. The value $\sigma_{y_{n+1}}^2$ (a function of n) converges very quickly to a stable value as the sample number n increases. For systems with small control gain K_c , the value $\sigma_{y_{n+1}}^2$ often converges in less than 5 samples.
5. The increase of output variance will decrease the process capability (C_{pk}), hence decreasing the quality of the process.
6. The variance amplification at lower gains is much gentler than at higher gains. We can still use CTC with small to medium gain to improve the process by speeding up the response time and reducing the steady-state error.

Figure 3.8 compares the Matlab simulation result versus the analytical result using equation (3.19):

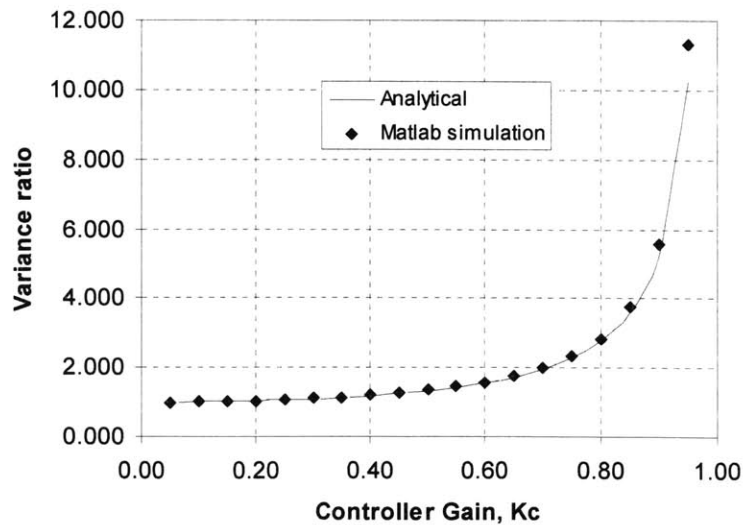


Figure 3.8: Matlab verification of the analytical result for a P-controller with NIDI disturbance

Figure 3.9 shows the results of Matlab simulation illustrating the time dependent transient effect of variance amplification. The data points obtained from Matlab simulation are the ensemble averages of 500,000 identical processes running in parallel ⁷.

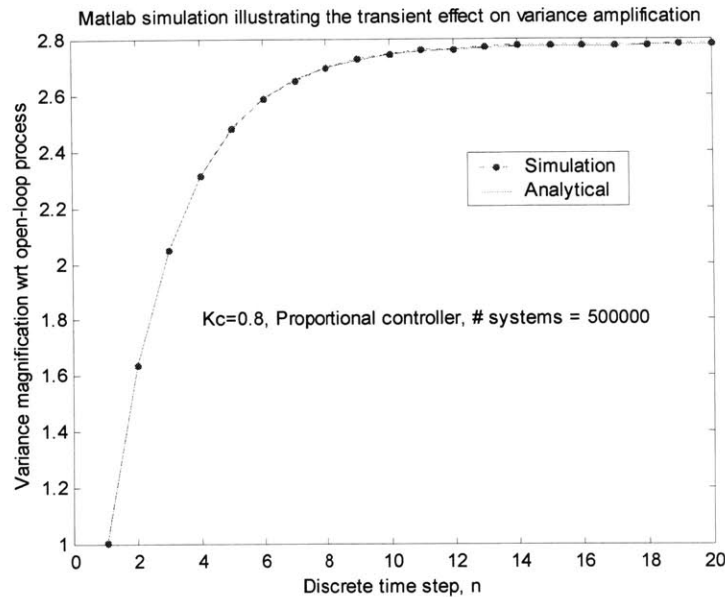


Figure 3.9: Time dependence of variance amplification for P-controller

When d_i 's are correlated

The time series analysis of correlated disturbance is found to be very tedious. Frequency domain analysis of correlated systems can be referred to work by Novak [22]. Matlab simulation result of the variance ratio is given in Figure 3.10. It shows clear variance reduction for the first order correlated disturbance shown in Figure 3.6. The correlation parameter, p , is 0.8 for the simulation.

⁷ If we only have one random process running, we cannot obtain the variance for a single time frame of the process because we only have one data point. In order to obtain variance statistics for the process at a single time frame, we need to perform the identical process many times.

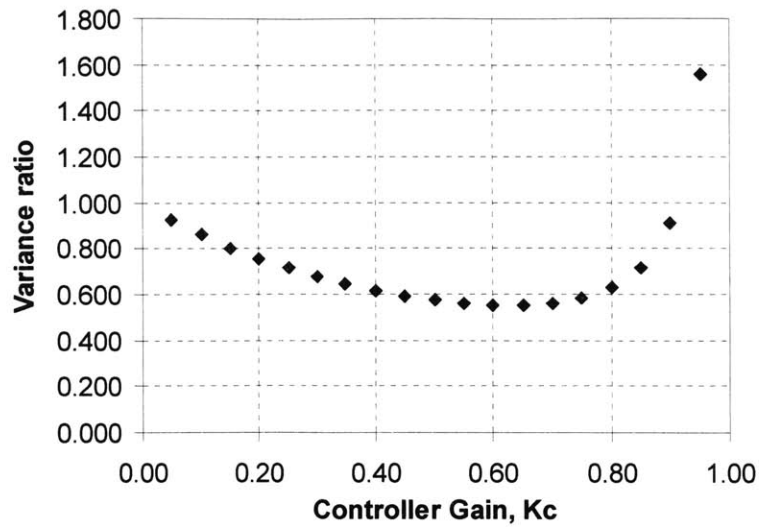


Figure 3.10: Matlab simulation result showing variance reduction for a P-controller

3.4.2. Integral control with direct feedback

The proportional controller presented in the previous section is simple to analyze but they cannot remove steady-state errors for step disturbances. This means that a closed-loop system using P-controller is not able to keep the process constantly at the desired target. An integral controller is needed to remove steady-state error from a step disturbance.

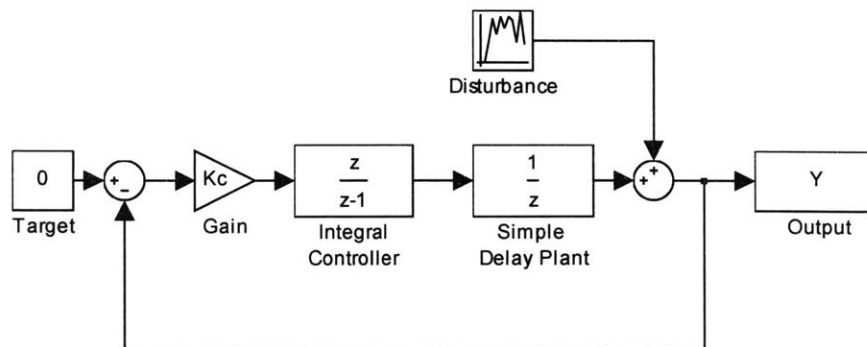


Figure 3.11: Control Block Diagram for Integral Controller

For an integral feedback control system illustrated in Figure 3.11, the transfer function is as follows:

$$Y = D + (-Y) \cdot K_c \cdot \left(\frac{z}{z-1} \right) \cdot \frac{1}{z} \quad (3.20)$$

$$G(z) = \frac{Y}{D} = \frac{z-1}{z-(1-K_c)}$$

The root locus plot is shown in Figure 3.12 and the stability region is $0 \leq K_c \leq 2$.

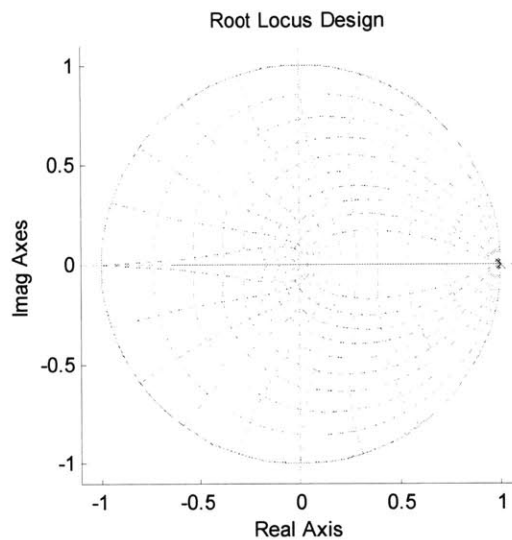


Figure 3.12: Root locus plot for a closed-loop integral control system

From the transfer function in equation (3.20), we can obtain a recursive difference equation for the system.

$$y_{n+1} - (1 - K_c) \cdot y_n = d_{n+1} - d_n \quad (3.21)$$

One can see that this equation is similar to the EWMA controller equation used commonly in RbR control.

One simple way to solve this recursive difference equation is to obtain the solution for both the homogeneous and particular equation. For the homogeneous equation, $y_{n+1} - (1 - K_c) \cdot y_n = 0$, the solution is obtained from Mickens [17] to be $y_n = y_o \cdot (1 - K_c)^n$. We can get the particular

solution by comparing to the solution we obtain for the proportional controller. The particular solution for a proportional controller system $y_{n+1} - (1 - K_c) \cdot y_n = d_n$ is $\sum_{i=1}^{n-1} [d_i \cdot (1 - K_c)^{n-i-1}]$.

Owing to the linear nature of the system, we can superimpose the solutions of the particular solution and the homogeneous solution. This gives us the complete solution for an integral controller system:

$$\begin{aligned} y_n &= y_1 \cdot (1 - K_c)^n - \sum_{i=1}^{n-1} [d_i \cdot (1 - K_c)^{n-i-1}] + \sum_{i=1}^n [d_i \cdot (1 - K_c)^{n-i}] \\ &= y_1 \cdot (1 - K_c)^n + d_n + (-K_c) \cdot \left[\sum_{i=1}^{n-1} d_i \cdot (1 - K_c)^{n-i-1} \right] \end{aligned} \quad (3.22)$$

When d_i 's are NIDI

When the disturbance sequence is uncorrelated, we can use the same method used for the proportional controller in the previous section. By substituting the stochastic properties of the disturbance, $d_i \sim (0, \sigma^2)$, into equation (3.22), we can obtain the stochastic properties of the output, y_n :

$$\begin{aligned} \sigma_{y_n}^2 &= \sigma^2 + (-K_c)^2 \cdot \left[\sum_{i=1}^{n-1} \sigma^2 \cdot (1 - K_c)^{2(n-i-1)} \right] \\ &= \sigma^2 \cdot \left\{ 1 + (-K_c)^2 \cdot \left[\sum_{i=1}^{n-1} (1 - K_c)^{2(n-i-1)} \right] \right\} \\ &= \sigma^2 \cdot \left\{ 1 + (-K_c)^2 \cdot \frac{1 - (1 - K_c)^{2(n-1)}}{K_c \cdot (2 - K_c)} \right\} \\ &= \sigma^2 \cdot \left\{ 1 + K_c \cdot \frac{1 - (1 - K_c)^{2(n-1)}}{2 - K_c} \right\} \end{aligned} \quad (3.23)$$

So the ratio between the variance of the disturbance and the variance of the output is:

$$\frac{\sigma_{y_n}^2}{\sigma^2} = 1 + K_c \cdot \frac{1 - (1 - K_c)^{2(n-1)}}{2 - K_c} \quad (3.24)$$

Since the stability region is $0 \leq K_c \leq 2$, solutions only exist for equation (3.24) within this limit.

Figure 3.13 summarizes the Matlab simulation result versus the analytical result using equation (3.24). Analytical results by Novak [22] in the frequency domain is included to provide a comparison with the time dependent result (for $n = 20$).

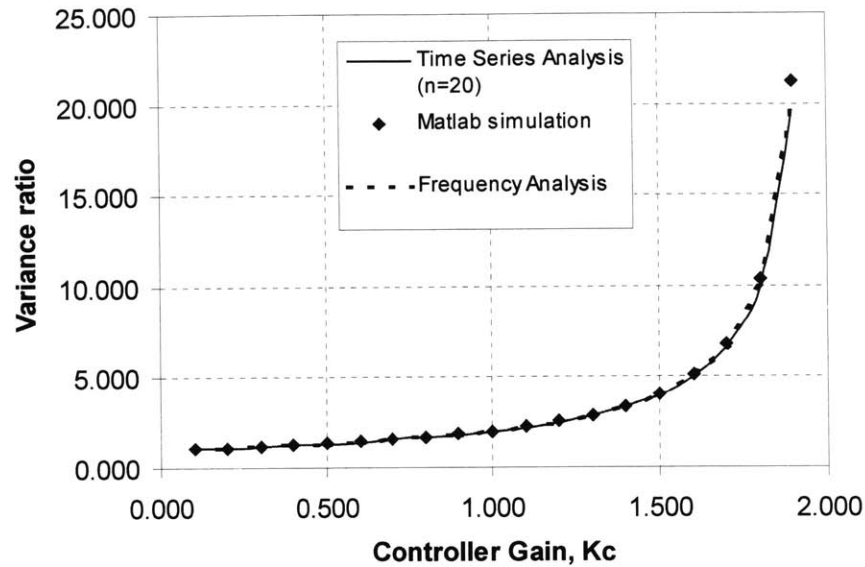


Figure 3.13: Matlab verification of the analytical result for I- controller with NIDI disturbance

As with the P-controller, the I-controller also results in variance amplification on the output. Both the P-controller and the I-controller have highly nonlinear variance amplification: the variance amplification is very moderate at small gains and then increases abruptly at higher gain. For example, as K_c increases from 0 to 1, the variance ratio only increases by a factor of two. If we have a large step disturbance (say more than twice the open-loop variance), using closed-loop control can eliminate the step disturbance completely and thus making the process better. So depending on the circumstances, we can use CTC control with small gains to improve process capability even if closed-loop control means variance amplification for uncorrelated processes. In the next chapter, we will combine the different factors affecting the quality of a process and come up with an analytical optimum for CTC systems.

Figure 3.14 shows the Matlab simulation of time dependence of the variance ratio at different feedback gains (K_c).

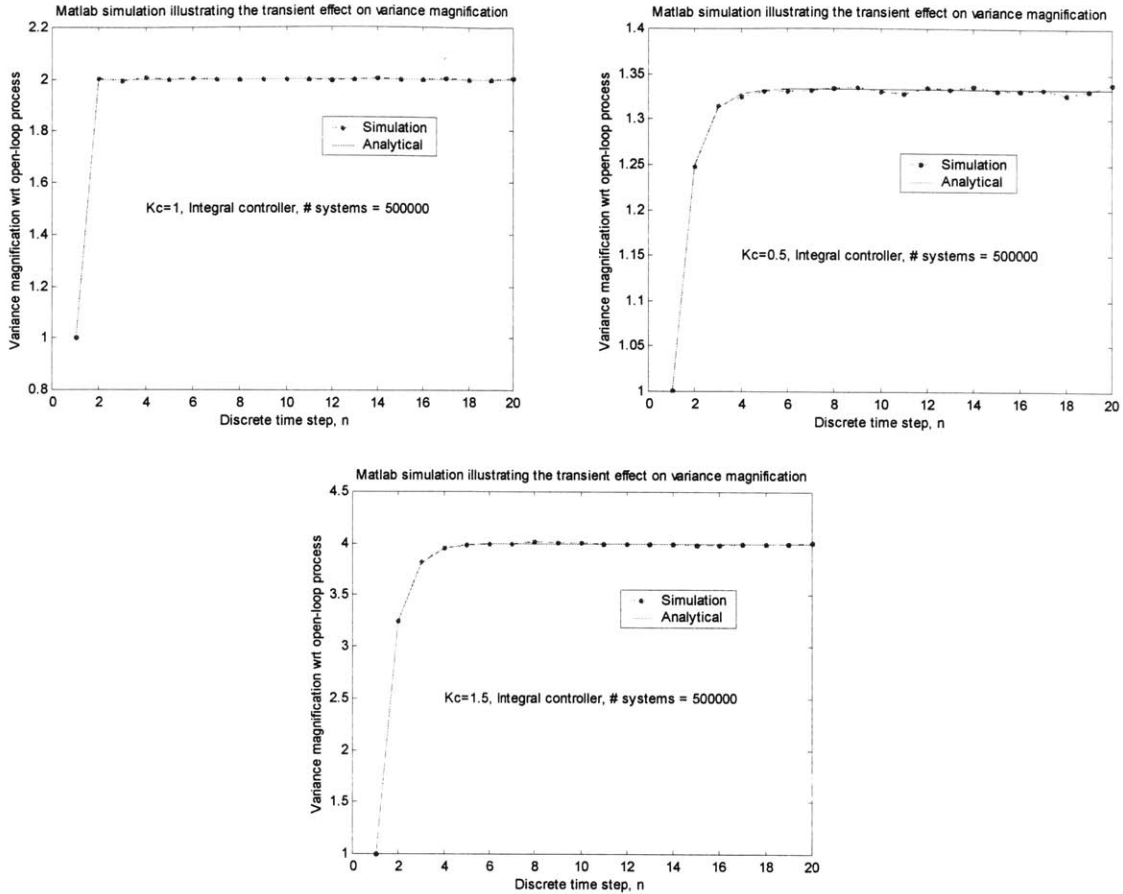


Figure 3.14: Time dependence of variance amplification for I-controller $K_c = 1$ (upper left), $K_c = 0.5$ (upper right), $K_c = 1.5$ (bottom)

When d_i 's are correlated

The correlated disturbance analysis is very tedious for time series method. The paper by Box & Kramer [4] presented in chapter 2 shows the result of an optimal PI-controller on a correlated process, and it shows properties of variance reduction. Novak [22] also showed variance reduction with frequency analysis. Both Box & Luceño [21] and Novak [22] contain the theoretical analysis to the problem.

Figure 3.15 shows a comparison of Matlab simulation results and frequency analysis results showing variance reduction. The correlation filter is a first order filter with $p=0.8$. Compared to the

simulation results of P-controller, the I-controller gives better variance reduction and also a bigger range of stable gain.

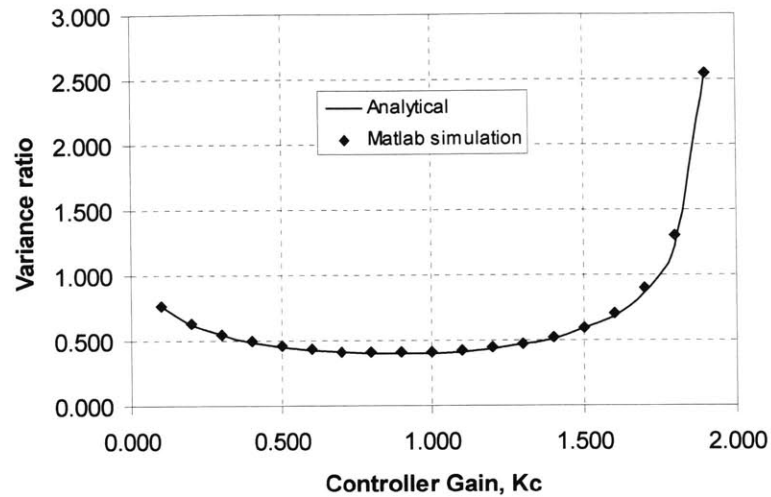


Figure 3.15: Matlab and frequency analysis results showing variance reduction for I-controller

3.5. Analysis Summary

In this chapter, we presented a simple linear process model with additive disturbances. The elegance of the model is to allow separate analysis of the deterministic and stochastic components of the model.

In the deterministic analysis, we showed the ability of the I-controller to remove steady-state error. We can also speed up the response time by increasing controller gain. From a quality point of view, eliminating the steady-state error and improving speed of response both result in better process capability (C_{pk}).

In the stochastic analysis, we showed both the amplification and reduction of variance. For uncorrelated processes, increasing controller gain would increase variance, thus decrease process capability. For correlated processes, on the other hand, we can have a range of controller gain that results in variance reduction.

Deterministic analysis demands higher K_c for better disturbance rejection and faster response time. Stochastic analysis, on the other hand, asks for lower K_c to avoid large variance amplification. This tension sets up an optimization problem for designing the optimal controller for CTC control system that will be presented in the next chapter.

Chapter 4: Design of Minimum Quality Loss Controller

4.1. Introduction to Controller Design

Various graphical and analytical tools have been developed to aid the design of control systems. As described in the previous chapter, we can use root locus diagrams to observe the change in system performance. In particular, we can learn about the speed of response as the controller gain (K_c) varies. Using mathematical tools such as the final value theorem, one can also obtain the relationship between controller gain and the steady-state error, e_{ss} . In state-space represented control systems, linear compensators and observers are used to shape systems dynamics [24]. For stochastic systems, Kalman filters and adaptive controllers are used to dynamically and precisely estimate the states or parameters of the system [24].

In this chapter, we first present various statistical methods to measure performance of manufacturing processes. Various techniques from the different sources described above are considered. We then develop a minimum quality loss method of designing an optimal feedback control system that would optimize the performance of a CTC system. Finally, we will present an analytical example for designing controllers under step disturbance situations for a discrete manufacturing process.

4.2. Performance Measuring Techniques

In manufacturing, the control objectives are no different than in other control systems. The primary goal is to constantly achieve (or stay at) the desired target with as little variation as possible; secondary concerns often include the speed of response of the system and the cost of implementation. As in designing any feedback control systems, the primary concerns for CTC systems are the stability and steady-state error of the system. It is not until the stability requirement is achieved that other system objectives can be met.

In manufacturing control, however, the stochastic property of the system has more of an effect than other applications of feedback control. The main reason for this is that manufacturing processes are generally considered stationary. We tend to model the output with mean value that should ideally be at the target value. Sampled data points are usually distributed normally around the mean. And process disturbances, such as material shifts, tool wear, temperature drifts, occur slowly and may not be observable unless statistical filtering is used. In other words, the natural random variation of the process (we characterize this as ideal white noise) is large with respect to the magnitude of disturbances that might be present.

As we learned in the stochastic analysis of discrete control systems, variance amplification of a white noise output disturbance increases as K_c increases. In most other feedback control applications, the random component of the disturbance is usually very small in magnitude and the effect of variance amplification would not be significant. So their most important goal is to speed up the system response. In manufacturing, our goal is to reduce the steady-state error without significantly increasing the variance.

4.2.1. Performance metrics used in Manufacturing Quality Control

One widely used performance parameter in manufacturing is the process capability index, C_{pk} . It is defined mathematically as follows:

$$C_{pk} = \min\left(\frac{USL - \mu}{3\sigma}, \frac{\mu - LSL}{3\sigma}\right) \quad (4.1)$$

where μ and σ are the mean and standard deviation of the process, and USL and LSL are the specification limits. The goal for the process designer to optimize a process is to maximize C_{pk} .

Another less widely used performance measure is the expected quality loss function, which is commonly defined as a quadratic cost function. Let the quality loss function be $L = (x - T)^2$, where x is the output of the process that contains a deterministic component and a stochastic component, and T is the desired target of the process. Taking the expectation of L , we have:

$$\begin{aligned}
 E[L] &= E[(x - T)^2] \\
 &= E[x^2] - 2 \cdot T \cdot E[x] + T^2 \\
 &= \{E[x^2] - E[x]^2\} + \{E[x]^2 - 2 \cdot T \cdot E[x] + T^2\} \\
 &= Var[x] + \{E[x] - T\}^2
 \end{aligned} \tag{4.2}$$

One can see that this performance measure penalizes the high variance of the process and large deviation from the target. The goal of the process designer is to minimize the expected quality loss, $E[L]$. This is the most direct measure of cost of bad quality, but coming up with a suitable quality loss function can be difficult.

The aforementioned techniques are designed to quantitatively describe the performance of an open-loop process, to monitor whether the system is behaving as desired and to determine whether process improvements have been made. These techniques cannot be applied directly to optimize a closed-loop systems because they cannot capture the dynamics in a closed-loop system.

4.3. Cycle-to-Cycle feedback control scheme and its design criteria

In manufacturing processes, the most significant factors are the overall production rate of the process and the quality of the product. In order to analyze the benefits of CTC feedback control, an appropriate performance-measuring scheme needs to be devised. This performance metric has to combine the needs of statistical quality control and discrete feedback control. The different goals of statistical process control and feedback control are listed as follows:

Quality measure of process control

1. Minimize the number or fraction of bad products manufactured ⁸.

⁸ The fraction of bad parts produced is directly related to the process capability, C_{pk} . The process capability gives the range of the specification limits relative to the process variation. If the distribution of a process is known (e.g. NIDI), the fraction of bad parts can be calculated directly.

2. Maximize the C_{pk} in the shortest time.
3. Maximize the overall C_{pk} over the entire production run of a given product.
4. Minimize the overall cost of production.

Design criteria for feedback control

1. Improve speed of response
2. Rejection and reduction of variance or disturbance
3. Minimize steady state error on the process

4.3.1. Performance Metric of Cycle-to-Cycle feedback controller

For CTC feedback control, we can combine the design objectives from both quality and controller performance. The quality of a process can be characterized by the parameter C_{pk} as described in equation (4.1).

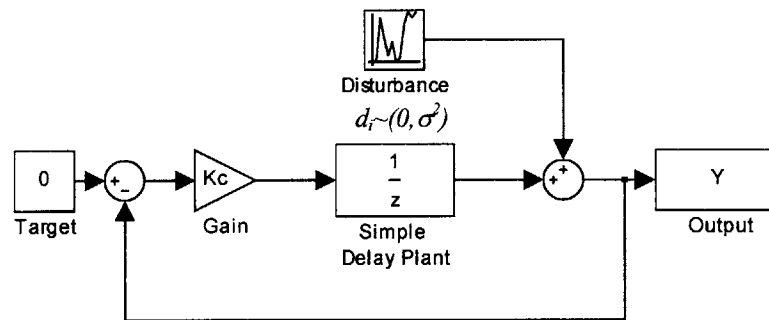


Figure 4.1: Discrete-time feedback implementation of a P-controller with random disturbance

As presented in the previous chapter, settling time and steady-state error can characterize the controller performance:

$$t_s|_{5\%} = \frac{3}{\ln|r|} \quad (4.3)$$

$$e_{ss}|_{step\ disturbance} = \frac{1}{1 + K_c} \quad (4.4)$$

where r is the distance of the closed-loop pole from the origin on a root-locus plot on z-plane. K_c is the gain of the controller. For the proportional controller shown in Figure 4.1, $r = K_c$.

The variance of the output, assuming a NIDI disturbance that has a mean of zero and standard deviation of σ^2 , is a function of K_c as proven in the previous chapter:

$$\sigma_y^2 = \sigma^2 \cdot \left[\frac{1}{1 - K_c^2} \right] \quad (4.5)$$

By combining and weighing the effect of the three parameters, we can obtain a performance metric that can be used to describe a CTC control system. Figure 4.2 below shows how the three parameters vary at different gains. Since the steady-state error decreases with increasing gain and the other two parameters increase with increasing K_c , an optimal performance can be reached.

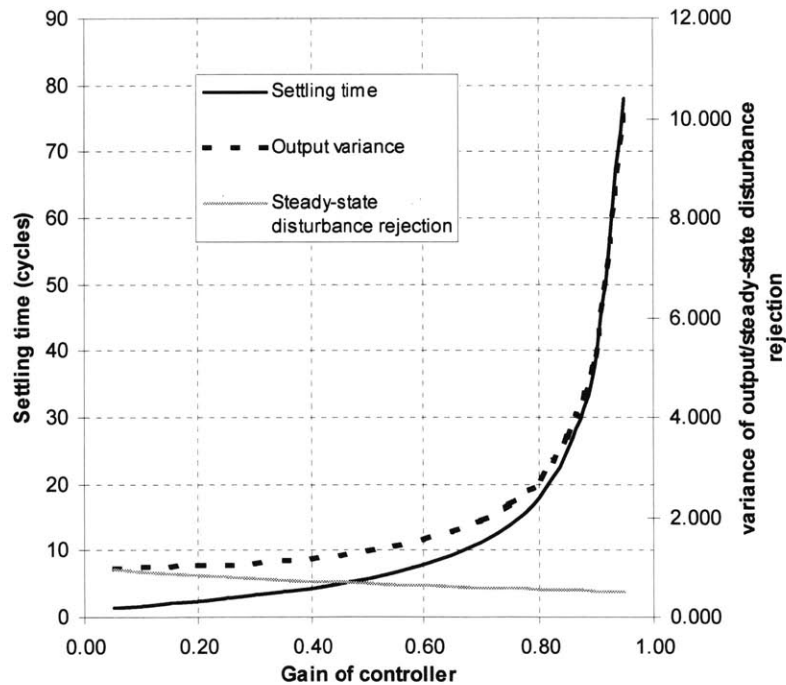


Figure 4.2: Variation of performance parameters for a P-controller with random disturbance

Combining the contributions of all performance measuring parameters, we can come up with the following unified performance index:

$$V(K_c) = \sum_{\text{all intervals}} (\text{Quality Loss}) \quad (4.6)$$

where the quality loss is evaluated instantaneously for each production interval.

Observations:

1. The index is a function of controller gain (K_c). The optimal controller design would give a value of K_c that has the smallest V .
2. Different values of V would be obtained for difference types of disturbances, so a controller is only optimal for a particular type of disturbance.
3. By considering the quality loss contribution for each cycle, we can better capture the transient effect of a closed-loop system ⁹.

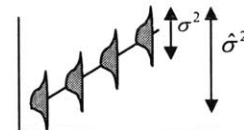
4.4. Optimal Controller Design for Cycle-to-Cycle Systems

As we learned from the discrete system analysis, closed-loop control of a system with an additive white noise output disturbance would only increase the output variance. However, we also know from discrete feedback control theory that increasing the feedback gain, K_c , will help reduce the steady-state error and system response time when a disturbance is injected. We can see that as K_c changes, an optimal point can be reached in reducing error and increasing variance. By collating all performance issues, we can come up with a simple minimum mean square error/quality loss performance index (V) for closed-loop control system that is somewhat similar to the quality loss function.

$$V = \frac{1}{N} \cdot \sum_{i=1}^N [e(i)^2] \quad (4.7)$$

where $e(i)$ is the error from the desired target for cycle i and N is the number of cycles in a manufacturing run. Because of the linear property of the system, the error $e(i)$ can be dissected into

⁹ For a process that is subjected to a ramp disturbance, for example, the sample variance ($\hat{\sigma}^2$), which is averaged over time, cannot distinguish the transient behavior from the steady-state behavior. The effect of the moving mean value in a ramp disturbance will be included in the sample variance. The calculated sample variance will, therefore, be much larger than the true process variance (σ^2).



two components: the deterministic error resulted from the deterministic component of the disturbances such as step or drift disturbances, and the stochastic error. Using the additive property of variances, equation (4.7) can be re-written as follow:

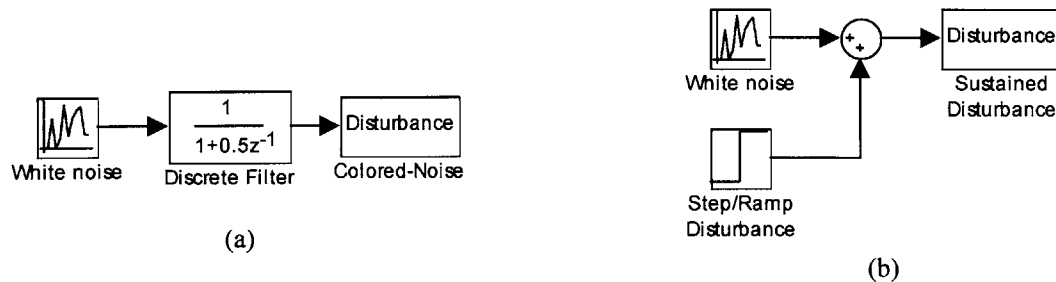
$$V = \frac{1}{N} \cdot \sum_{i=1}^N [d(i)^2 + n(i)^2] \quad (4.8)$$

where $d(i)$ is the deterministic component of the error and $n(i)$ is the stochastic (white noise) component of the error.

The key difference between V and $E[L]$ is that $E[L]$ only gives the expected value for a steady-state cost function while V tries to capture the dynamic behavior of the process that is caused by feedback control actions.

4.5. Step disturbance example

From the modeling of process outputs, we learned that process disturbances come in all sorts of shapes and forms. But from an analytical point of view, process disturbances can be categorized into two types: ‘colored-noise’ (white noise through a linear filter), and ‘sustained disturbance’ (a summation of white noise and deterministic disturbances). The block diagram illustration of the two types of disturbances is shown in Figure 4.3.



**Figure 4.3: The two types of disturbances:
a) Colored-Noise, b) White Noise added to a deterministic disturbance**

Research work on colored-noise disturbance model has been done by Box [21] (in the time domain) to obtain an optimal gain K_c that would give the minimum output variance. The optimization criterion for a colored-noise process is simply to minimize variance because the

output of a colored-noise process has a mean of zero (i.e. the output is wandering around the target). For the deterministic disturbance that is added to a white noise component, more variables (in addition to K_c) need to be considered for optimization. Simply minimizing the variance about the average output is not sufficient, as the average of the output can shift from the target as well. The performance index needs to take into consideration the mean being off target as well. The performance metric (V) achieves this goal by measuring the total quality loss. Some comments about the performance index when applied to step disturbance are as follows:

1. Both $d(i)$ and $n(i)$ are functions of feedback gain (K_c). K_c changes the transient behavior of the system and thus changes the error attributed to $d(i)$. K_c also changes the steady state value of the output caused by $d(i)$.
2. The length of the manufacturing run, N , affects the degree of importance of the transient. The longer the length N , the more time we have to bring the process to target without magnifying the white noise component. The speed of response becomes less important to the overall performance and a smaller K_c can be used.
3. The magnitude of the deterministic disturbance with respect to the white noise also affects the calculation of performance index (V). We can see that if the white noise component is significantly smaller than the magnitude of a step disturbance, a larger K_c value should be used because the need to bring the output to target quickly out-weights the need to reduce the magnification effect on the white noise.

An integral controller on a process with a step disturbance is used as an example to illustrate the remarks stated above. A discrete control system block diagram is shown in Figure 4.4.

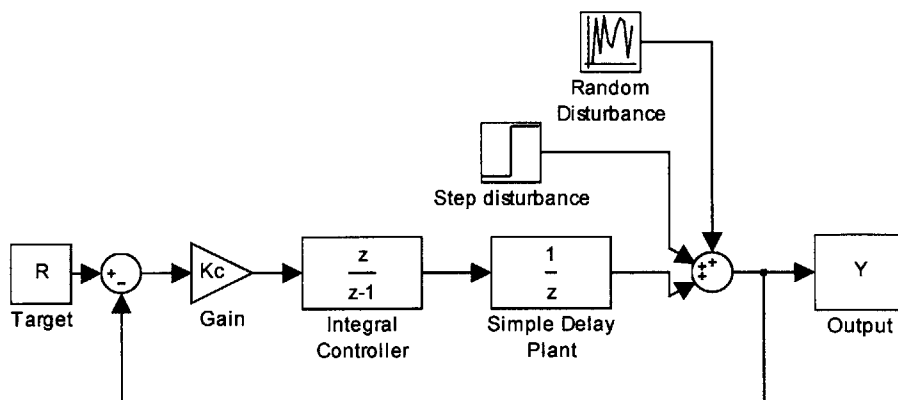


Figure 4.4: Block diagram of a feedback control system with an I-controller on a shifted process

Since the system illustrated above is linear, we can separate the two components of V for easier analysis.

$$V = \frac{1}{N} \cdot \sum_{i=1}^N n(i)^2 + \frac{1}{N} \cdot \sum_{i=1}^N d(i)^2 \quad (4.9)$$

We can see that the first term in equation (4.9) is the error component caused by the white noise and the second term is the error component caused by the step disturbance

In the previous chapter, we proved that the white noise component is amplified when closed-loop feedback control is used and the expression for $n(i)$ as a function of K_c and production run length (N):

$$n(i)^2 = \left(1 + K_c \cdot \frac{1 - (1 - K_c)^{2(N-1)}}{2 - K_c} \right) \cdot \sigma^2 \quad (4.10)$$

where σ^2 is the variance of the white noise disturbance and can be measured in a real manufacturing process by performing an open-loop production run¹⁰.

Also, using time series analysis of the response of the integral-controlled system to a step input, $d(i)^2$ can be expressed as follows:

$$d(i)^2 = S^2 \cdot (1 - K_c)^{2 \cdot (i-1)} \quad (4.11)$$

where S is the size of the unit step disturbance.

Combining the results of deterministic and stochastic analysis, we have the follow expression for the performance metric, V :

$$\begin{aligned} V &= \left\{ \frac{1}{N} \cdot \sum_{i=1}^N \left(1 + K_c \cdot \frac{1 - (1 - K_c)^{2(i-1)}}{2 - K_c} \right) \cdot \sigma^2 \right\} + \left\{ \frac{1}{N} \cdot \sum_{i=1}^N S^2 \cdot (1 - K_c)^{2(i-1)} \right\} \\ &= \left\{ \left(1 + \frac{K_c}{2 - K_c} - \frac{1}{N} \cdot \frac{1 - (1 - K_c)^{2N}}{(2 - K_c)^2} \right) \cdot \sigma^2 \right\} + \left\{ \frac{1}{N} \cdot S^2 \cdot \left[\frac{1 - (1 - K_c)^{2N}}{K_c \cdot (2 - K_c)} \right] \right\} \end{aligned} \quad (4.12)$$

¹⁰ Novak [22] obtained a similar result for variance amplification. His analysis was done in the frequency domain and the result was $n(i)^2 = \left(\sqrt{\frac{K_c^2}{(K_c - 2)^2} - 1} \right) \cdot \left(\frac{\sigma^2}{K_c - 1} \right)$. We can see that the time dependence of the expression was lost in his expression. But the two results converge rapidly as the value of N approaches 20. This observation can be important for short run manufacturing system because we can take advantage of the “transient” behavior of the variance amplification.

We can immediately see that V is a function of K_c , σ^2 , S and N . Some observations on the expression are as follows:

1. As K_c increases, the term in the first bracket increases due to the amplification of the white noise. At the same time, however, the second bracket decreases due to a faster approach to steady state. An optimum can, therefore, be reached between the two opposing terms.
2. As the ratio $\frac{\sigma^2}{S^2}$ decreases, we would expect the optimal K_c to become smaller. This is because the quality loss is influenced more significantly by the variance amplification effect compared to the transient effect.
3. As the production run gets longer, i.e. N becomes larger, the optimal K_c would become smaller. This is because the longer production run negates the effect of the relatively short transient behavior. In other words, a longer production run results in a higher weight on the variance magnification effect.

For a well defined manufacturing process, σ^2 , S and N can either be specified or measured, leaving K_c to be the only remaining variable. As a result, we can obtain the optimal feedback control gain by using analytical or numerical techniques.

Another commonly used controller for continuous systems is the PI-controller. It contains one additional gain parameter (proportional gain) in the controller as shown in Figure 4.5. The proportional gain allows us to move the open-loop zero to the right of the origin (see Figure 4.6).

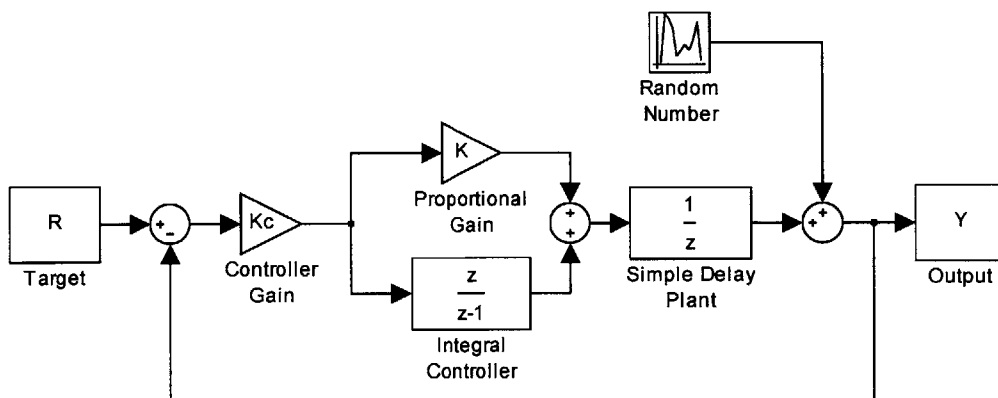


Figure 4.5: Control block diagram for a PI-controller

The closed-loop transfer function of the PI-controller system is

$$G(z) = \frac{(K_c \cdot K + K_c) \cdot z - K_c \cdot K}{z^2 + (K_c \cdot K + K_c - 1) \cdot z - K_c \cdot K},$$

where K is the proportional gain and K_c is the

controller gain. In discrete control system, the open-loop zero on the positive real axis will deteriorate the performance of the closed-loop process. This is because the open-loop zero cannot cancel out the open-loop pole at the origin, resulting in oscillatory behavior for the closed-loop system.

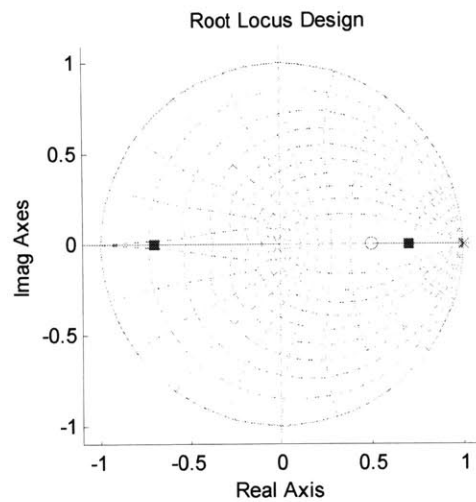


Figure 4.6: Root locus diagram for a PI-controller (with $K=1$, so the open-loop zero is at 0.5)

In the next chapter, we will present experimental results from metal bending process. The experimental results using the optimal control strategy discussed in this chapter will also be presented.

Chapter 5: Application to Sheet Metal Bending Process

5.1. Introduction

5.1.1. Manufacturing Process Taxonomy

There are hundreds of different manufacturing processes: from removal processes to forming processes, from chemical processes to mechanical operations. To simplify the learning of all the processes, we can group similar processes together and classify the processes into different categories.

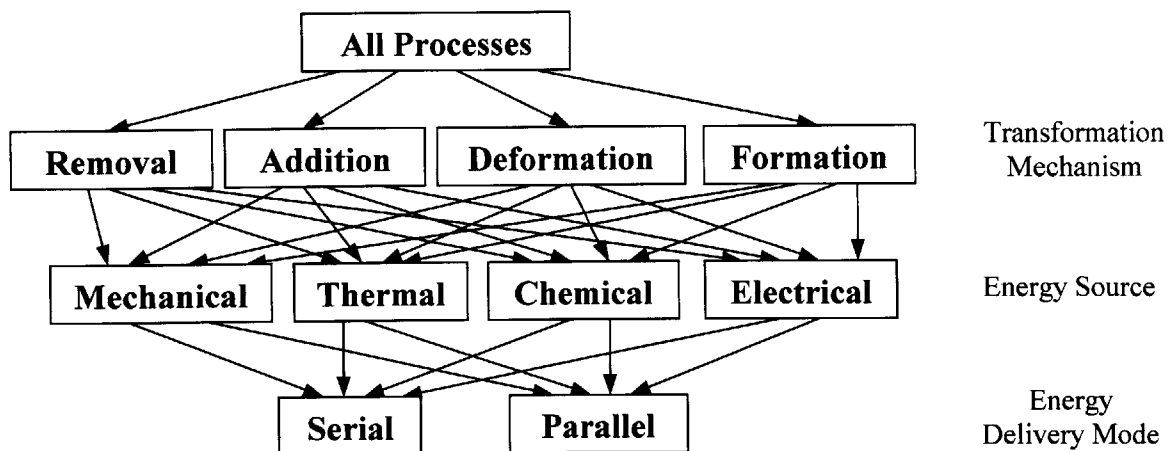


Figure 5.1: Manufacturing Process Taxonomy

Manufacturing is the transformation of material into desired shapes and properties from different energy sources. Based on the transformation mechanism of each process, they can be divided into four subgroups: removal, addition, deformation and formation. Within each transformation group, we can further divide the processes according to the sources of energy involved. The four common sources of energy delivery mechanisms are mechanical operations, thermal processes, chemical processes and electrical processes. Some of these energy transfers occur locally and are therefore called serial processes. Other processes involve the transfer of energy all at once and are called parallel processes. Figure 5.1 shows the different levels of classification of manufacturing processes.

Most semiconductor manufacturing processes, for example, are parallel chemical processes: etching is a removal process, ion implantation is an addition process. Machining is a serial mechanical removal process, while stamping is a parallel mechanical deformation process.

In manufacturing, the energy delivery mode is crucial in deciding methods of control. Serial processes can usually be controlled sufficiently by regulating machine states such as position or force. Serial processes such as machining usually have very high degree of precision so output control is generally not needed. Also, because the energy transfer is local, partially finished outputs are assessable before the entire process is completed. So output control can be done within each process cycle in a continuous manner. For parallel processes, the entire output is not accessible within a manufacturing cycle. As a result, parallel processes would benefit more from CTC control.

5.1.2. Selection of appropriate processes for experimentation

In choosing the appropriate candidate for experimentation, some of the criteria considered for selection of suitable processes for CTC control are as follows:

1. Good representative of a family of processes commonly performed in industry.
2. Easily accessible inputs that can be changed rapidly for the next cycle.
3. Able to do quick and easy measurements that would allow immediate feedback control.
4. Ability to introduce disturbances: drift, abrupt shifts, exponential and cyclic.
5. Detectable and significant variation (i.e. measurement error \ll process noise).

5.1.3. Description of Air Bending process

Sheet metal bending process is selected as the first experiment to verify some of the theories proposed. Figure 5.2 illustrates the mechanics of the air bending process. It represents a family of processes that is typical in discrete parts manufacturing such as stamping, forming and extrusion. In air bending, input can be easily and quickly changed for the next cycle. There is no need to change any equipment or dies to obtain different bending angles because the depth of the punch stroke (input) determines the bend angle (output). The forces required to form the parts are relatively small, but accurate control of the punch stroke is necessary to obtain the desired bend angle.

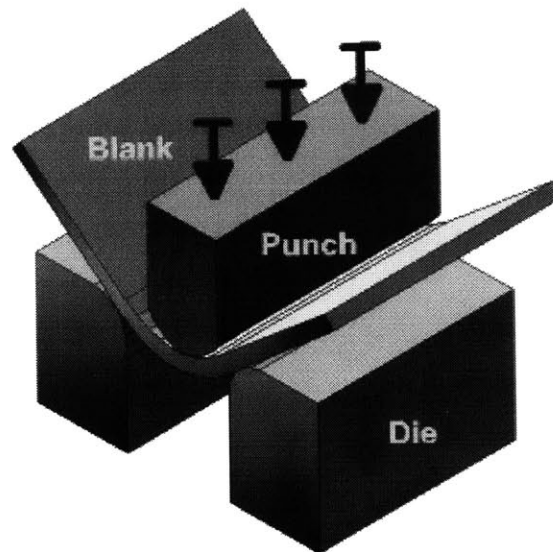


Figure 5.2: Illustration of Air Bending Process

Source: [25]

Measurements can be quickly and accurately made using a Vernier Protractor. The measurement noise is about 0.12° . The major source of process disturbance is from material variations. Both material thickness and material constitutive property will affect the springback on the part, which is the major uncertainty in the metal bending process. The ease of simulating common disturbances experimentally is also a major advantage of the air bending process. Step disturbances can easily be introduced by a change of material. A ramp disturbance can also be introduced by moving the punch away from the die (this can indeed happen in an actual production and is caused by a slip in punch position). In addition, it is a simple discrete process that has no process dynamics; meaning

subsequent outputs are virtually independent of each other. Finally, the input-output relationship can be easily found empirically.

5.1.4. Process Model and Assumptions

To derive a suitable stochastic control model for the process, certain assumptions need to be made. The following are the assumptions and observations made for sheet metal air bending process:

1. There is no dynamics or state dependence in the process from cycle to cycle. In other words, the process has reached steady state before the cycle is over and the output of a prior cycle has no effect on the next cycle. Thus, the variation of the output can simply be characterized by a white noise random disturbance.
2. The air bending process can be assumed to be a linear system so that simple linear control strategies can be applied¹¹.
3. There will be only one cycle delay on the process. (i.e. the measurements are fed back for immediate adjustment for the next cycle)

A schematic of the model is shown in the Figure 5.3.

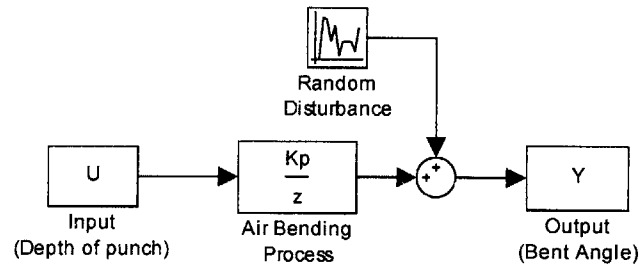


Figure 5.3: Model Schematics for Air Bending Process

¹¹ If we only use a small range of input for feedback adjustment, the local process gain can be assumed to be linear.

5.2. Experimental Setup

The setup of the experiment is very simple. A manual lathe is used as the basis for the air bending process. A forming die is mounted onto the chuck of the lathe and a punch is mounted to the tailstock of the lathe. The chuck is locked in position so the die cannot rotate. A picture of the experimental setup is shown in Figure 5.4. By turning the tailstock dial, the depth of each punch stroke can be precisely controlled. This is the primary mode of feedback input for the entire experiment. A picture of the tailstock dial is shown in Figure 5.5. The precision of the dial is 0.001”.

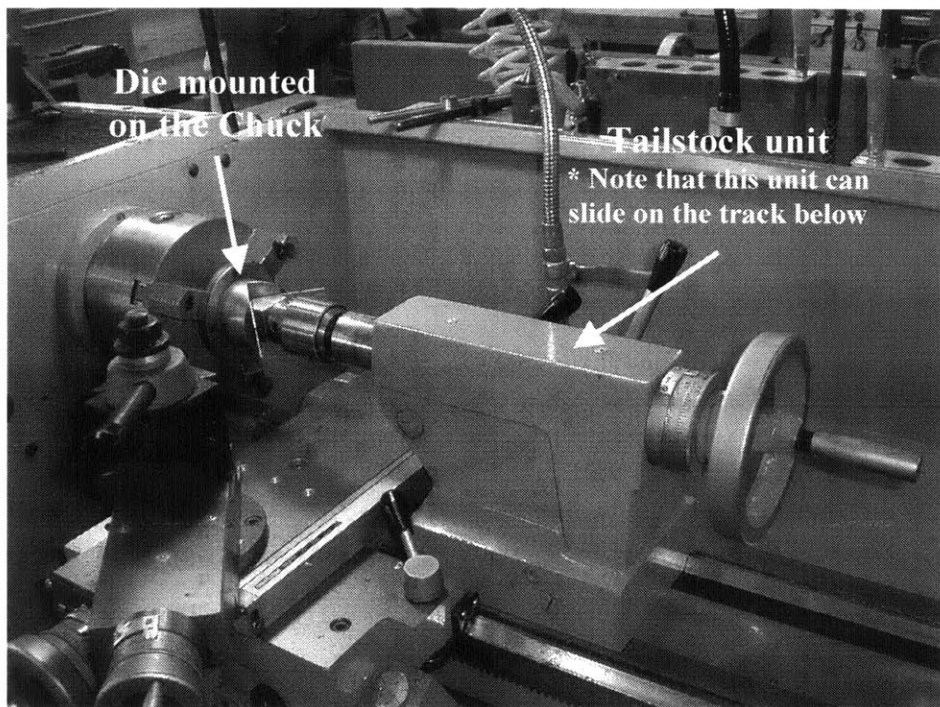


Figure 5.4: Setup for the metal air bending experiment on a lathe

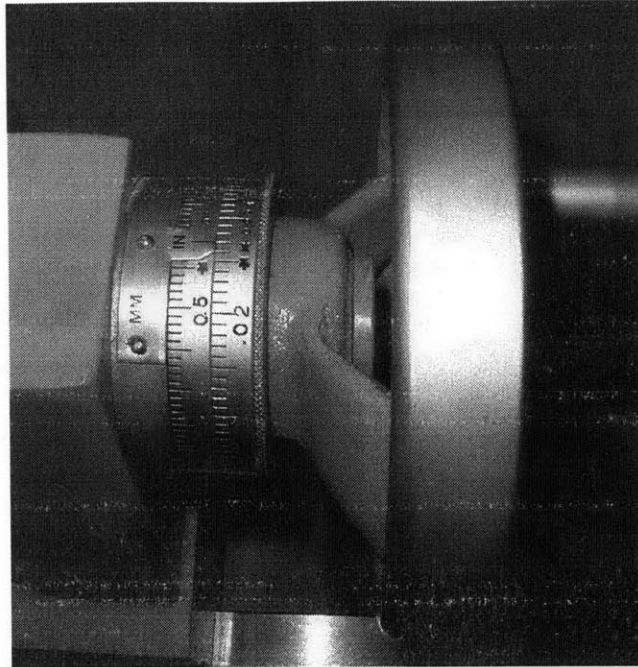


Figure 5.5: Punch depth control using the precision dial on a lathe

Sheet metal is used for the experiment. The different materials used are as follows:

1. 0.025" thickness steel (Materials I and II)
2. 0.02" thickness steel (Materials III and IV)
3. 0.032" thickness aluminum (Materials V and VI)

We anticipate that the orientation of the rolling process might affect the directional property of the materials, so each sheet was cut into 4.8"x0.9" strips in two different direction; thus a total of 6 labels were given. (It was later found that the direction property of the materials was insignificant compared to the measurement error).

A Vernier Protractor (see Figure 5.6) is used for precise measurement of the bent parts. The resolution of the device is 5 minutes (or approximately 0.1°). The measurements are entered into a laptop computer running a spreadsheet program. It contains the feedback control algorithm that provides the punch depth input for the next cycle. Actuation is then performed by manually turning the tailstock dial to the appropriate punch depth for the next cycle. The punch is returned to the zero position at the end of each cycle.

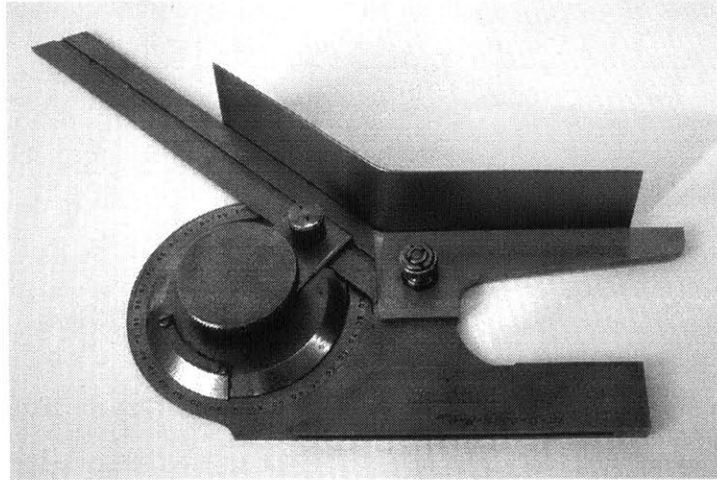


Figure 5.6: A Vernier Protractor measuring part angle

5.2.1. Expected Results

Based on the system model given in Figure 5.3, we would expect the air bending process to demonstrate the following behavior in the actual experiment:

1. Closed-loop control of the undisturbed process (white noise disturbance only) would increase the variance. While closed-loop control of the disturbed process (intentional drift, cyclic, shifts) would decrease the variance.
2. Using a closed-loop controller would tend to center a process at its desired target (i.e. steady-state error become less). Also, using an integral controller would reject both step disturbances completely.
3. Improved performance with optimal controller technique (in terms of quality loss) compared with other quality control methodology.

5.3. Experimental Procedure and Observations

The goals of the experiment are to compare the results to the theoretical prediction; mainly to show the behavior of the process under different control schemes and the ability to design an optimal controller using discrete control theory.

The input of the process is the depth of punch stroke and the output is the ‘excluded’ angle of the part. (‘Included angles’ are measured using the Vernier Protractor. They are then converted to the ‘excluded angles’ by subtracting them from 180°). The effect on bend angles by changing punch depth is illustrated in Figure 5.7.

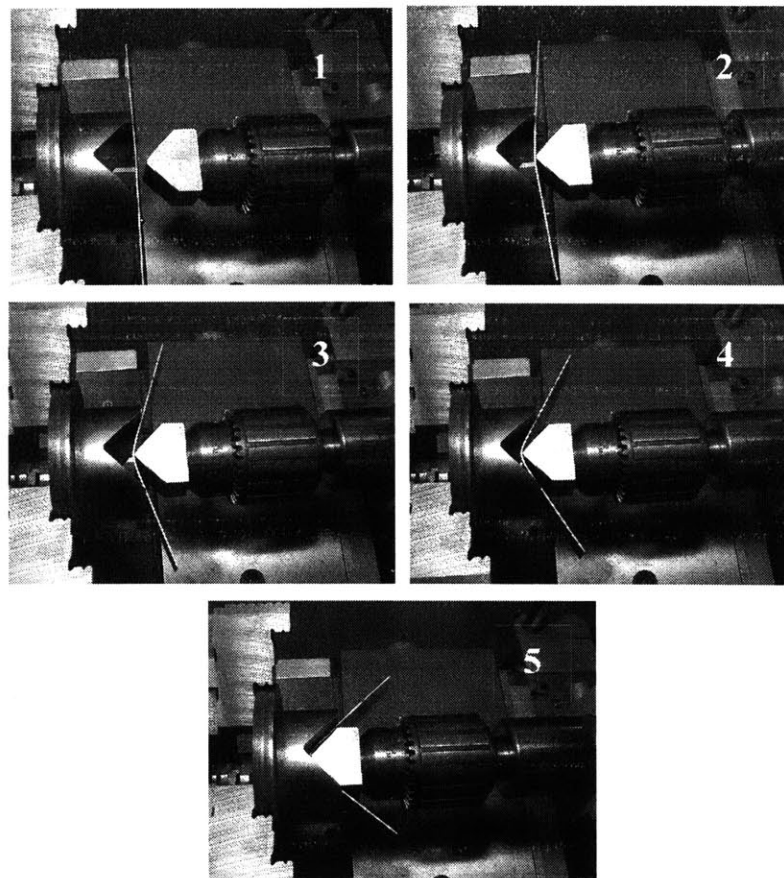


Figure 5.7: Steps showing different bend angles at different punch depths

The expected natural variations of the process include the variation in material properties and the error in punch location. Disturbances can be intentionally injected by changing the material used and also adjusting the position of the tailstock or create a false zero position. Feedback control strategies to be used are proportional, integral and integral-differential. Sample size for the experiments varies from 20 to 50 depending on the behavior of the output and the accuracy of the parameters needed.

The experiments are divided into four sections:

1. Characterization of process gain
2. Open-loop run of the process to characterize the open-loop process statistics
3. Closed-loop control of the process with and without disturbances
4. Optimal control run

Characterization of process gain is needed to understand the input-output relationship of the process. The punch depth is varied and the unloaded output angle is recorded. A linear relationship can be obtained from the experiment and it represents the plant gain, K_p , for the process.

The open-loop run acts like a control experiment for comparison to the closed-loop counterpart. Process statistics such as mean and standard deviation can be obtained. Measurements need not be made in real-time.

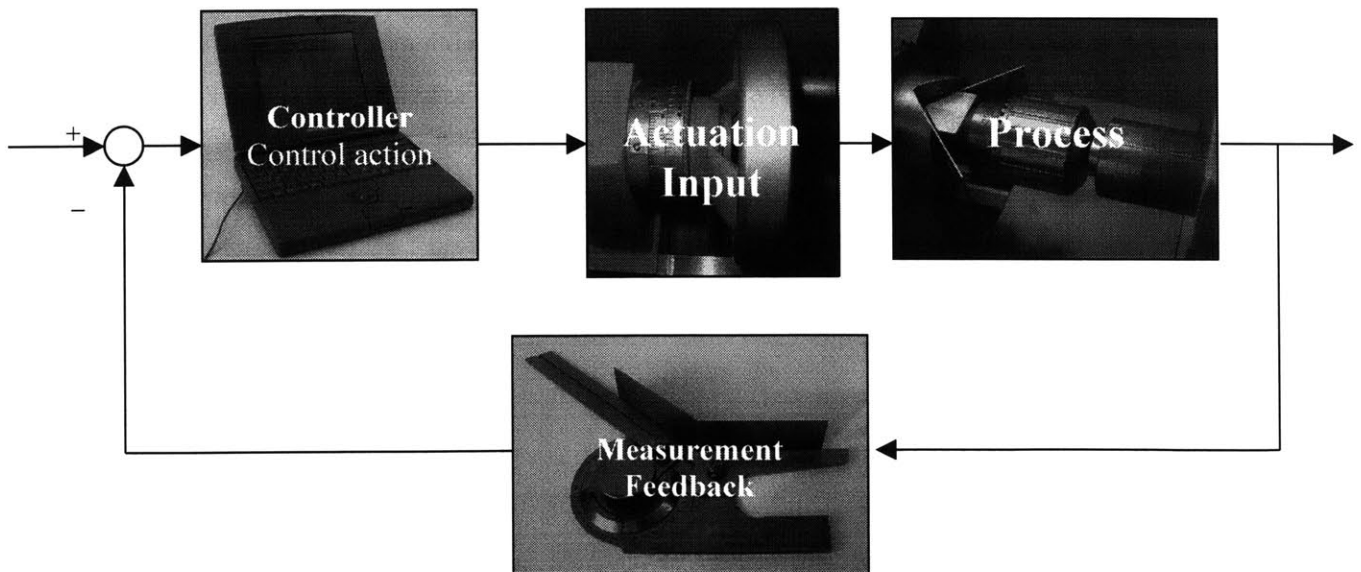


Figure 5.8: Feedback Control schematics for air bending process

When operating in closed-loop mode, measurements would be fed back after each cycle to adjust for the next cycle. A schematic diagram showing the components of the feedback loop is given in Figure 5.8. The different control schemes differ only in the algorithm used in the spreadsheet program.

5.4. Results and Analysis

The results and analysis of the experiments are summarized in this section. More detailed calculations for steady-state error and settling time are given in the Appendix A.

5.4.1. Characterization of Process Gains

The input depth reading¹² varies from 1.1” to 1.65” (the corresponding actual punch depth is from 0” to 0.55”) and the output angle is measured. For check of accuracy, two samples are obtained for each punch depth. The experiment is performed on all three materials with two orientations for each material, so a total of 6 separate series are performed. For the steel sheets, the direction of the grain is not detectable using naked eye, so the directional information is based on the direction of the cut from the original sheet. For the aluminum sheets, the direction of the grain is easily distinguishable. The results show that although the input-output relationship is not perfectly linear, a linear approximation can be used locally to satisfy the linear assumption of the model. The r-squared value shows that the experimental data fits the linear model extremely well. The key results of the experiment are summarized in the Table 5.1. As expected, the effect of strip direction is not significant for steel where grain directions cannot be seen but it is significant for aluminum where the grain direction is evident.

¹² The input depth is the reading on the dial and is not the actual depth of punch. Calibrating the actual punch depth is very difficult; the compliance of the sheet metal makes it impossible to take an accurate reading. Calibration is based on the distance between the chuck and the tailstock instead.

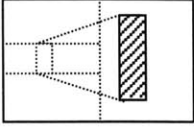
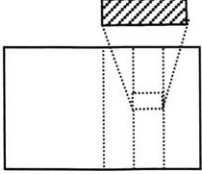
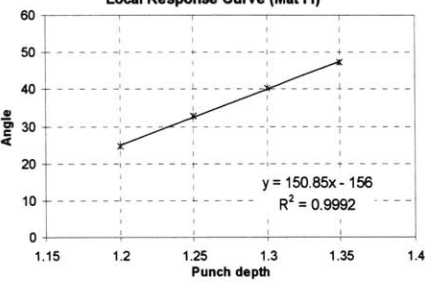
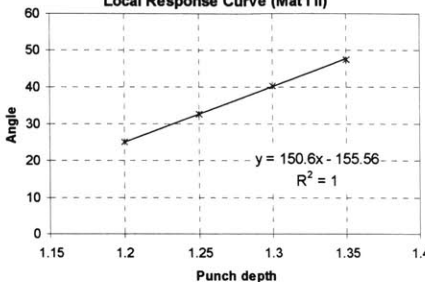
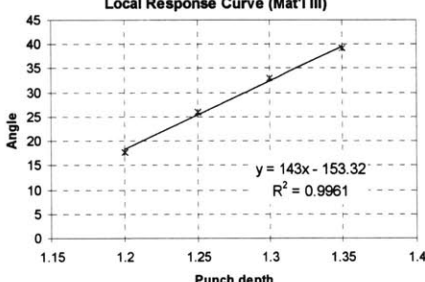
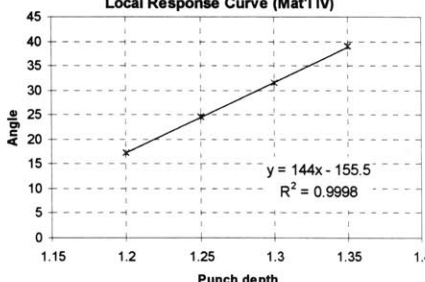


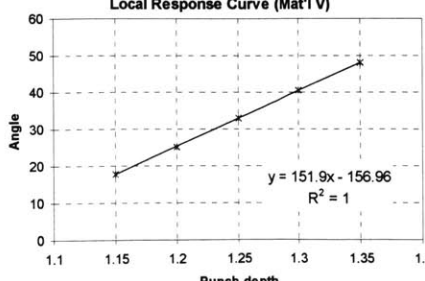
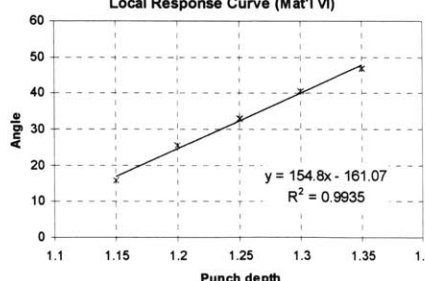
<u>Material</u>	<u>Fitting chart with linear relationship</u>	
Steel	Vertical strip 	Horizontal strip 
I. & II. 0.025" steel	Local Response Curve (Mat'l I)  $K_p = 151$	Local Response Curve (Mat'l II)  $K_p = 151$
III. & IV. 0.02" steel	Local Response Curve (Mat'l III)  $K_p = 143$	Local Response Curve (Mat'l IV)  $K_p = 144$
Aluminum	Vertical grain 	Horizontal grain 
V. & VI. 0.032" aluminum	Local Response Curve (Mat'l V)  $K_p = 144$	Local Response Curve (Mat'l VI)  $K_p = 155$

Table 5.1: Results of Process Gain Characterization experiments

5.4.2. Open-loop Run

An undisturbed open-loop run is performed for each material to obtain process statistics (mean and standard deviation). Input punch depths of 1.25, 1.265 and 1.35 are used. Run lengths are between 15 and 30. The standard deviations for steel are similar in value while aluminum differs according to the grain direction. The summary of results is shown in Table 5.2.

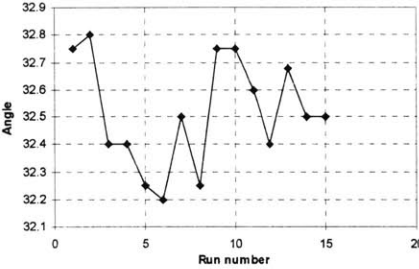
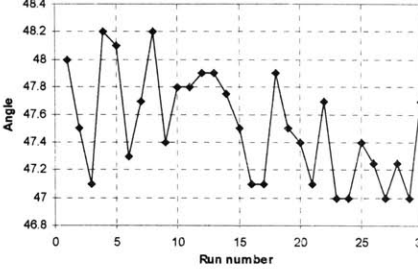
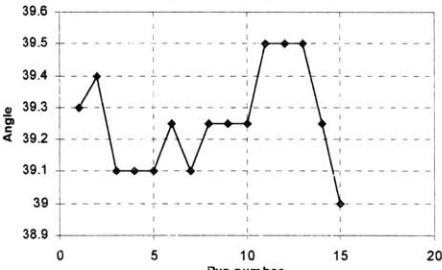

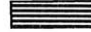
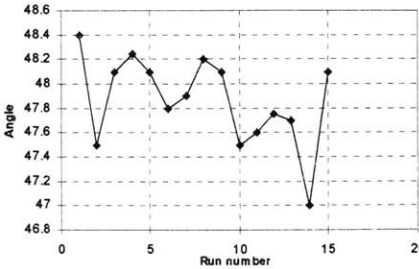
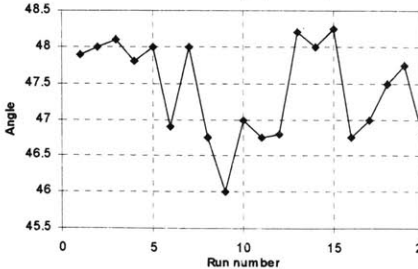
<u>Material</u>	<u>Open-loop process statistics</u>	
Steel		
I. & II. 0.025" steel	<p data-bbox="527 674 943 695">Run Chart for Mat'I I (Depth = 1.25)</p>  <p data-bbox="609 976 862 1010">$\mu = 32.5^\circ, \sigma = 0.200^\circ$</p>	<p data-bbox="1015 674 1430 695">Run Chart for Mat'I I (Depth = 1.35)</p>  <p data-bbox="1096 976 1349 1010">$\mu = 47.5^\circ, \sigma = 0.383^\circ$</p>
III. & IV. 0.02" steel	<p data-bbox="868 1024 1096 1045">Run Chart for Mat'III (Depth = 1.35)</p>  <p data-bbox="852 1344 1105 1377">$\mu = 39.2^\circ, \sigma = 0.161^\circ$</p>	
Aluminum	Vertical grain 	Horizontal grain 
V. & VI. 0.032" aluminum	<p data-bbox="527 1497 943 1518">Run Chart for Mat'IV (Depth = 1.35)</p>  <p data-bbox="609 1799 862 1833">$\mu = 47.9^\circ, \sigma = 0.368^\circ$</p>	<p data-bbox="1015 1497 1430 1518">Run Chart for Mat'VI (Depth = 1.35)</p>  <p data-bbox="1096 1799 1349 1833">$\mu = 47.4^\circ, \sigma = 0.663^\circ$</p>

Table 5.2: Results of open-loop run experiments

Repeatability tests are also performed. Twenty measurements are made on the same part and it is found that the repeatability of the measurement is about 0.120° .

5.4.3. Closed-loop with no deterministic disturbance

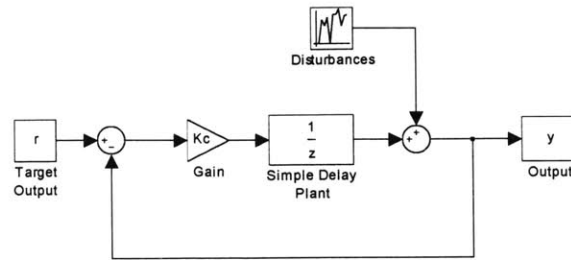
Undisturbed closed-loop experiment is performed using all 0.025" steel material. The target angle (included angle) for all experiments is 35° . Both proportional and integral control strategies are used. For the P-controller, only the error from the previous cycle is used for control. For the I-controller, the sum of all previous errors is multiplied by the controller gain to get the actuator input. Results for P-controller and I-controller are shown in Table 5.3 and Table 5.4 respectively (The solid dot in the root locus diagram represents the closed-loop pole at the specified controller gain, K_c)

As expected, there is variance amplification by closing the loop. This shows that the disturbance is purely random in nature and using closed-loop control would only decrease the process capability. This result conforms with the assumption that the disturbance is independent and random.

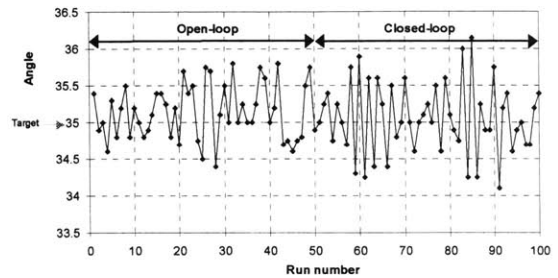
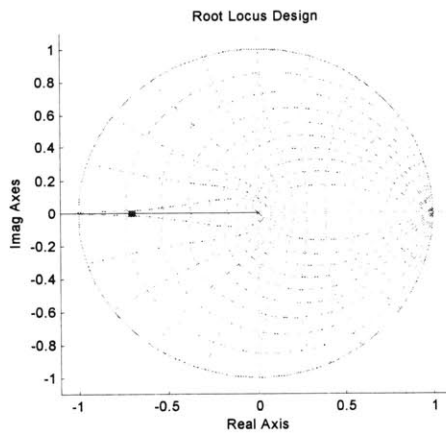
Two different values of K_c are used for P-controller. When $K_c = 0.7$, it is found that closed-loop variance is significantly larger than open-loop variance using hypothesis testing. The theoretical variance ratio is 1.961, with a 95% confidence interval of 1.22 and 3.15. The experimental variance ratio is 1.665, indicating that it is statistically equivalent to the theoretical result. Also, since the pole is to the left of imaginary axis on the root locus plot, we can observe some oscillatory behavior. Finally, the open-loop mean is 35.14° while the mean for the closed-loop runs is 35.06° . This demonstrates the target centering property of a closed-looped system.

When $K_c = 1$, we can see from the root locus diagram that the system is marginally stable because there is a closed-loop pole located on the unit circle. Highly oscillatory behavior is observed experimentally together with highly amplified variance.

P-Controller: Closed-loop results with no disturbance



$K_c = 0.7$



$K_c = 1$

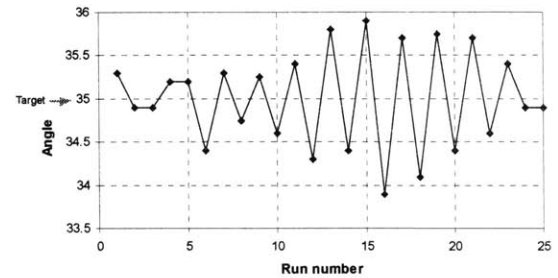
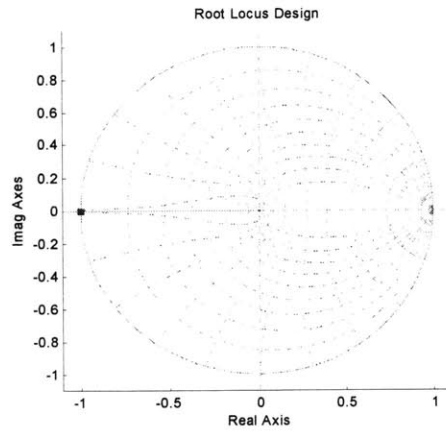
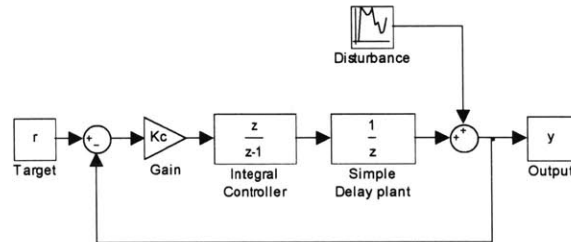


Table 5.3: Results from undisturbed closed-loop experiment with P-controller

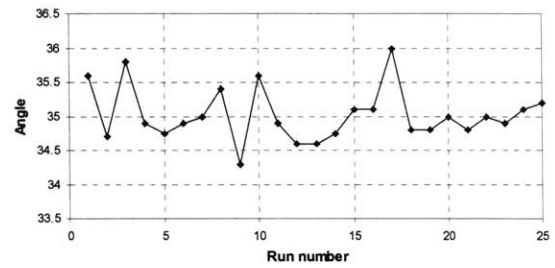
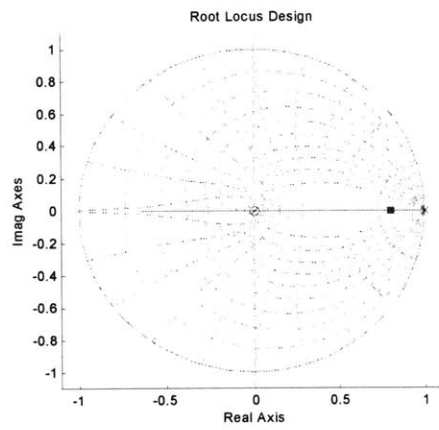
For the I-controller, expected results are also observed. When $K_c = 0.2$, the closed-loop pole is located on the real axis to the right of the imaginary axis, which means the system response should be non-oscillatory and fast. Similar behavior can be seen on the experimental plot. The variance amplification is 1.015, which is also very close to the theoretical value of 1.115.

For $K_c = 1.8$, oscillatory response is observed as expected. The variance amplification is 10.20, comparable to the theoretical value of 10.00.

I-Controller: Closed-loop results with no disturbance



$K_c = 0.2$



$K_c = 1.8$

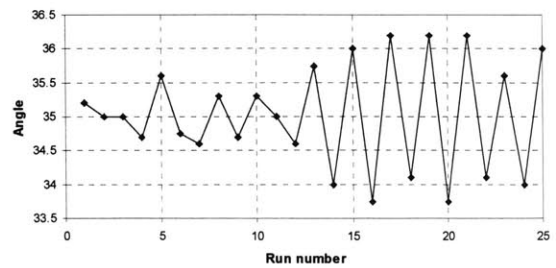
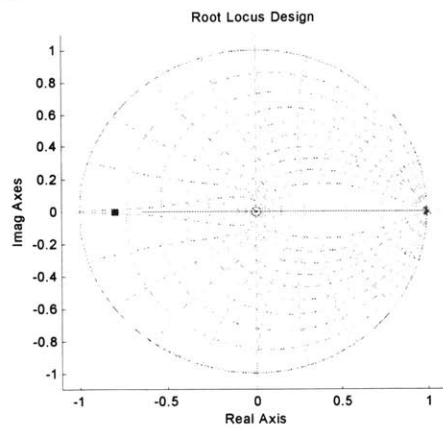


Table 5.4: Results from undisturbed closed-loop experiment with I-controller

5.4.4. Closed-loop with step disturbance (sudden shift of material properties)

A step disturbance is simulated by changing the material used from 0.025" steel to 0.02" steel, and for the experiment using ID-controller from 0.02" steel to 0.025" steel. In the previous experiment, we observe that closed-loop systems have mean values that are closer to the desired target. In this section, we will demonstrate in a more dramatic fashion the centering effect of a closed-loop system trying to bring the shifted process closer to the target. All three controllers were tested on the step disturbance. We initiate each experiment with one material for a few runs and then switch to the other material for the rest of the experiment. The experiment is stopped when steady-state behavior is observed or the transient effect diminished. The results of the experiments are shown in Table 5.5 with the root locus diagram on the left showing the closed-loop pole location.

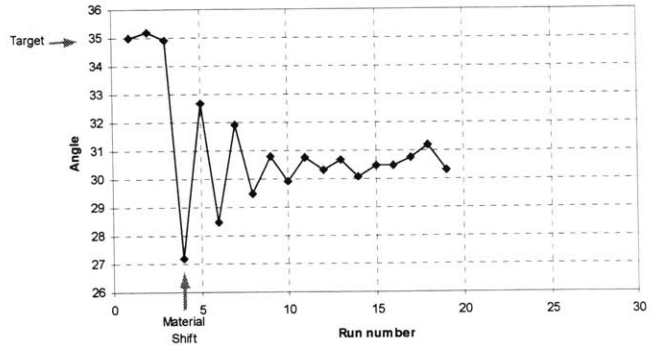
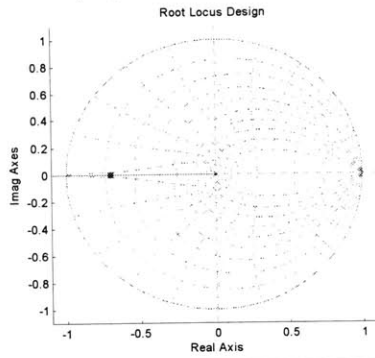
For the P-controller, a gain of 0.7 is used to ensure stability. It is expected to have some oscillatory behavior and it is indeed observed in the experimental plot. There is a steady-state error for the P-controller and it is found to be 4.65° . A shift from 0.025" to 0.02" steel represents a step disturbance of 7.29° and the theoretical is calculated to be 4.29° . The 5% settling time is expected to be 9 cycles and it is found to be about 10~11 cycles. The slight discrepancies between prediction and experimentation can be attributed to the imperfect model and the random disturbance affecting the system.

For the I-controller, a gain of 0.5 is used to produce a non-oscillatory response. The result shows almost no oscillation compared with the P-controller response. The experimental steady-state error is zero, meaning that the output achieved the desired target. This is as expected because the free integrator associated with the I-controller should remove the steady-state error. The 5% settling time is about 4~5 cycles, compared to 5 cycles in the calculation.

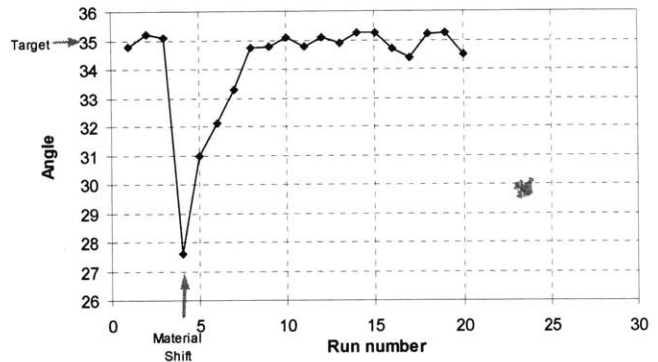
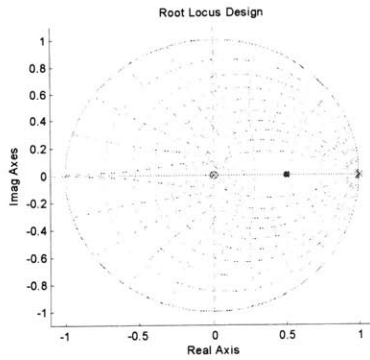
For the ID-controller, a gain of 0.2 is used, giving one oscillatory pole and two non-oscillatory poles. The result shows some oscillatory behavior and no steady-state error. This is as expected due to the effect of the free integrator. The 5% settling time is expect to be 13 cycles and the experiment shows a settling time of about 14~15 cycles. The results also prove that ID-controller is undesirable in controlling a discrete system because of its sluggish performance. The slowest pole that is farthest away from the origin limits its performance.

Closed-loop results with step disturbance

P-controller, $K_c = 0.7$



I-controller, $K_c = 0.5$



ID-controller, $K_c = 0.2$

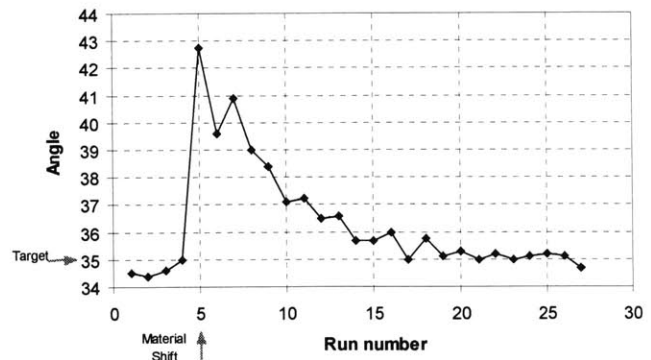
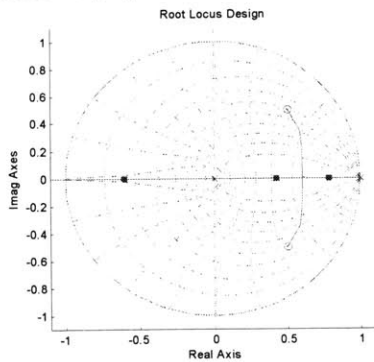


Table 5.5: Results from shifted closed-loop experiment

5.4.5. Closed-loop with ramp disturbance (gradual change of tailstock position)

We simulate a ramp disturbance by sliding the tailstock away from the chuck. This is a realistic disturbance because the punch stroke could force the tailstock to slide away if it is not locked in position (See Figure 5.4 for the tailstock unit). The experiments start out with the tailstock at its nominal position (3" away from the chuck). The tailstock unit would then be intentionally slid away at a rate of 0.01" per cycle, which translates into a disturbance of 1.51° per cycle on the output. The experiment is stopped when steady-state behavior is observed or the transient effect diminished. The results of the experiments are shown in Table 5.6.

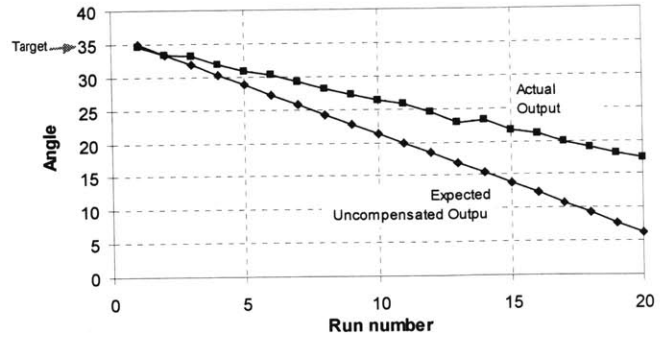
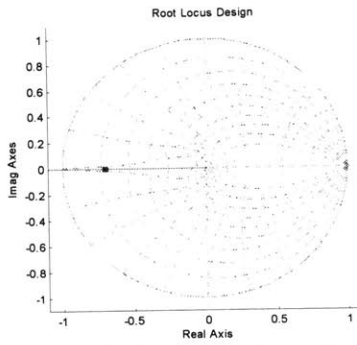
For the P-controller, a gain of 0.7 is used as usual. The output is expected to follow the ramp behavior of the disturbance but at a shallower slope. As expected, the steady-state error for the P-controller is found to be infinite because the output never approaches the target. We expect the slope of the output to be 0.89° per cycle and it is observed to be 0.91° per cycle from the experiment. The predicted output for an open-loop system is also shown on the plot.

For the I-controller, a gain of 0.5 is used. As expected, the result shows almost no oscillation. The steady-state error is no longer infinite, but at a finite value. This is because the free integrator associated with the I-controller can only reduce the order of the infinite ramp to a steady-state error. The steady-state error is 3.03° , comparable with a theoretical value of 3° . The 5% settling time is about 5~6 cycles, compared to 5 cycles in the calculation. One might wish to use a second integrator to remove the steady-state error, but it will make the discrete system marginally stable.

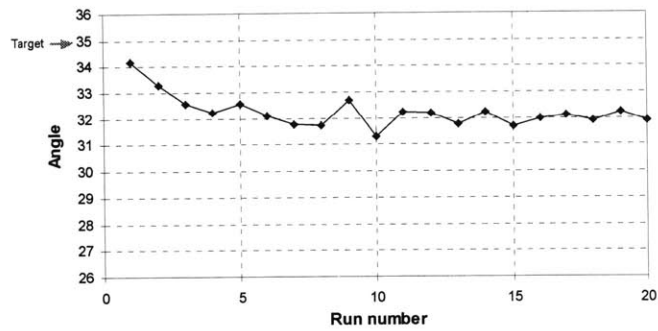
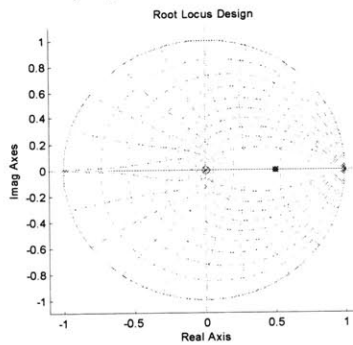
For the ID-controller, gains of 0.2 and 0.5 are used. The experiments show a steady-state error in both cases. A 0.5 gain makes the system unstable with high oscillation; this is because one of the poles is outside the unit circle on the root locus diagram. The experimental result shows a local steady-state error of 3.24° , comparable to the expected value of 3° . At 0.2 gain, it results in a steady-state error of 7.48° . The calculated value was 7.5° . The 5% settling time is expected to be 13 cycles and the experiments shows settling times of about 15 cycles. One interesting observation is that an unstable gain of 0.5 for the ID-controller gives us a steady-state error of 3.24° while a stable gain of 0.5 for I-controller gives us the same steady-state error. This again demonstrates the poor performance of an ID-controller.

Closed-loop results with ramp disturbance

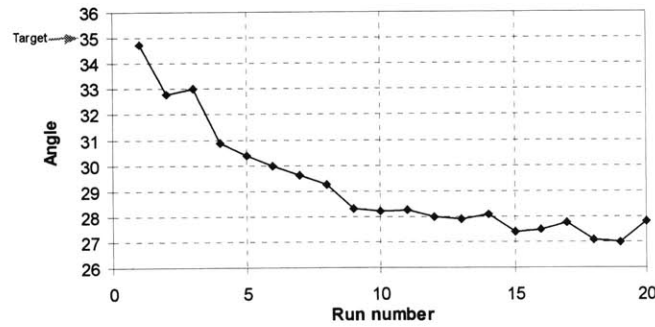
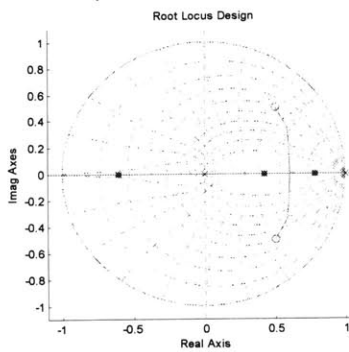
P-controller, $K_c = 0.7$



I-controller, $K_c = 0.5$



ID-controller, $K_c = 0.2$



ID-controller, $K_c = 0.5$

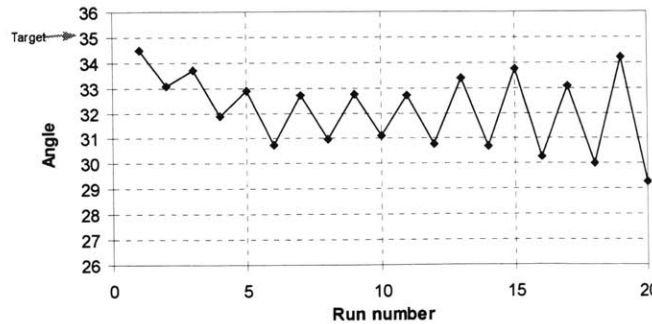
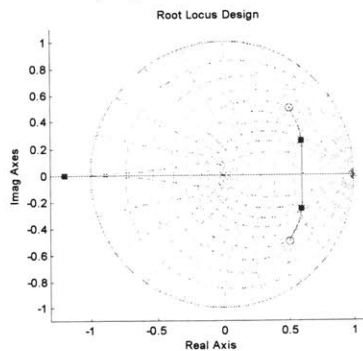


Table 5.6: Results from closed-loop experiment with ramp disturbance

5.4.6. Optimally designed gain with material shift

The minimum mean square error optimizing technique described in the previous chapter is tested on the metal bending process. Again, we try to achieve a target angle by changing the input punch depth based on feedback information from previous cycles. An integral controller is used for the experiment to ensure zero steady state error. The control system representation for the metal bending process is identical to the one presented in Figure 4.4. A material shift is injected to provide a realistic step disturbance to the process.

The known parameters for the bending process are $\sigma^2 = 0.062$, $S = 7.26^\circ$, and $N = 20$. Substituting these parameters into the equation (4.12),

$$V = \left\{ \left(1 + \frac{K_c}{2 - K_c} - \frac{1}{N} \cdot \frac{1 - (1 - K_c)^{2N}}{(2 - K_c)^2} \right) \cdot \sigma^2 \right\} + \left\{ \frac{1}{N} \cdot S^2 \cdot \left[\frac{1 - (1 - K_c)^{2N}}{K_c \cdot (2 - K_c)} \right] \right\}, \text{ and using}$$

Microsoft Excel's solver function, a numerical solution for the optimal feedback gain, K_c , is found to be 0.98. A simulation for the deterministic output¹³ of the system with $K_c = 0.98$ is shown in Figure 5.9 below. It shows the short transient behavior of the system. This is because of the large step size relative to the random noise, which needs to be quickly adjusted to avoid high quality loss. The expected value of average quality loss (V) is 2.83.

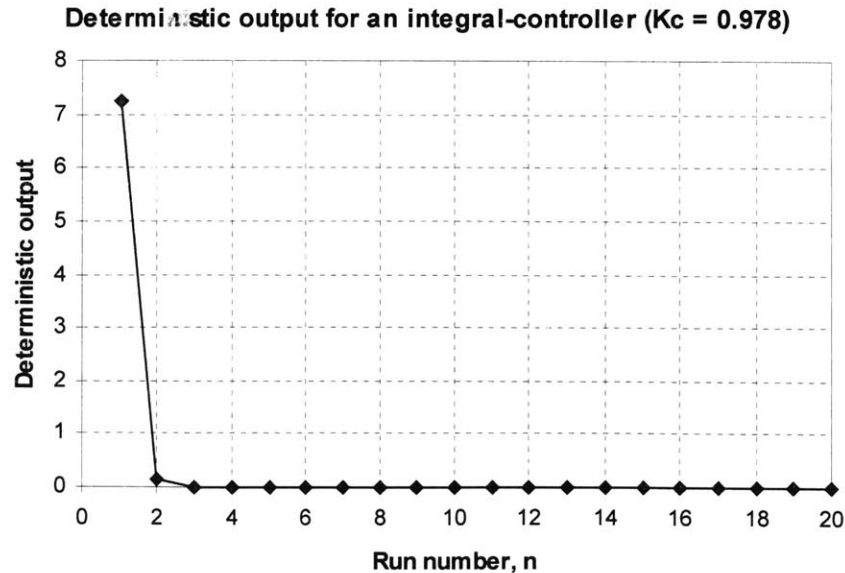


Figure 5.9: Simulated deterministic output using optimal feedback gain

¹³ The deterministic output is the output of the closed-loop system without any disturbance.

Because of the relatively small $\frac{\sigma^2}{S^2}$ ratio, coupled with a short production run, we can see in

Figure 5.9 that the optimum response approaches the steady state in less than 3 cycles. Figure 5.10 below shows how the performance index (V) varies with K_c .

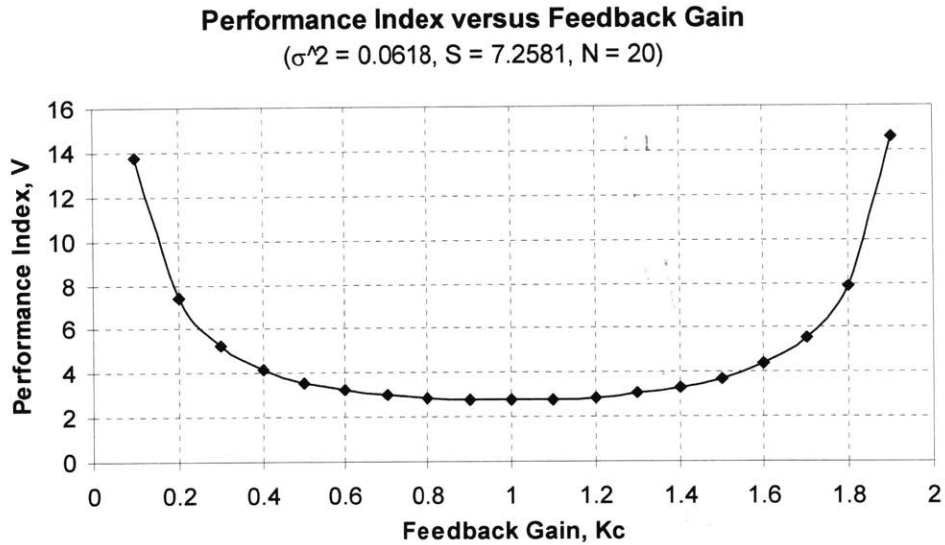


Figure 5.10: Performance Index minimization by K_c

Metal bending experiments are performed for $K_c = 0.5$, 0.98 and 1.5 for comparison. We expect to see a lower quality loss value for the optimum K_c . The results for the experiments are summarized in Table 5.7. The expected values of V for $K_c = 0.5$ and 1.5 are 3.73 and 3.76 respectively.

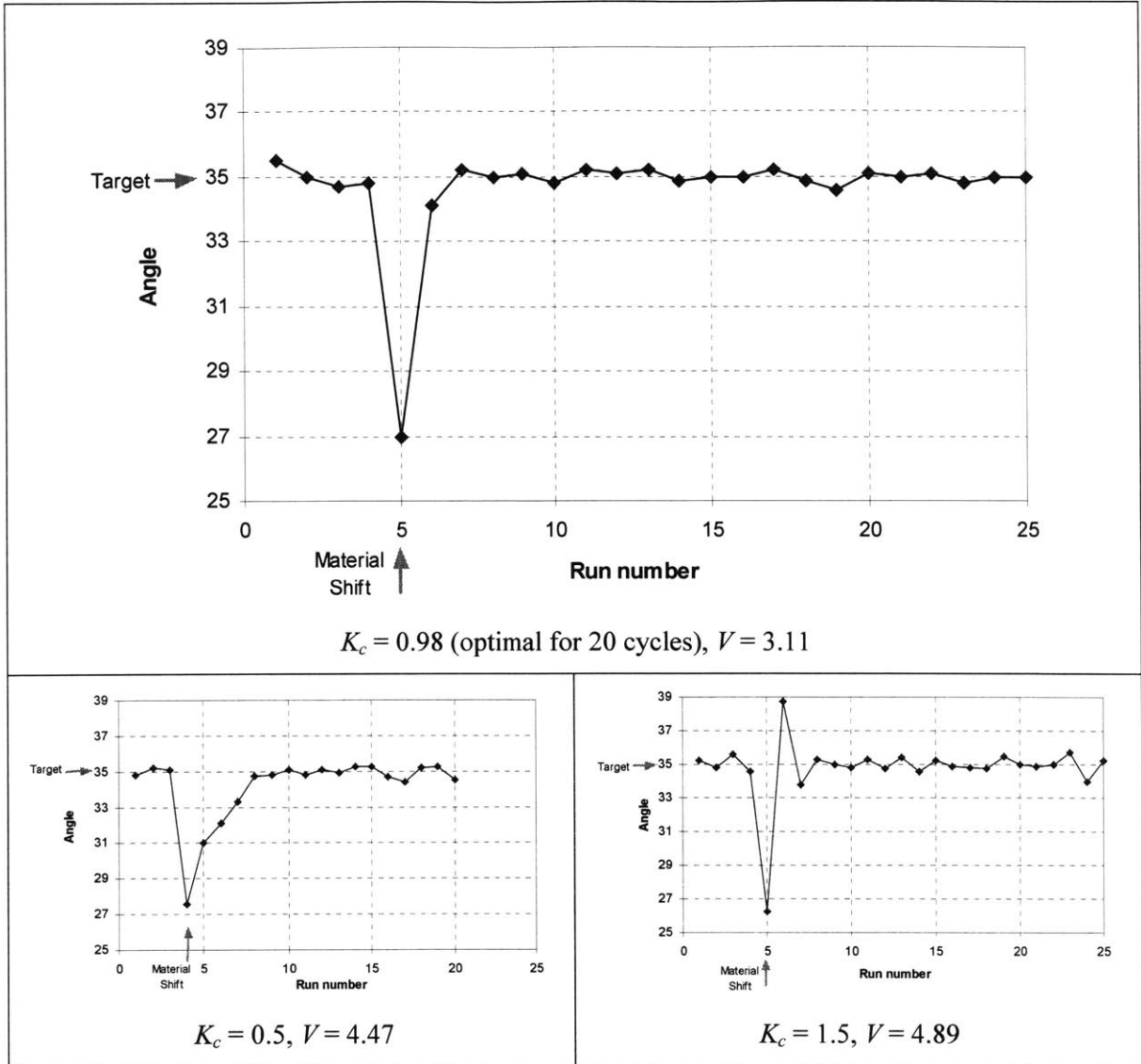


Table 5.7: Experimental result for Minimum Quality Loss I-controller design

The experimental result matches the predictions very well. For $K_c = 0.98$, the step disturbance is rejected in less than 3 cycles after the material shift. The values of the performance index (V) are also within the range of prediction.

5.5. Conclusions

All the experiments behave as expected. Three key properties of CTC feedback control is demonstrated:

1. The increase of variance in a process that has uncorrelated disturbance.
2. The ability of closed-looped system to center towards the desired target, especially for I-controller where steady-state error is eliminated for a step disturbance.
3. Differential controllers have poor performances for discrete systems and thus should not be used.

We can conclude that the bending process is well modeled by the linear simple delay process model with the additive uncorrelated disturbance.

We also demonstrate the use of discrete control theory and root locus diagram to predict some of the closed-loop behavior of the system. They prove to be easy to use and very accurate.

This chapter serves as a verification for the theory of CTC feedback control in an uncorrelated process. We also point out some of the implementation issues of the concept. In the next chapter, we will try to characterize an injection molding system and to CTC control to the process.

Chapter 6: Application to Injection Molding Processes

6.1. Introduction

6.1.1. Description of Injection Molding Process

Injection molding is a widely used polymeric manufacturing process. It evolved from metal die-casting. Unlike molten metals, however, polymer melts have high viscosity and cannot flow into a mold on their own. Large pressures must be exerted to force the polymer into the mold cavity. After the mold is filled, more polymer melt must also be packed into the mold during solidification to avoid shrinkage in the mold.

Injection molding can be used to form a wide variety of products. Complexity is virtually unlimited, sizes may range from very small to very large, and excellent control of tolerances is also possible. Most polymers may be injection molded, including thermoplastics, fiber reinforced thermoplastics, thermosetting plastics, and elastomers. Structural injection molding is also possible in which a core and skin may be made of different polymers.

In a reciprocating screw injection molding machine, pelletized material flows under gravity from the hopper onto a turning screw. The frictional energy supplied by the screw, together with barrel heaters, converts the resin into a molten state. While the molten plastic is being transferred to the

front of the barrel, the screw retracts toward the hopper end. When a sufficient amount of resin is melted, the screw is pushed forward, acting as a ram and forcing the polymer melt through a gate into the cooled mold. Once the plastic has solidified in the mold, the mold is unclamped and opened, and the part can be pushed from the mold by automatic ejector pins. The mold is then closed and clamped to repeat the cycle. For small parts, the process can be as fast as several cycles per minute.

The design of customized molds creates the flexibility of the process. The polymer flows from the nozzle to the mold through a sprue. The advantages of injection molding include high production rates, design flexibility, repeatability within tolerances, ability to process a wide range of materials, relatively low labor content, little to no finishing of parts and minimal scrap losses. Disadvantages are mainly capital cost related: high initial equipment investment, high startup and tooling costs. Parts must be custom designed for effective molding; accurate cost prediction is also difficult. Although the repeatability of the process is very high, the increasing use of the injection molding process in high tolerance, large size, low volume parts demands better quality control methodologies such as CTC control.

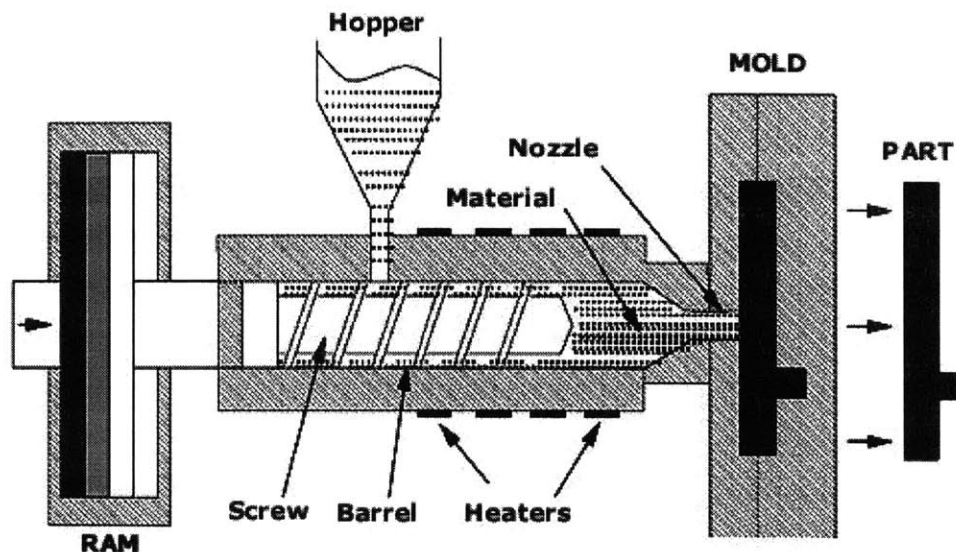


Figure 6.1: Illustration of Injection Molding Process

Source: [26]

6.1.2. Process Model and Assumptions

The injection molding process differs from air bending process fundamentally in the way the disturbance is modeled. Because of the involvement of heat transfer, which is an inherently slow process for plastic, the effect of a thermal disturbance can span several cycles. In other words, the air bending assumption that the process is uncorrelated is no longer valid. The revised assumptions are as follows:

1. There is correlation in the process disturbance model from cycle to cycle. In other words, one would expect the variation of the output to be correlated.
2. The process can still be assumed as a linear system so that simple linear control strategies can be applied.
3. There is a one-cycle process delay.

A schematic of the model is shown in Figure 6.2 below. The correlation filter shown here is a first order filter, but the correlation can be of any order or form (can also be non-linear).

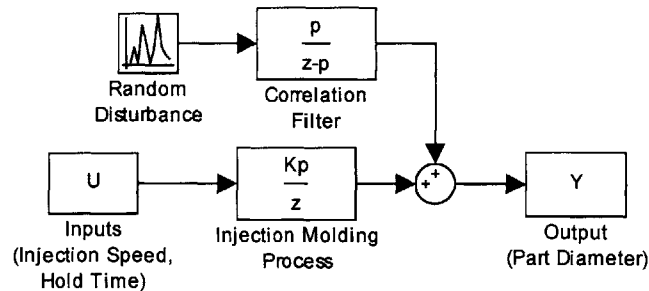


Figure 6.2: Model Schematics for Injection Molding Process

Based on the model given above, we would expect the following results to be shown in the actual experiments:

1. Feedback control of the correlated process would decrease the variance and bring a process closer to its desired target.
2. Using an integral controller would reject step disturbances completely.
3. Improved performance (in terms of quality loss, C_{pk} etc) compared with other quality control methodology such as acceptance sampling, SPC etc.

6.2. Experimental Setup

Injection molding machines consist of two basic parts, an injection unit and a clamping unit. Figure 6.3 below is a photograph that shows the injection molding machine used for the experiment at the Massachusetts Institute of Technology. The injection molding machine operation is fully automated. The control panel allows the setting of different input setting and is used for feedback input during the experiment. The adjustable inputs include packing pressure, injection boost pressure, nozzle/barrel temperatures, injection speed and packing hold time. A picture of the control panel is shown in Figure 6.4.

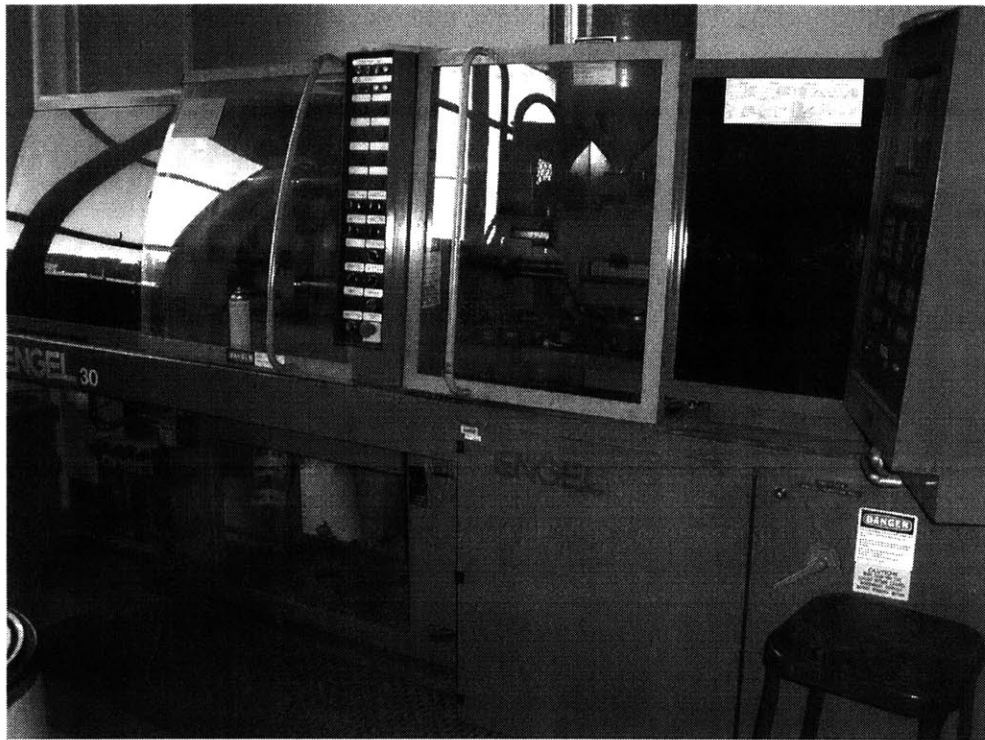


Figure 6.3: Injection Molding Machine used for experiment



Figure 6.4: Injection Molding Machine controller panel

The plastic material used throughout the experiment is ABS. The mold used for the experiment forms a cylindrical part that has a slit gap at one end. It is believed that the existence of the gap would increase the variability of the part and thus have more room for improvement. Figure 6.5 shows a picture of one-half of the mold with the final part still on the mold.



Figure 6.5: Injection Molding Die Close-up with Part

A Precision Dial Caliper (see Figure 6.6) is used for measurement of the part diameters. Measurements are made for the diameter of the cylinder at the top of the part across the gap (see Figure 6.7). The accuracy of the device is 0.001". The measurement is entered into a laptop computer running a spreadsheet program. It contains the feedback control algorithm that provides the adjusted input parameters for the next cycle. Control action is then carried out manually by entering inputs at the control panel for the next cycle.

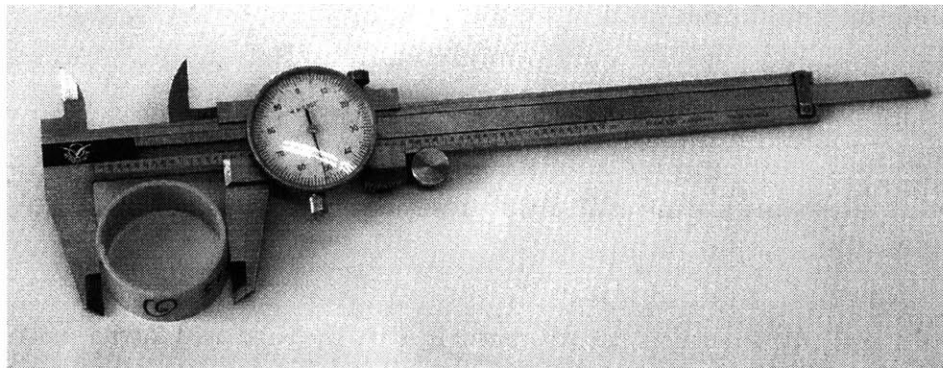


Figure 6.6: Dial Caliper measuring an injection molded part

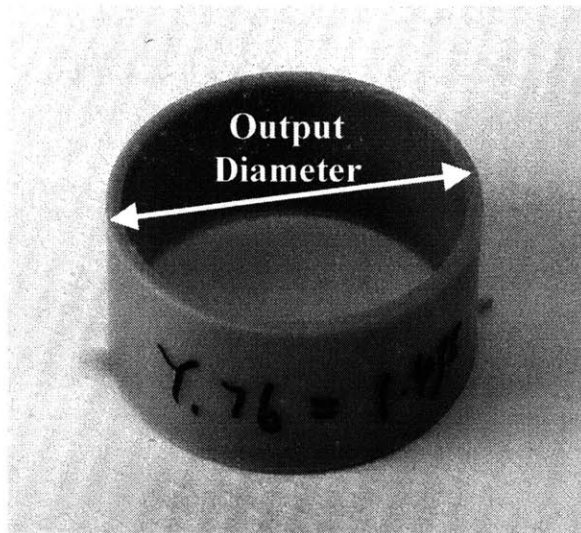


Figure 6.7: Output Part Dimension

6.3. Experimental Procedure and Observations

The goals of the experiment are to examine the correlated nature of the process, to show the behavior of the process under different control schemes and to demonstrate the ability to improve the process using CTC control.

The process is modeled as a multiple-input single-output (MISO) system (it is later found statistically that the only one input parameter is affecting the output). The expected natural disturbances of the process include the variation in material properties and temperatures. A simulated disturbance can be introduced by adjusting the nozzle/barrel temperature of the injection unit. Feedback control strategies to be tested include proportional and integral. Sample size for the experiments vary from 20 to 50 depends on the behavior of the output and the accuracy of the parameters needed.

6.3.1. Procedures

The experimental procedure is divided into three steps:

1. Design of experiment to characterize process gain.
2. Open-loop run and closed-loop control using P-controller.
3. Closed-loop control of the process using I-controller.

Design of experiments (DOE) is used to characterize the process gains because the process has multiple inputs. One necessary assumption for this step is that steady state is reached within each process cycle and it is necessary to carry out the DOE. A linear input-output relationship can be obtained from the designed experiments.

We obtain process statistics such as mean and standard deviation during the open-loop run. Unlike the bending experiment, however, measurements have to be made immediately after each cycle while the part is still warm. Because cooling of plastic is slow, it will cause the closed-loop cycle time to be unacceptably long if cold measurements are used. Since the dimension of the cooled parts is important, measurements are also obtained for the cooled samples to get a correlation between hot and cold measurements. If there is strong correlation between hot and cold measurements, we can simply rely on the “real-time” (hot) measurement for feedback.

When operating in closed-loop mode, measurements would be fed back after each cycle to adjust for the next cycle. A schematic diagram showing the components of the feedback loop is given in Figure 6.8 below. The different control schemes differ only in the algorithm used in the spreadsheet program.

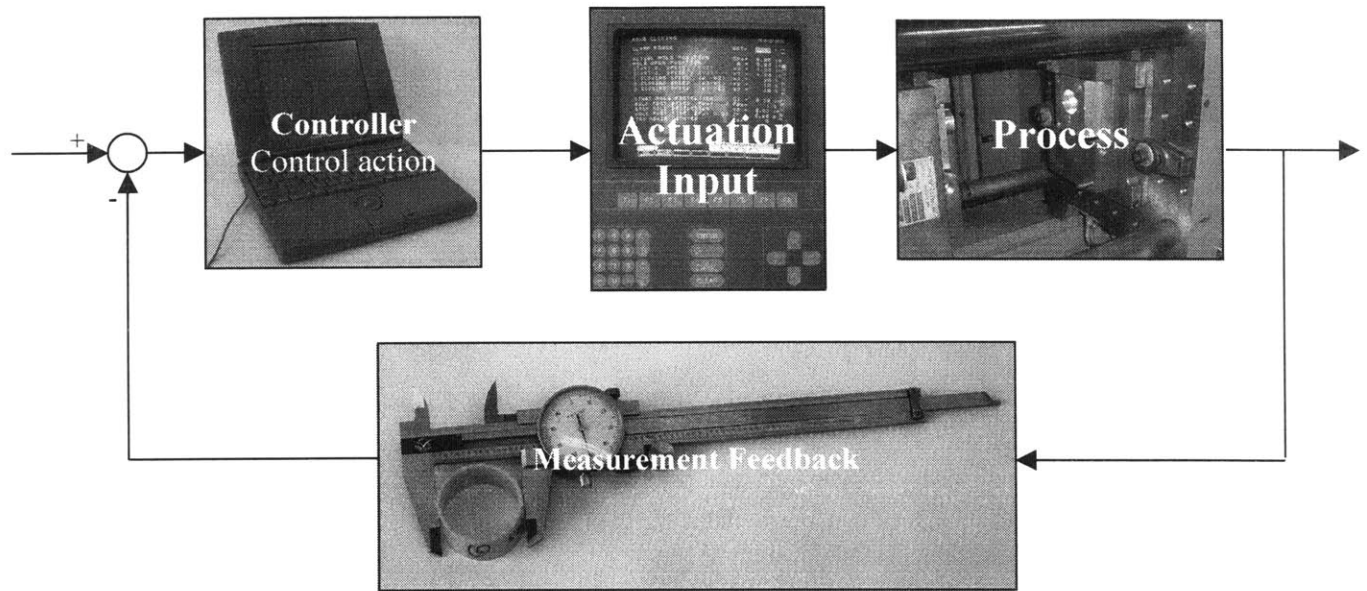
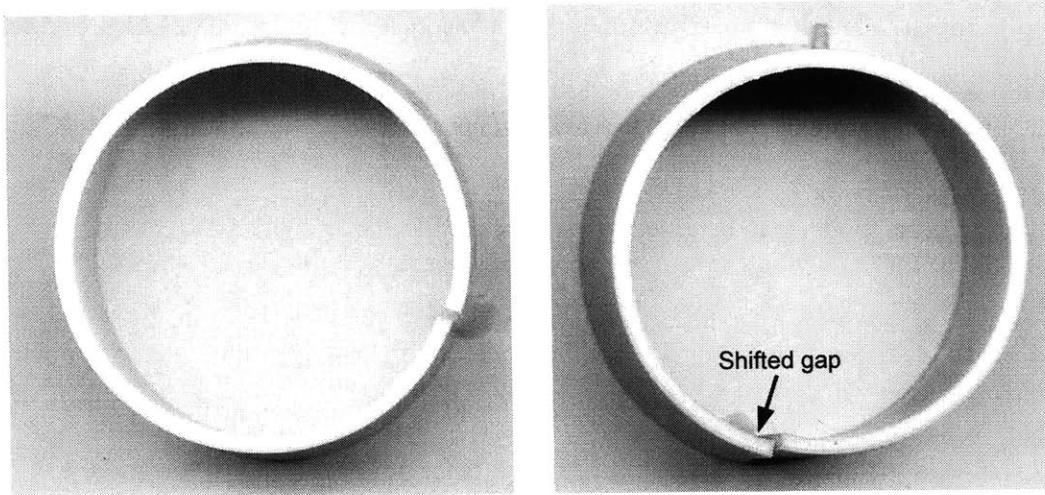


Figure 6.8: Feedback Control schematics for Injection Molding process

6.3.2. Observations

One observation of the experiment is the defective parts generated by the process. Because of the presence of the gap, some of parts have one side of the gap shifted outward (see Figure 6.9). An average increase of about 0.01” among the defective parts is resulted in the measurements. In addition, it is noted that the average number of defective parts during closed-loop runs is lower than the open-loop runs.



**Figure 6.9: Comparison of a good and bad part
Good part after cooling (left), Defective parts cooling (right)**

6.4. Data analysis

6.4.1. Design of experiment to characterize process gain

The goal of the design of experiment (DOE) is to obtain the input-output relationship for the injection molding process. From previous experience, three inputs are believed to have significant effect and are thus considered. The valid range of operations are given in Table 6.1:

Process inputs	Limits	
X_1 = Nozzle/Barrel temperatures ($^{\circ}\text{C}$)	430 $^{\circ}\text{F}$	450 $^{\circ}\text{F}$
X_2 = Hold time (seconds)	1 sec	50 sec and up
X_3 = Injection speed (in/sec)	0.2 in/sec	6.3 in/sec

Table 6.1: Input parameters and the range of operations

Temperatures have three settings on the machine (referred to different locations in the barrel) and we keep all three settings the same. We feel that varying the nozzle/barrel temperatures would not be practical for CTC control because the settling would be too long. As a result, the nozzle/barrel temperatures are fixed for each set of design of experiment. Three sets of DOE's are performed at three temperature levels: 430 $^{\circ}\text{F}$, 440 $^{\circ}\text{F}$ and 450 $^{\circ}\text{F}$. Only the result for 450 $^{\circ}\text{F}$ is presented here

because the closed-loop experiments are conducted only at this temperature. The DOE results for the other two temperatures can be found in Appendix B. In contrast to the result of 450 °F, a different input factor is significant at the two lower temperatures.

The following linear model is to be tested by each set of 2^2 DOE experiments:

$$\hat{Y} = \beta_0 + \beta_2 \cdot X_2 + \beta_3 \cdot X_3 + \beta_{23} \cdot X_2 \cdot X_3 \quad (6.1)$$

where \hat{Y} is the predicted output and β_i 's are the model coefficients to be determined through experiments.

The experiment utilizes two levels for each factor and we use 6 replicates for each experiment to get good estimates of variance. A total of 24 parts are made. Table 6.2 indicates the input levels used.

Process inputs	Levels	
X ₂ = Hold time (seconds)	5 sec	20 sec
X ₃ = Injection speed (in/sec)	0.5 in/sec	6 in/sec

Table 6.2: Design of experiment input levels used

The results of the first DOE analysis are shown in Table 6.3. Only the hold time is found to have significant effect on the output. Detailed explanation of the DOE procedure can be found in Devor et al. [1].

Effect	beta	SS	DOF	MS	F	F _{crit}	p-value
1	1.437	49.568	1	49.568	20163205	4.351	0.000
X2 (Hold time)	-1.04E-03	0.000	1	2.6E-05	10.593	4.351	0.004
X3 (Injection speed)	-3.75E-04	0.000	1	3.38E-06	1.373	4.351	0.255
X2X3 (Hold time*Injection speed)	2.92E-04	0.000	1	2.04E-06	0.831	4.351	0.373
Error		0.000	20	2.46E-06			
Total		49.568	24				

Table 6.3: First round ANOVA table

A second round of DOE is conducted with the simplified model in equation (6.2) and the experimental results are presented in Table 6.4:

$$\hat{Y} = \beta_0 + \beta_2 \cdot X_2 \quad (6.2)$$

Effect	beta	SS	DOF	MS	F	F _{crit}	p-value
1	1.437	49.568	1	49.57	19978504	4.301	0.000
X2 (Hold time)	-1.04E-03	0.000	1	2.604E-05	10.496	4.301	0.004
Error		0.000	22	2.481E-06			
Total		49.568	24				

Table 6.4: Second round design of experiment result

The coefficients of the model are found to be 1.439 for the constant term and -1.389×10^{-4} for the hold time, giving the following linear relationship for the process:

$$\hat{Y} = 1.439 - 1.389 \times 10^{-4} \cdot X_2 \quad (6.3)$$

The process gain (K_p) is, therefore, estimated to be -1.389×10^{-4} with hold time as the only effective input. For an input range from 1 sec to 30 sec, the process gain will result in a change of 0.004” on the output.

Although this process gain (for hot measurements) is useful for “real-time” feedback adjustment, the only useful output is the dimension of the cooled part. The CTC control scheme would be useless if the cold measurement have no correlation with the hot measurement. A correlation analysis is, therefore, performed to check this assumption. The correlation coefficient between hot and cold measurements for all the results in the DOE experiments shows a positive correlation of 0.601. The positive correlation means that a larger hot measurement generally leads to a larger cold measurement. Hypothesis testing shows that it is 95% confident that the correlation coefficient is greater than 0.485. A plot showing correlation of cold and hot measurements is given in Figure 6.10.

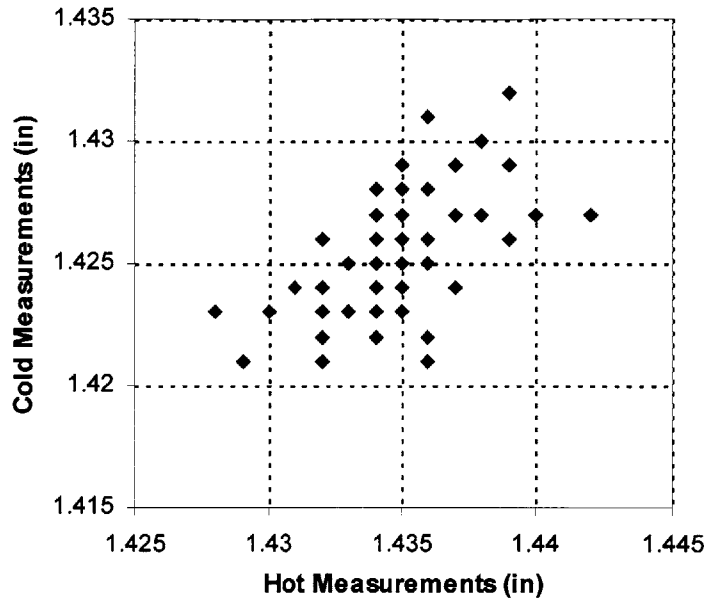
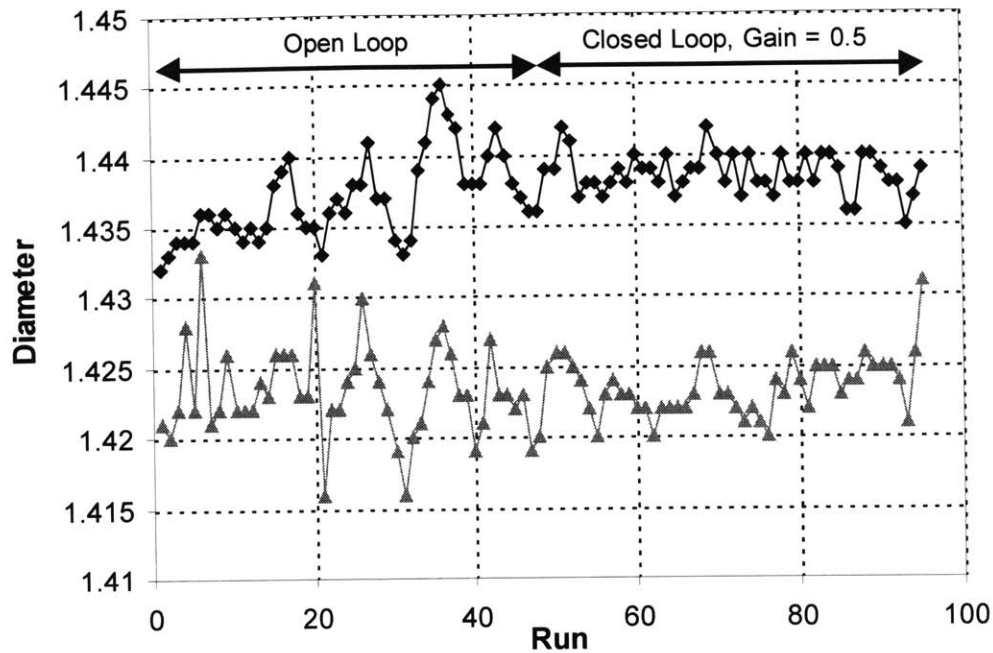


Figure 6.10: Correlation plot between hot and cold measurement

6.4.2. Closed-loop control of the process with P-controller

Due to the sensitive nature of the injection molding process, open-loop experiments are performed together with the closed-loop experiment on the same day for more accurate comparisons. This is to ensure that the effect of ambient temperature and moisture level would not corrupt the result of the experiments. The target of the experiments is 1.437", which is the mean value obtained in the DOE analysis.

In the first experiment, we wish to demonstrate the variance reduction property of CTC control. The experiment starts out with 45 cycles of open-loop runs and is then followed by 45 cycles of closed-loop run. We use a P-controller with a gain of 0.5 for the closed-loop control. It should be noted that different values of controller gain are experimented but it is found that a gain higher than 0.5 would result in saturation of the process and thus lead to erratic behavior. The run chart of the experiment is shown in Figure 6.11.



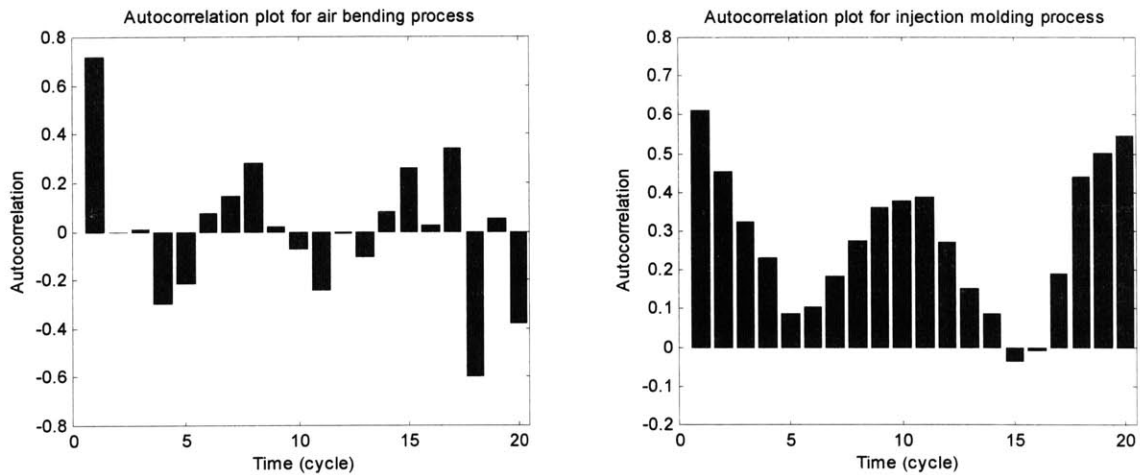
**Figure 6.11: P-controller closed-loop run
Hot measurement (top), Cold measurements (bottom)**

It can be seen that the open-loop portion of the experiment has a higher variance than closed-loop section. The run statistics are tabulated in Table 6.5 below. The variance ratio is found to be 0.234. Hypothesis testing results show that the variance ratio is outside the limits of 95% F-statistics (0.612 and 1.623 respectively). So the conclusion is that the closed-loop variance is 2.6 times smaller than the open-loop variance with 95% certainty. Or it could also mean that the closed-loop variance is smaller than the open-loop variance with 99.999% certainty. The theoretical variance ratio, for an uncorrelated process, is 1.333. This part of the experiment shows significant evidence that the injection molding process is correlated. Some oscillatory behavior can also be seen in closed-loop run, which is expected for P-controllers.

Experiment	Mean (Hot measurement)	Variance	Variance Ratio
Open-loop	1.437	9.97E-06	-
Closed-loop	1.439	2.34E-06	0.234

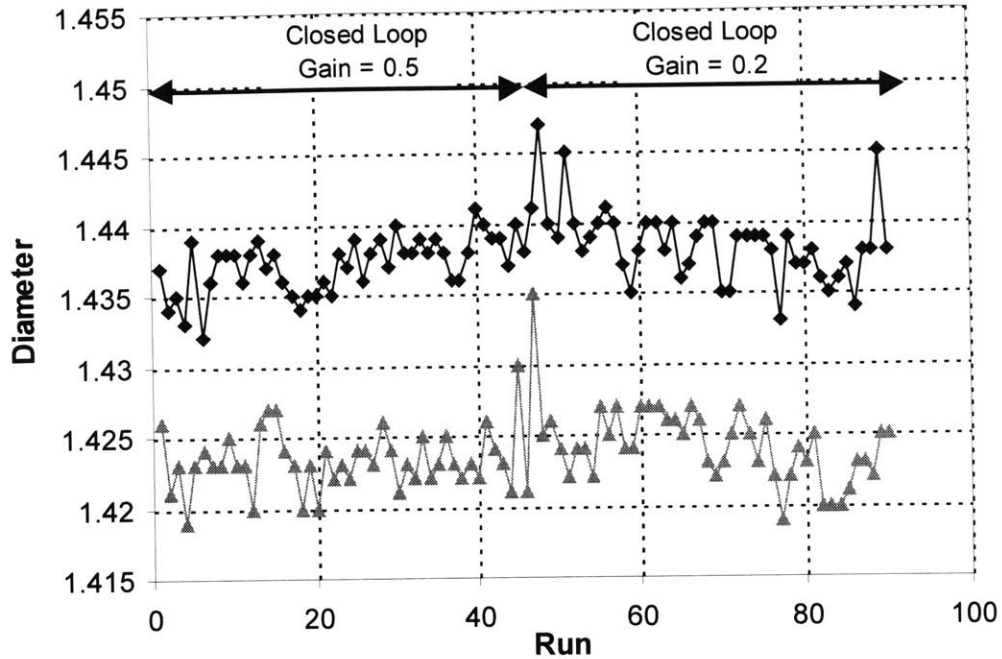
Table 6.5: Run statistics for P-controller run

In addition to the variance ratio, we also perform an autocorrelation test for the open-loop experiment. Figure 6.12 below shows a comparison of the autocorrelation plots between open-loop bending and injection molding processes. The contrast is overwhelming, with injection molding process showing significant correlation between cycles. A run test is also performed to test for autocorrelation statistically. It is found that there are 6 runs for the injection molding process, way outside the 97.5% statistical limits of 14 and 27. The cold measurements, eliminating results of defective part, also show significant autocorrelation; the run value is 11, outside the run test limits of 14 and 27. For air bending experiment, on the other hand, we can not statistically prove that there is autocorrelation in the open-loop experiment. Detailed explanations of autocorrelation and run test calculations can be found in Bendat and Piersol [27].



**Figure 6.12: Autocorrelation comparison between open-loop process
Air bending process (left), Injection Molding Process (right)**

Immediately following the first experiment, we intentionally try to introduce a step disturbance by changing the nozzle/barrel temperature to 440°F. The change is made at the beginning of the experiment. 45 cycles of closed-loop run with a gain of 0.5 is followed by 45 cycles of closed-loop run with gain of 0.2. The run chart is shown in Figure 6.13. It shows slightly higher variance for K_c of 0.5 than 0.2.



**Figure 6.13: P-controller closed-loop run with gain change
Hot measurement (top), Cold measurements (bottom)**

The run statistics are tabulated in Table 6.6 below. The open-loop variance from the previous experiment is used. For K_c of 0.5, the variance ratio is 0.390. For K_c of 0.2, the variance ratio is clearly larger at 0.737. Hypothesis testing shows no evidence of variance reduction for K_c of 0.2 (limits for 95% F-statistics were 0.612 and 1.623). As expected, the mean value is closer to the target when K_c is 0.5 than when K_c is 0.2. Also, slightly more oscillatory behavior is observed for a closed-loop gain of 0.5 than a gain of 0.2, which conforms to analytical prediction (see Figure 6.14 for root locus diagrams).

Experiment	Mean (Hot measurement)	Variance	Variance Ratio
Closed-loop, $K_c = 0.5$	1.437	3.89E-06	0.390
Closed-loop, $K_c = 0.2$	1.439	7.35E-06	0.737

Table 6.6: Run statistics for disturbed P-controller run

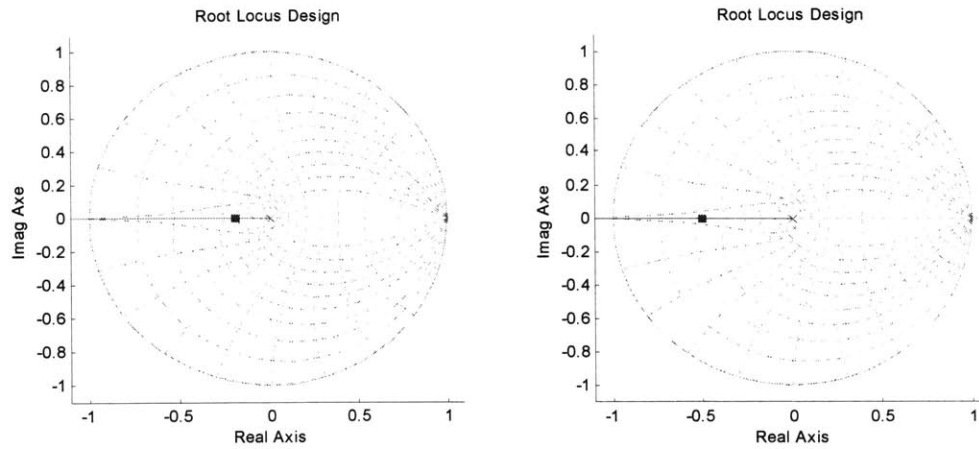


Figure 6.14: Root locus diagram for P-controller
 $K_c = 0.2$ (left), $K_c = 0.5$ (right), more oscillation for poles away from the origin

In the third experiment, we try to demonstrate the target centering capability of the closed-loop system. The experiments start out with the target set at 1.436" for 45 cycles, then we shift to a target of 1.440" for another 45 cycles; finally, we perform an open-loop run for 50 cycles. The controller gain is set at 0.5 throughout and the barrel temperature is fixed at 450°F. The run chart is shown in Figure 6.15. The run statistics is given in Table 6.7. Some saturation behavior is observed when the target is set at 1.436", possibly explaining why the output is slightly off the target. There is a difference in the mean value for the two closed-loop runs. Hypothesis testing is performed to see if the difference is statistically significant. It is shown with 95% confidence that the second mean is larger than the first mean, with the difference in mean value to be at least 0.0012". The results of this experiment demonstrate the target centering ability of a closed-loop system.

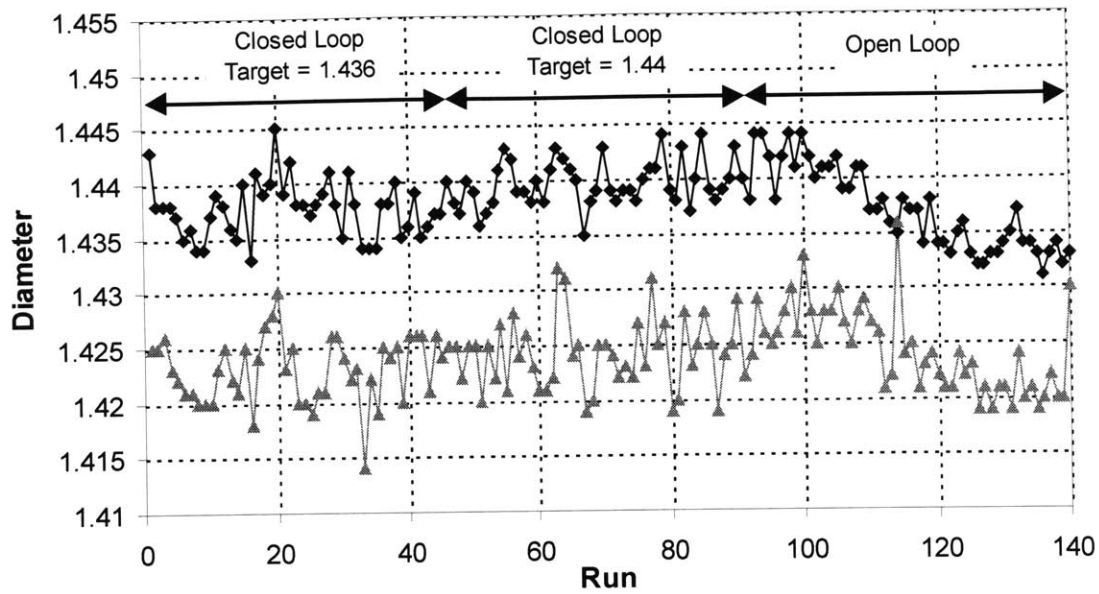


Figure 6.15: Closed-loop P-controller target shifted

Experiment	Mean (Hot measurement)	Variance	Variance Ratio
Closed-loop, target = 1.436"	1.438	6.79E-06	0.471
Closed-loop, target = 1.440"	1.440	4.54E-06	0.315
Open-loop	1.437	1.44E-05	-

Table 6.7: Run statistics for P-controller with varying target

6.4.3. Closed-loop control of the process with I-controller

Finally, an I-controller is used for the injection molding process. The process seems to be biased towards one side of the target and is thus prone to accumulating a large sum of error for the I-controller. A controller gain of only 0.2 is used to try to compensate this. But the result still shows over-compensation and saturation of the process. This can be attributed to the process having a rather narrow operating range. The run chart and run statistics are given in Figure 6.16 and Table 6.8 respectively. The variance ratio is 0.395 and hypothesis testing shows that there is a variance reduction. The theoretical variance amplification for an uncorrelated process is 1.111.

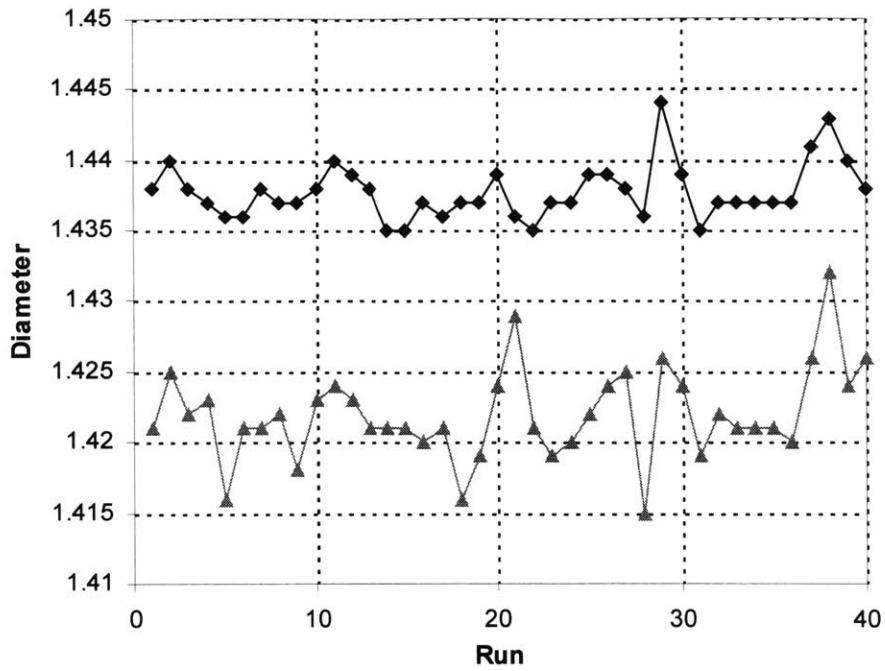


Figure 6.16: I-controller closed-loop run

Experiment	Mean (Hot measurement)	Variance	Variance Ratio
Closed-loop, target = 1.436"	1.438	3.94E-06	0.395
Open-loop, from first experiment	1.437	9.97E-06	-

Table 6.8: Run statistics for I-controller

As expected, there is no obvious oscillatory behavior for the I-controller system (see Figure 6.17 for root locus diagram). But this might have been a result of the saturation that took place during the experiment. A different part, which has less intrinsic variation, together with a more precise measurement system can be used to redo this part of the experiment for better results in the future. A heuristic algorithm controller that has actuation limits can also be used to ensure operation within the operating limits.

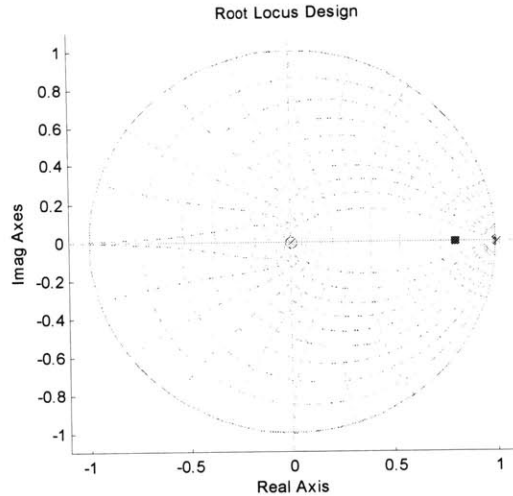


Figure 6.17: Root locus diagram for I-controller
Non-oscillatory behavior expect with closed-loop pole on the real axis

6.5. Conclusions

Most experiments behave as expected. Some key findings in the experiment include:

1. Injection molding process is highly correlated.
2. Cycle-to-cycle control using hot measurement results in process improvement of the cooled part. This is because the two measurements are highly correlated.
3. We can use CTC control to reduce the variance and move the process closer to the target for the injection molding process.
4. In closed-loop control, an integral controller that accumulates all errors can cause over-adjustment and saturation on a process with narrow operating range.

A thermoforming experiment is also conducted to try to come up with similar results as the injection molding experiment. The shape of the thermoformed part is shown in Figure 6.18. Measurement of the output part, however, proved to be problematic. First of all, the flexibility of the thermoformed part gives inaccurate measurements. Thicker material helped to reduce the problem but it was still a delicate operation. Secondly, the side of the part is tapered (see Figure 6.19), making the measurement inconsistent from part to part.

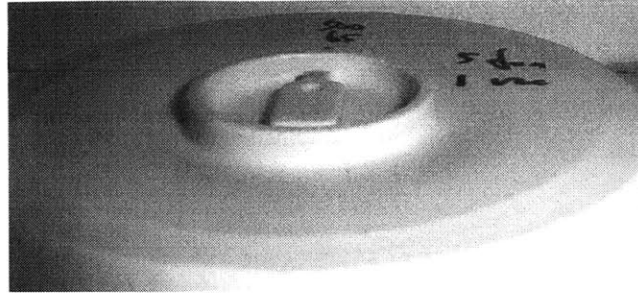


Figure 6.18: Illustration of a thermoformed part

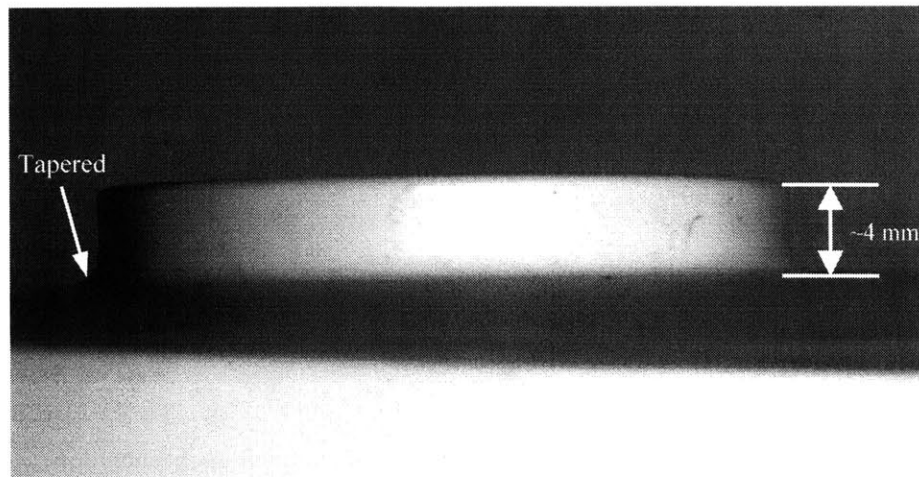


Figure 6.19: The side of a thermoformed part is tapered at the bottom

A more proper thermoforming experiment would require a part that has a much longer vertical feature so that the tapered effect would be much less of an issue.

The results from the injection molding experiment complement the results of the air bending experiment very well. Injection molding is an inherently correlated process with large random noise. Air bending, on the other hand, is uncorrelated with relative low random noise. Together, they are able to represent a wide range of the parallel manufacturing processes commonly used today. This concludes the core experimental component of the research, which is intended to verify some of the theories of CTC control and to demonstrate applications to new processes.

Chapter 7: Conclusions and Recommendations

7.1. Summary of results

7.1.1. Experimental results

Because of the target centering ability of the closed-loop systems, we expect that CTC feedback control would provide better quality when compared to traditional quality control methodologies such as SPC, acceptance sampling, etc. The two key advantages of CTC feedback control that the experiments in this research demonstrated are:

1. In the ever-increasing demands of flexible manufacturing, the average production run length of a manufacturing process tends to decrease. New setups usually mean a change in operation conditions; and this can be represented by shift disturbances. Cycle-to-cycle control is especially effective in short run systems because it can remove the shift disturbance quickly.
2. Some manufacturing processes are inherently correlated. This means that the outputs of subsequent cycles are related and can be defined by a mathematical function (e.g. EWMA correlation or first order correlation.). Utilizing CTC control can reduce the output variance and thus improve the process capability.

Some drawbacks of CTC feedback control are also prevalent in the experiments.

1. The cost of implementation from two perspectives: high measurement cost to inspect all output parts and high adjustment cost for some processes.
2. The increase of cycle time while waiting for measurement can be an obstacle for high rate processes.
3. If the disturbances of the process are uncorrelated with stable outputs (i.e. no deterministic disturbances such as step or ramp disturbance), we may end up increasing the variance of the process and thus corrupt the quality of the output.

The drawbacks are important for us to better understand the concept of CTC control. Over time, however, these drawbacks can be overcome with more research and implementation. The following are some of the expectations:

1. Cost of measurement is coming down with new sensor technologies that are faster and more accurate.
2. Adaptive control can dynamically model the process online and adjust the controller gain accordingly to achieve optimal performance.
3. Automatic feedback system incorporating advanced vision systems and robotic systems for handling outputs can bring CTC feedback control to high production processes.

7.1.2. Additional insights

In addition to quality improvement on each individual process, CTC feedback control provides a framework for improving process capability of the entire system. Information collected on output parameters and cycle time can be used to improve the manufacturing system as a whole. It is almost like further expanding the concept of CTC control by closing the loop at the system level. The most important attribute for a manufacturing system is to meet customer needs. Only the final output of the manufacturing system is of interest from a customer point of view. By closing the loop on the entire system, we can control the final output of the system just like we did for each process.

7.2. Recommended future work

Future research work for CTC feedback control can be classified into short-term and long-term research. For short-term research, it can be accomplished mainly by acquiring results from established areas and adapting it to existing applications. The long-term research interest would involve applying the method to more complex processes and also to the system level.

7.2.1. Short-term research goals

1. Continue the development of CTC feedback control theory, particularly in the area of system identification. This would allow the study of online model fitting and adaptive control of manufacturing processes.
2. The process model used in this research assumes an additive disturbance, meaning the disturbance is added to the linear plant output at the output end. In reality, however, the plant gain is the parameter that varies. For example, material property is the main source of variation and the plant gain, K_p , is the parameter subjected to disturbance.
3. Implementation of CTC feedback control to manufacturing processes that are economically viable without the need of automatic measurement system (e.g. metal bending, injection molding and thermoforming of large parts).

7.2.2. Long-term research goals

1. Industrial adaptation of CTC feedback control to high volume processes by using advanced metrology devices such as laser measurement.
2. The use of measurement information to improve quality at a system level.
3. Study the practicality of implementing fully autonomous equipment using CTC feedback control methodology.

7.3. Final words

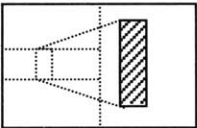
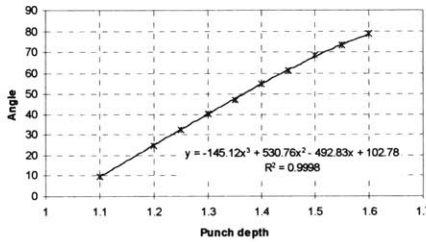
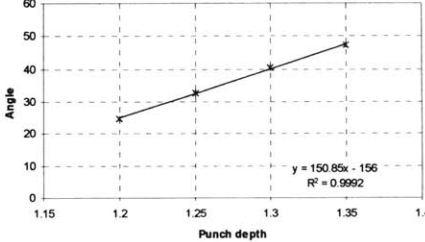
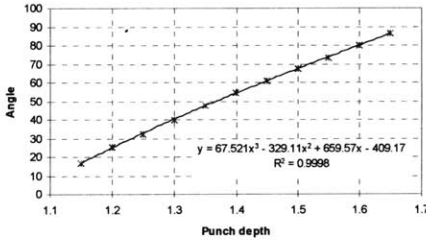
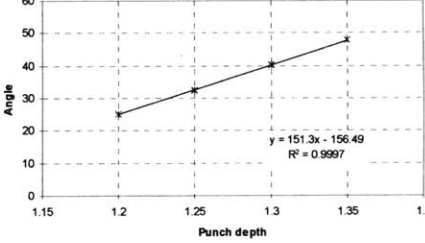
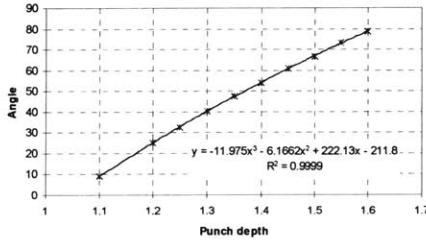
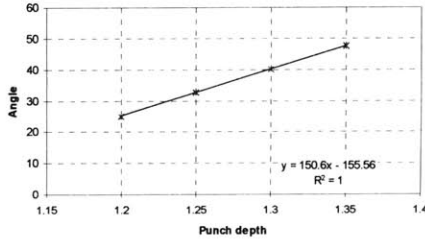
A great deal is learned throughout this research. A seemingly break-through idea is found to be shared by numerous colleagues in manufacturing. We realize that this field would share many ideas with subjects such as discrete signal processing, time series analysis and operations research. There is also a match of CTC control with vision of the next generation manufacturing concept.

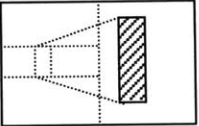
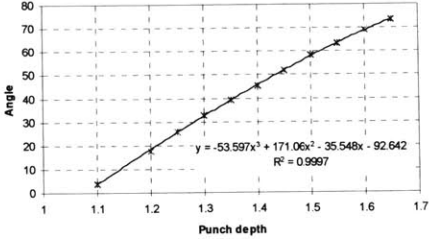
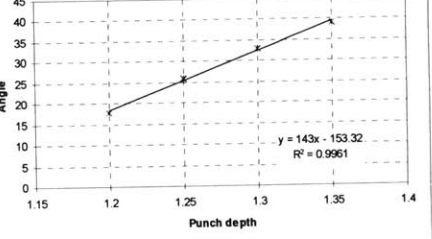
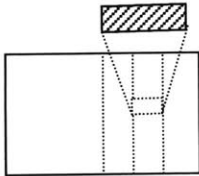
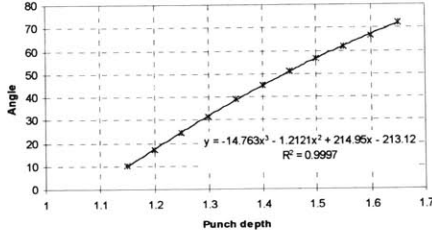
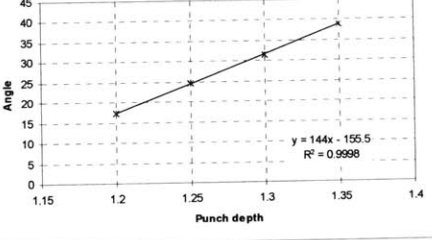

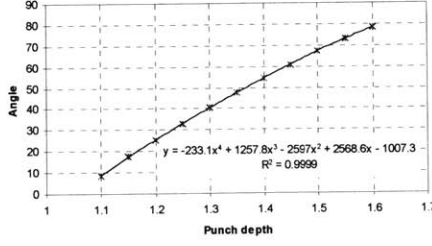
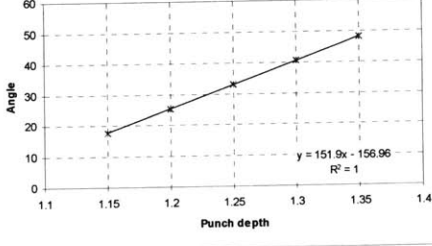
When I discussed with my friends and colleagues about my research, most of them seemed to be surprised by the simplicity of the concept. Yet many of them could not believe that this idea has not been studied and used widely in industry. As one proverb says, “simplicity is as common as tall grass on a busy highway”, perhaps it is not always easy to realize something simple and obvious in life.


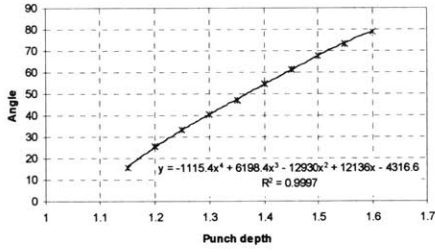
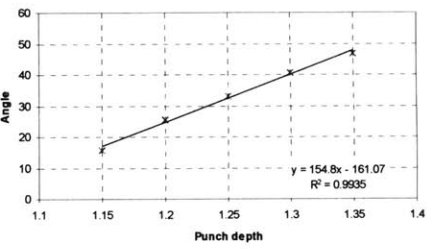
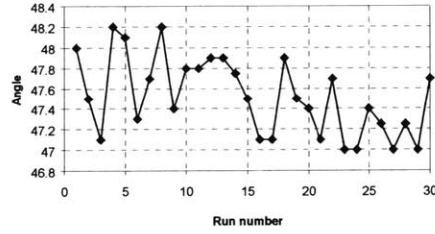
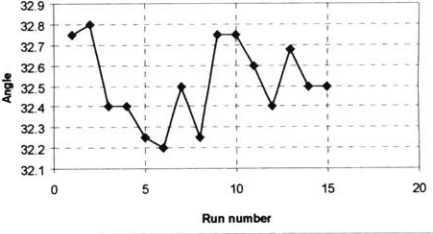
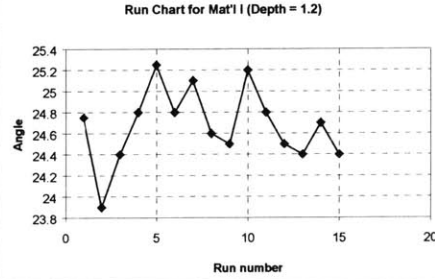
Appendix A

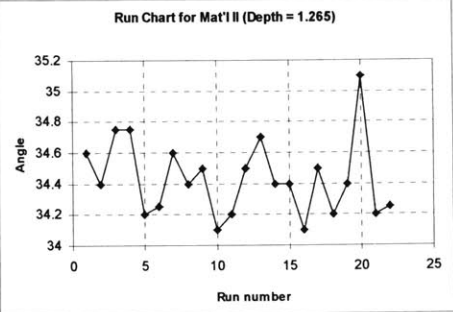
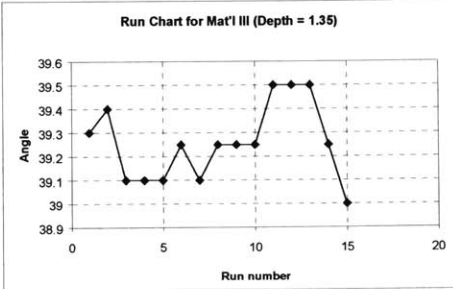
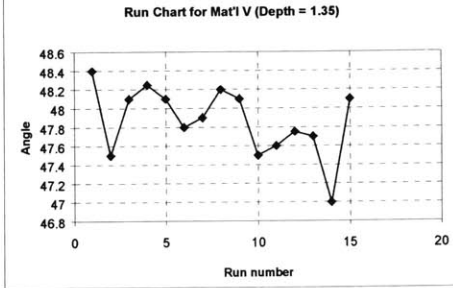
Summary of analysis for air bending process

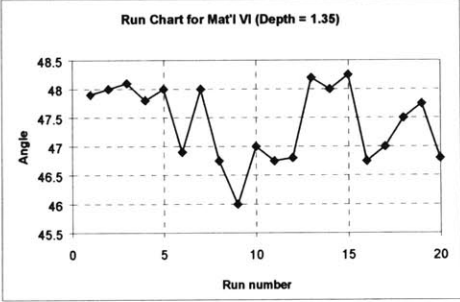
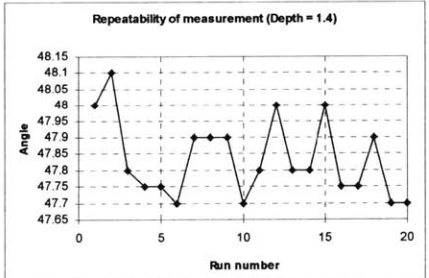
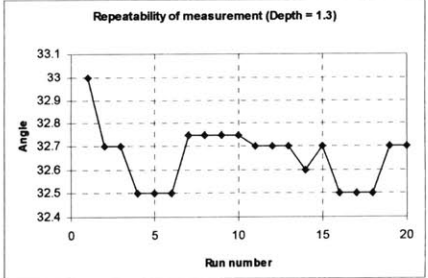
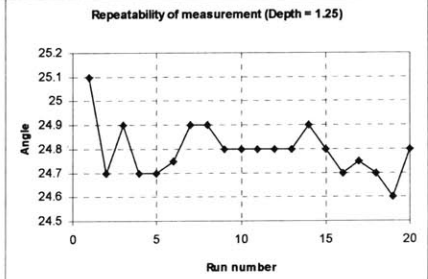
1. Open-loop characterization of the processes and materials

Experiments	Material	Results or Characterization Chart	
a. Characterization of plant gain 	I. 0.025" steel (vertical strip)	<p>Response Curve (Mat'I I)</p>  <p>$y = -145.12x^3 + 530.76x^2 - 492.83x + 102.78$ $R^2 = 0.9998$</p>	<p>Local Response Curve (Mat'I I)</p>  <p>$y = 150.85x - 156$ $R^2 = 0.9992$</p>
	Ia. 0.025" steel (vertical strip)	<p>Response Curve (Mat'I Ia)</p>  <p>$y = 67.521x^3 - 329.11x^2 + 659.57x - 409.17$ $R^2 = 0.9998$</p>	<p>Local Response Curve (Mat'I Ia)</p>  <p>$y = 151.3x - 156.49$ $R^2 = 0.9997$</p>
	II. 0.025" steel (horizontal strip)	<p>Response Curve (Mat'I II)</p>  <p>$y = -11.975x^3 - 6.1662x^2 + 222.13x - 211.8$ $R^2 = 0.9999$</p>	<p>Local Response Curve (Mat'I II)</p>  <p>$y = 150.6x - 155.56$ $R^2 = 1$</p>

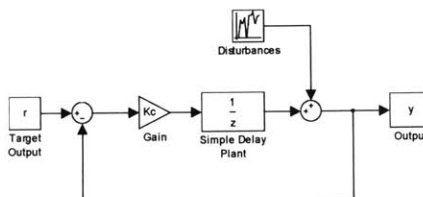
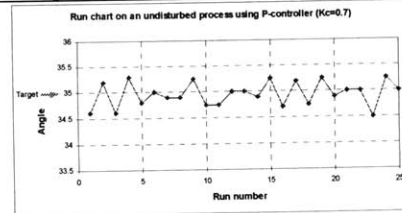
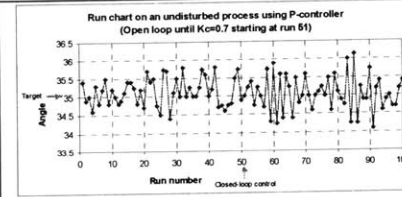
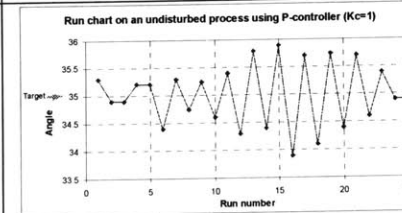
<p>a. Characterization of plant gain</p>	<p>III. 0.02" steel (vertical strip)</p> 	<p>Response Curve (Mat'l III)</p>  $y = -53.597x^3 + 171.06x^2 - 35.548x - 92.642$ $R^2 = 0.9997$	<p>Local Response Curve (Mat'l III)</p>  $y = 143x - 153.32$ $R^2 = 0.9961$
	<p>IV. 0.02" steel (horizontal strip)</p> 	<p>Response Curve (Mat'l IV)</p>  $y = -14.763x^3 - 1.2121x^2 + 214.95x - 213.12$ $R^2 = 0.9997$	<p>Local Response Curve (Mat'l IV)</p>  $y = 144x - 155.5$ $R^2 = 0.9998$
	<p>V. 0.032" aluminum (vertical grain)</p> 	<p>Response Curve (Mat'l V)</p>  $y = -233.1x^3 + 1257.8x^2 - 2567x^2 + 2568.6x - 1007.3$ $R^2 = 0.9999$	<p>Local Response Curve (Mat'l V)</p>  $y = 151.9x - 156.96$ $R^2 = 1$

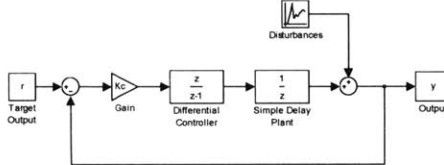
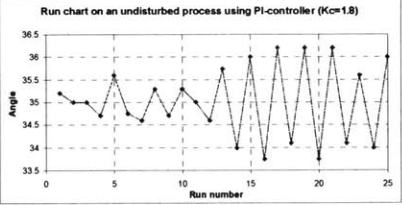
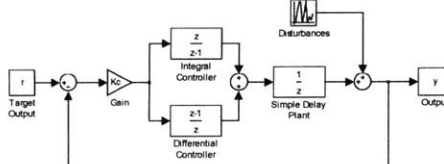
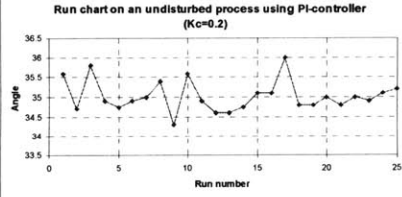
	<p>VI. 0.032" aluminum (horizontal grain)</p> 	<p>Response Curve (Mat'l VI)</p> 	<p>Local Response Curve (Mat'l V)</p> 
<p>b. Open-loop Control Run</p>	<p>I. 0.025" steel (vertical strip)</p> <p>(1.35) Standard deviation = 0.383 (1.25) Standard deviation = 0.200 (1.2) Standard deviation = 0.352</p>	<p>Run Chart for Mat'l I (Depth = 1.35)</p> 	<p>Run Chart for Mat'l I (Depth = 1.25)</p>  <p>Run Chart for Mat'l I (Depth = 1.2)</p> 

<p>b. Open-loop Control Run</p>	<p>II. 0.025" steel (horizontal strip) (1.265) Standard deviation = 0.249</p>	
	<p>III. 0.02" steel (vertical strip) (1.35) Standard deviation = 0.161</p>	
	<p>IV. 0.02" steel (horizontal strip)</p>	<p>- None -</p>
	<p>V. 0.032" aluminum (vertical grain) (1.35) Standard deviation = 0.368</p>	

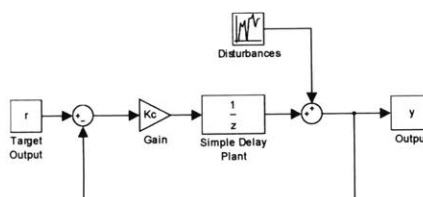
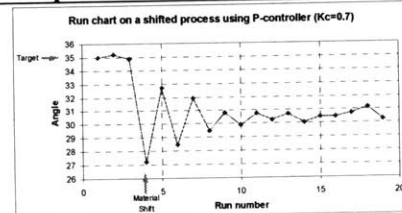
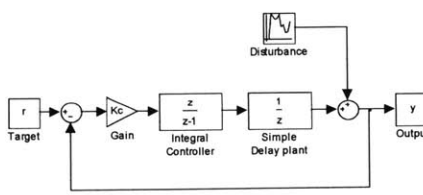
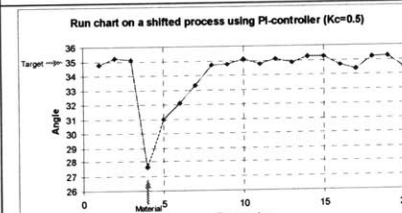
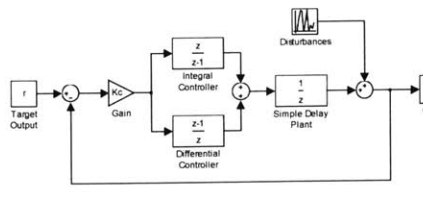
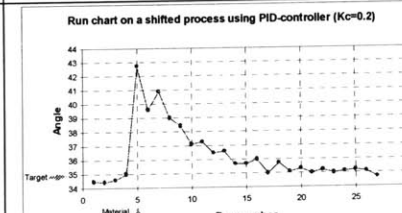
<p>b. Open-loop Control Run</p>	<p>VI. 0.032" aluminum (horizontal grain)</p> <p>(1.35) Standard deviation = 0.663</p>		
<p>c. Repeatability Test</p>	<p>I. 0.025" steel (vertical strip)</p>	<p>Depth = 1.4, Angle = 47.8; Repeatability = 0.120</p> 	<p>Depth = 1.3, Angle = 32.7; Repeatability = 0.129</p> 
		<p>Depth = 1.25, Angle = 24.8; Repeatability = 0.109</p> 	

2. Response of an undisturbed process to close-loop control

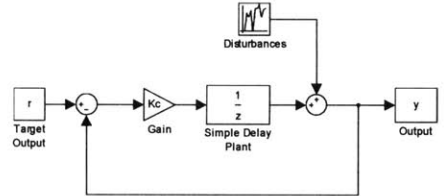
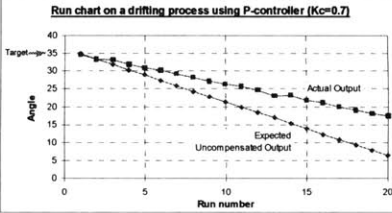
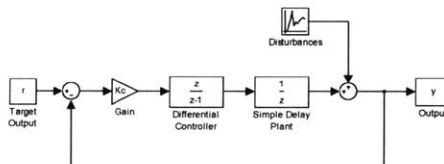
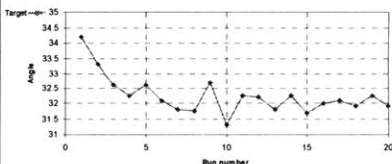
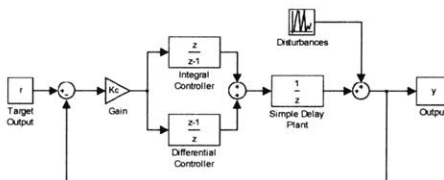
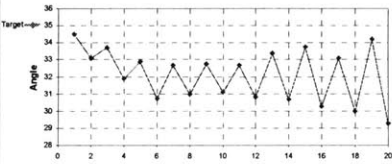

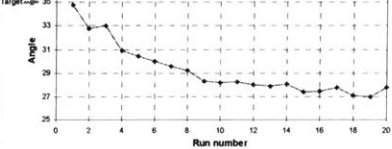
Controller Type	Expected Results	Experimental Results	Output Chart
<p>P-Controller</p> 	<p>$K_c = 0.7$ (sample size = 25)</p> $\frac{\sigma_Y^2}{\sigma_D^2} = 1.961$	<p>$K_c = 0.7$ (sample size = 25)</p> <p>$\sigma_Y^2 = 0.0535, \sigma_D^2 = 0.0618$</p> $\frac{\sigma_Y^2}{\sigma_D^2} = 0.8664! \text{ (variance reduction)}$ <p>but, both σ_D^2 and σ_Y^2 are subjected to measurement error, σ_e^2</p> <p>performing hypothesis testing</p> <p>$F^* = 0.4418,$</p> <p>$F(0.95) = 0.5141, F(0.05) = 1.901$</p>	
	<p>$K_c = 0.7$ (sample size = 50)</p> $\frac{\sigma_Y^2}{\sigma_D^2} = 1.961$	<p>$K_c = 0.7$ (sample size = 50)</p> <p>$\sigma_Y^2 = 0.237, \sigma_D^2 = 0.142$</p> <p>using $\sigma_e^2 = \text{repeatability error} = 0.0167$</p> $\frac{\sigma_Y^2}{\sigma_D^2} = 1.665, \frac{\sigma_Y^2}{\sigma_D^2} \Big _{adj} = 1.754$ <p>performing hypothesis testing</p> <p>$F^* = 0.8496,$</p> <p>$F(0.95) = 0.6222, F(0.05) = 1.607$</p>	
	<p>$K_c = 1$</p> $\frac{\sigma_Y^2}{\sigma_D^2} = \infty$	<p>$K_c = 1$</p> <p>$\sigma_Y^2 = 0.3186, \sigma_D^2 = 0.0618$</p> $\frac{\sigma_Y^2}{\sigma_D^2} = 5.155$	

<p>PI-Controller</p> 	<p>$K_c = 1.8$</p> $\frac{\sigma_Y^2}{\sigma_D^2} = 10.0005$	<p>$K_c = 1.8$</p> $\sigma_Y^2 = 0.630, \sigma_D^2 = 0.0618$ $\frac{\sigma_Y^2}{\sigma_D^2} = 10.197$ $\frac{\sigma_Y^2}{\sigma_D^2} \Big _{adj} = 13.603$ <p>performing hypothesis testing $F^* = 1.360,$ $F(0.95) = 0.5141, F(0.05) = 1.901$</p>	
<p>PID-Controller</p> 	<p>- None -</p>	<p>- None -</p>	<p>- None -</p>
	<p>$K_c = 0.2$</p> $\frac{\sigma_Y^2}{\sigma_D^2} = 1.115$	<p>$K_c = 0.2$</p> $\sigma_Y^2 = 0.144, \sigma_D^2 = 0.142$ $\frac{\sigma_Y^2}{\sigma_D^2} = 1.015$	

3. Response to a sudden shift of material – Step disturbance

Controller Type	Expected Results	Experimental Results	Output Chart
P-Controller  $Y = D - Y \cdot \frac{K_c}{z}, \text{ so } \frac{Y}{D} = \frac{z}{z + K_c}$	$K_c = 0.7$ $Y_{ss} _{r=0} = \frac{C}{1 + K_c} = -4.286$ <p>where C is the magnitude of the step disturbance = 7.287, and K_c is that of the shifted material.</p> $t_s _{5\%} = \frac{3}{ \ln(K_c) } = 9 \text{ cycles}$	$K_c = 0.7$ Steady-state value $\approx 30.35^\circ$ $\Rightarrow -4.65$ off target $t_s _{5\%} \approx 10 \text{ to } 11 \text{ cycles}$	
PI-Controller  $Y = D - Y \cdot K_c \cdot \frac{z}{z \cdot (z - 1)}$	$\frac{Y}{D} = \frac{z - 1}{z - 1 + K_c}$ $Y_{ss} _{r=0} = 0, \text{ due to free integrator}$ $t_s _{5\%} = \frac{3}{ \ln(K_c) } = 5 \text{ cycles}$	$K_c = 0.5$ Steady-state value $\approx 34.95^\circ$ $\Rightarrow -0.05$ off target $t_s _{5\%} \approx 4 \text{ to } 5 \text{ cycles}$	
PID-Controller  $Y = D - Y \cdot K_c \cdot \frac{1}{z} \cdot \left[\frac{z}{(z - 1)} + \frac{z - 1}{z} \right],$	$\frac{Y}{D} = \frac{z^2 \cdot (z - 1)}{z^3 - z^2 + K_c \cdot (2z^2 - 2z + 1)}$ $Y_{ss} _{r=0} = 0, \text{ due to free integrator}$ $t_s _{5\%} = \frac{3}{ \ln(0.785) } = 13 \text{ cycle}$	$K_c = 0.2$ Steady-state value $\approx 35.08^\circ$ $\Rightarrow 0.08$ off target $t_s _{5\%} \approx 14 \text{ to } 15 \text{ cycles}$	

4. Response to a gradual change of tailstock position – Ramp disturbance

Controller Type	Expected Results	Experimental Results	Output Chart
<p>P-Controller</p> 	<p>$K_c = 0.7$</p> <p>$Y_{ss} = -\infty$</p>	<p>$K_c = 0.7$</p> <p>$Y_{ss} = -\infty$</p>	
<p>PI-Controller</p> 	<p>$K_c = 0.5$</p> <p>$Y_{ss} _{r=0} = \frac{m}{K_c} = -3$</p> <p>where m is the slope of the ramp disturbance</p>	<p>$K_c = 0.5$</p> <p>Steady-state value $\approx 31.97^\circ$ $\Rightarrow -3.03$ off target</p>	
<p>PID-Controller</p> 	<p>$K_c = 0.5$</p> <p>$Y_{ss} _{r=0} = \frac{m}{K_c} = -3$</p> <p>where m is the slope of the ramp disturbance</p>	<p>$K_c = 0.5$</p> <p>Steady-state value $\approx 31.76^\circ$ $\Rightarrow -3.24$ off target</p>	
<p>PID-Controller</p> 	<p>$K_c = 0.2$</p> <p>$Y_{ss} _{r=0} = \frac{m}{K_c} = -7.5$</p> <p>where m is the slope of the ramp disturbance</p>	<p>$K_c = 0.2$</p> <p>Steady-state value $\approx 27.52^\circ$ $\Rightarrow -7.48$ off target</p>	

Appendix B

Complete DOE analysis for injection molding process

- The purpose of the DOE analysis is to obtain the input-output relationship of a complex system. It is a statistical method that utilizes hypothesis testing to tell the significance of each input factor on the output.
- The scheme used in our analysis is a 2-level (high and low) and 2-factor (hold time and injection speed) design. The 2-level design will give us linear relationships between the two input factors and the output. Each factor and level combination is repeated 6 times for accuracy. In DOE terminology, it is denoted as a 2^2 experiment with 6 replicates. The total number of experiments is $6 \cdot 2^2 = 24$. The linear model to be fitted by the DOE is $\hat{Y} = \beta_0 + \beta_2 \cdot X_2 + \beta_3 \cdot X_3 + \beta_{23} \cdot X_2 \cdot X_3$, where X_2 and X_3 are the two input factors, β_i 's are the coefficients to be estimated by the DOE, and \hat{Y} is the output.
- A complete description of the DOE analysis and its procedures are given in DeVor [2] and Montgomery [1].

1. Barrel temperature fixed at 450°F

X1 = 450 X2 = (5, 20) X3 = (0.5, 6)

X1 = Barrel temp

X2 = Hold time

X3 = Injection speed

DOE Matrix

	1	X2	X3	X2X3	y
1	1	-1	-1	1	1.436
2	1	-1	1	-1	1.436
3	1	1	-1	-1	1.436
4	1	1	1	1	1.435
5	1	-1	-1	1	1.439
6	1	-1	1	-1	1.436
7	1	1	-1	-1	1.439
8	1	1	1	1	1.435
9	1	-1	-1	1	1.439
10	1	-1	1	-1	1.439
11	1	1	-1	-1	1.435
12	1	1	1	1	1.435
13	1	-1	-1	1	1.437
14	1	-1	1	-1	1.438
15	1	1	-1	-1	1.435
16	1	1	1	1	1.437
17	1	-1	-1	1	1.442
18	1	-1	1	-1	1.438
19	1	1	-1	-1	1.437
20	1	1	1	1	1.437
21	1	-1	-1	1	1.44
22	1	-1	1	-1	1.438
23	1	1	-1	-1	1.435
24	1	1	1	1	1.437

First round DOE

Effect	beta	SS	DOF	MS	F	F _{crit}	
1	1.437125	49.56787838	1	49.56788	20163205	4.35125	Significant
X2	-0.00104	2.60417E-05	1	2.6E-05	10.59322	4.35125	Significant
X3	-0.00038	0.000003375	1	3.38E-06	1.372881	4.35125	Insignificant
X2X3	0.000292	2.04167E-06	1	2.04E-06	0.830508	4.35125	Insignificant
Error		4.91667E-05	20	2.46E-06			
Total		49.567959	24				

Second round DOE

Effect	beta	SS	DOF	MS	F	F _{crit}	
1	1.437125	49.56787838	1	49.56787838	19978504	4.300944	
X2	-0.001041667	2.60417E-05	1	2.60417E-05	10.49618	4.300944	
Error		5.45833E-05	22	2.48106E-06			
Total		49.567959	24				

2. Barrel temperature fixed at 440°F

X1 = 440 X2 = (5, 20) X3 = (0.5, 6)

X1 = Barrel temp
 X2 = Hold time
 X3 = Injection speed

DOE Matrix

	1	X2	X3	X2X3	y
1	1	-1	-1	1	1.432
2	1	-1	1	-1	1.437
3	1	1	-1	-1	1.434
4	1	1	1	1	1.435
5	1	-1	-1	1	1.436
6	1	-1	1	-1	1.435
7	1	1	-1	-1	1.432
8	1	1	1	1	1.435
9	1	-1	-1	1	1.432
10	1	-1	1	-1	1.435
11	1	1	-1	-1	1.434
12	1	1	1	1	1.436
13	1	-1	-1	1	1.436
14	1	-1	1	-1	1.434
15	1	1	-1	-1	1.431
16	1	1	1	1	1.436
17	1	-1	-1	1	1.434
18	1	-1	1	-1	1.436
19	1	1	-1	-1	1.433
20	1	1	1	1	1.434
21	1	-1	-1	1	1.436
22	1	-1	1	-1	1.435
23	1	1	-1	-1	1.432
24	1	1	1	1	1.436

First round DOE

Effect	beta	SS	DOF	MS	F	F _{crit}	
1	1.434417	49.38122817	1	49.38123	27951639	4.35125	Significant
X2	-0.00042	4.16667E-06	1	4.17E-06	2.358491	4.35125	Insignificant
X3	0.000917	2.01667E-05	1	2.02E-05	11.41509	4.35125	Significant
X2X3	0.000417	4.16667E-06	1	4.17E-06	2.358491	4.35125	Insignificant
Error		3.53333E-05	20	1.77E-06			
Total		49.381292	24				

Second round DOE

Effect	beta	SS	DOF	MS	F	F _{crit}	
1	1.434416667	49.38122817	1	49.38122817	24879092	4.300944	
X3	0.000916667	2.01667E-05	1	2.01667E-05	10.16031	4.300944	
Error		4.36667E-05	22	1.98485E-06			
Total		49.381292	24				

3. Barrel temperature fixed at 430°F

$X1 = 430$ $X2 = (5, 20)$ $X3 = (0.5, 6)$

X1 = Barrel temp

X2 = Hold time

X3 = Injection speed

DOE Matrix

	1	X2	X3	X2X3	y
1	1	-1	-1	1	1.432
2	1	-1	1	-1	1.435
3	1	1	-1	-1	1.432
4	1	1	1	1	1.434
5	1	-1	-1	1	1.43
6	1	-1	1	-1	1.434
7	1	1	-1	-1	1.432
8	1	1	1	1	1.434
9	1	-1	-1	1	1.428
10	1	-1	1	-1	1.435
11	1	1	-1	-1	1.432
12	1	1	1	1	1.435
13	1	-1	-1	1	1.432
14	1	-1	1	-1	1.434
15	1	1	-1	-1	1.432
16	1	1	1	1	1.435
17	1	-1	-1	1	1.433
18	1	-1	1	-1	1.434
19	1	1	-1	-1	1.432
20	1	1	1	1	1.435
21	1	-1	-1	1	1.429
22	1	-1	1	-1	1.435
23	1	1	-1	-1	1.43
24	1	1	1	1	1.435

First round DOE

Effect	beta	SS	DOF	MS	F	F _{crit}	
1	1.432875	49.27513838	1	49.27514	38647167	4.35125	Significant
X2	0.000292	2.04167E-06	1	2.04E-06	1.601307	4.35125	Insignificant
X3	0.001708	7.00417E-05	1	7E-05	54.93464	4.35125	Significant
X2X3	-0.00021	1.04167E-06	1	1.04E-06	0.816993	4.35125	Insignificant
Error		2.55E-05	20	1.27E-06			
Total		49.275237	24				

Second round DOE

Effect	beta	SS	DOF	MS	F	F _{crit}	
1	1.432875	49.27513838	1	49.27513838	37926054	4.300944	
X3	0.001708333	7.00417E-05	1	7.00417E-05	53.90962	4.300944	
Error		2.85833E-05	22	1.29924E-06			
Total		49.275237	24				

Originally, it appears strange that a different input parameter is significant at different temperatures. If we try to interpret the phenomenon with physical understanding, it may actually sound reasonable.

At a higher temperature (450°F), the polymer melt is less viscous so injection speed would not affect the amount of polymer melt injected. A longer hold time, on the other hand, can increase the amount of polymer injected.

At lower temperatures, the polymer melt is more viscous and also freezes faster. A longer hold time would not increase the amount of injected polymer because the gate is frozen before the hold time ends. A faster injection speed would result in more injected polymer.

References

- [1] Montgomery, D. C., *Introduction to Statistical Quality Control*, Third edition, John Wiley & Sons, Inc., New York, 1997
- [2] DeVor, R. E., Chang, T., and Sutherland, J. W., *Statistical Quality Design and Control: Contemporary Concepts and Methods*, Prentice-Hall, Inc., Upper Saddle River, New Jersey, 1992
- [3] Hardt, D.E., *MIT Course 2.830 lecture notes: Lecture 3*, 2000
- [4] Box, G. E. and Kramer, T., *Statistical Process Monitoring and Feedback Adjustment: A Discussion*, Technical report, Center for Quality and Productivity Improvement, 1990
- [5] Box, G. E., Jenkins, G. M. and Reinsel, G. C., *Time Series Analysis: Forecasting and Control*, Third Edition, Prentice-Hall, Inc., Upper Saddle River, New Jersey, 1994
- [6] Wickens, C. D. and Hollands, J., *Engineering Psychology And Human Performance*, Third Edition, Prentice-Hall, Inc., Englewood Cliffs, New Jersey, 1999
- [7] Valjavec, M., *A closed-loop shape control methodology for flexible stretch forming over a reconfigurable tool*, PhD Thesis, Department of Mechanical Engineering, MIT, 1999
- [8] Ingolfsson, A., *Run by Run Process Control*, MS Thesis, Department of Electrical Engineering and Computer Science, MIT, 1997
- [9] Sachs, E. M., Hu, A. and Ingolfsson, A., *Run by Run Process Control: Combining SPC and Feedback Control*, IEEE Transaction on Semiconductor Manufacturing, Vol. 8, No. 1, 1995, pp. 26-43
- [10] Ingolfsson, A. and Sachs, E. M., *Stability and Sensitivity of an EWMA Controller*, Journal of Quality Technology, Vol. 25, No. 4, 1993, pp. 271-287
- [11] Vander Wiel, S. A. and Tucker, W. T., *Algorithmic Statistical Process Control: Concepts and an Application*, Technometrics, Vol. 34, No. 3, 1992, pp. 286-297
- [12] Smith, T. and Boning, D., *A Self-Tuning EWMA Controller Utilizing Artificial Neural Network Function Approximation Techniques*, International Electronics Manufacturing Symposium, IEMT '96, Oct. 1996
- [13] Del Castillo, E. and Hurwitz, A., *Run-to-Run Process Control: Literature Review and Extensions*, Journal of Quality Technology, Vol. 29, No. 2, 1997, pp. 184-196
- [14] Del Castillo, E., *A multivariate self-tuning controller for run-to-run process control under shift and trend disturbances*, IIE Transactions, Vol. 28, No. 12, 1996, pp. 1011-1021
- [15] *Next-Generation Manufacturing – A Framework for Action*, Agility Forum, Leaders for Manufacturing and Technologies Enabling Agile Manufacturing, 1997

- [16] Hardt, D.E., *MIT Course 2.830 lecture notes: Lecture 22*, 2000
- [17] Mickens, R. E., *Difference Equations*, Van Nostrand Reinhold Company Inc., New York, 1987
- [18] Van De Vegte, J., *Feedback Control Systems*, Third Edition, Prentice-Hall, Inc., Englewood Cliffs, New Jersey, 1994
- [19] Boyce, W. E. and DiPrima, R. C., *Elementary Differential Equations and Boundary Value Problems*, Fifth edition, John Wiley & Sons, Inc., New York, 1992, pp. 98-109
- [20] Rice, J. A., *Mathematical Statistics and Data Analysis*, 2nd edition, Wadsworth, Inc., Belmont, California, 1995, pp. 111-154
- [21] Box, G. and Luceño, A., *Statistical Control by Monitoring and Feedback Adjustment*, John Wiley & Sons, Inc., New York, 1997
- [22] Novak, J. P., PhD Research, Department of Mechanical Engineering, MIT, In progress
- [23] Box, G. E. P. and Luceño, A., "Discrete Proportional-Integral Control with Constrained Adjustment", *Journal of the Royal Statistical Society, Series D – The Statistician*, Vol. 44, 1995, pp. 479-495
- [24] Friedland, B., *Control System Design: An introduction to State-Space Methods*, McGraw-Hill, Inc., New York, 1986
- [25] Ohio State University ERC/NSM Laboratory Website - <http://nsmwww.eng.ohio-state.edu>
- [26] Michigan State University Intelligent Systems Laboratory Website - <http://islnotes.cps.msu.edu/trp/inj/index.html>
- [27] Bendat, J. S. and Piersol, A. G., *Random Data: Analysis and Measurement Procedures*, John Wiley & Sons, Inc., New York, 1971
- [28] Kalpakjian, S., *Manufacturing Processes for Engineering Materials*, Third edition, Addison Wesley Longman, Inc., Menlo Park, California, 1997
- [29] Lakshmikantham, V. and Trigiante, D., *Theory of Difference Equations: Numerical Methods and Application*, Academic Press, Inc., San Diego, California, 1988
- [30] Mix, D. F., *Random Signal Processing*, Prentice-Hall, Inc., Englewood Cliffs, New Jersey, 1995
- [31] Leon-Garcia, A., *Probability and Random Processes for Electrical Engineering*, Second Edition, Addison-Wesley, Inc., Reading, Massachusetts, 1994
- [32] Åström, K. J., *Adaptive control*, Addison-Wesley, Reading, Massachusetts, 1989
- [33] Houpis, C. H. and Lamont, G. B., *Digital Control Systems: Theory, Hardware, Software*, Second Edition, McGraw-Hill, Inc., New York, 1992

- [34] Elsner, J. B. and Tsonis, A. A., *Singular Spectrum Analysis: A New Tool in Time Series Analysis*, Plenum Press, New York, 1996
- [35] Goldratt, E. M., *The Goal: A Process is Ongoing Improvement*, Second Revised Edition, North River Press, Inc., Great Barrington, Massachusetts, 1992
- [36] Oppenheim, A. V. and Schaffer, R. W., *Discrete-Time Signal Processing*, Prentice-Hall, Inc., Englewood Cliffs, New Jersey, 1989
- [37] Oppenheim, A. V., *Digital signal processing: video course manual*, Massachusetts Institute of Technology, Center for Advanced Engineering Study, Cambridge, Massachusetts, 1975
- [38] Simon, H. A., *The Sciences for the Artificial*, MIT Press, Cambridge, Massachusetts, 1969
- [39] Cover, T. and Thomas, J. A., *Elements of Information Theory*, John Wiley & Sons, Inc., New York, 1991
- [40] Gallager, R. G., *Discrete Stochastic Process*, Kluwer Academic Publishers, Norwell, Massachusetts, 1996

Bibliographical Note

Tsz-Sin Siu was born on March 26, 1977 in Shanghai, P.R.China. He is commonly known as George Siu among friends and relatives. While he was brought up in Hong Kong, he finished his high school education in Earl Haig Secondary School in Ontario, Canada. He received a B.A.Sc. degree in Engineering Science with honor from the University of Toronto in 1999. At the same year, he came to the Massachusetts Institute of Technology to pursue his Master's degree in Mechanical Engineering. After completing his Master's degree, he will be working full time as an engineer in sunny California.

201-52